The synthesis and evaluation of benzosuberone derivatives as inhibitors of monoamine oxidase

C Bakker

orcid.org/ 0000-0002-0992-3528

Dissertation submitted in partial fulfillment of the requirements for the degree *Magister Scientiae* in Pharmaceutical Chemistry at the Potchefstroom Campus of the North-West University

Supervisor:	Prof A Petzer
Co-supervisor:	Prof JP Petzer
Co-supervisor:	Prof LJ Legoabe

Graduation May 2018

Student number: 23517700

NWU®
NORTH-WEST UNIVERSITY
NOORDWES-UNIVERSITEIT
UNIBESITI YA BOKONE-BOPHIRIMA

The financial assistance of the National Research Foundation (NRF) towards this research is hereby acknowledged. Opinions expressed and conclusions arrived at, are those of the author and are not necessarily to be attributed to the NRF.

ACKNOWLEDGEMENTS

I would like to thank the following people who helped me in the last two years with their love and support:

- My studyleaders: **Prof. Anél Petzer & Prof. Jacques Petzer.**
- My parents: **Stephen and Adri Bakker.**
- **Ouma Corrie.**
- My brother: **Christiaan Bakker**
- **Andrea Bezuidenhout**: My Best Friend.
- **Nicolene "Nicci" Joubert**: My other Best Friend
- **Christopher Munday, Hayley Ward & Phillip Munday:** Friends who became family.
- Fellow masters students: **Elani Aucamp, Lianie Pieterse, Heleen Jansen van Rensburg, Mandi Erasmus & Suné Boshoff.**

"Magic happens when you don't give up, even though you want to. The universe always falls in love with a stubborn heart."

ABSTRACT

Monoamine oxidase (MAO) is responsible for the catabolism of neurotransmitters such as serotonin and dopamine in the central nervous system and peripheral tissues. MAO inhibitors such as selegiline play a vital part in the treatment of neurodegenerative diseases including Parkinson's disease (PD) and Alzheimer's disease. Inhibition of MAO-B elevates dopamine levels in the striatum and provides symptomatic relief for patients with PD. MAO-B inhibitors can be used as monotherapy or in combination with L-dopa to provide symptomatic relief.

1-Benzosuberone and structural derivatives thereof have not yet been evaluated as potential MAO inhibitors. 1-Benzosuberone, however, is structurally similar to rasagiline, a well-known MAO-B inhibitor. 1-Benzosuberone also is structurally similar to α-tetralone, which is a moderately potent reversible inhibitor of MAO-B. In this study, 1-benzosuberone was used as lead compound for the design of new MAO inhibitors. 1-Benzosuberone derivatives were thus synthesised and the structures of the compounds that were successfully synthesised were verified by NMR and MS. The purities of the compounds were determined by HPLC. Although difficulties were encountered during synthesis, four 1-benzosuberone derivatives were successfully synthesised.

Recombinant human MAO-A and MAO-B were used as enzyme sources to determine the MAO inhibition potencies of 1-benzosuberone and the synthesised derivatives. The inhibition potencies were expressed as the IC_{50} values. The results showed that three 1-benzosuberone derivatives display moderately potent inhibition of MAO-B. 6,7,8,9-Tetrahydro-*5H*-benzo[7]annulen-5-yl acetate is the most potent MAO-B inhibitor with an IC_{50} value of 8.31 µM. Weak or no inhibition of MAO-A was observed for the derivatives. 1-Benzosuberone showed no MAO-A inhibition and only weak inhibition of MAO-B.

The reversibility of MAO inhibition was investigated by dialysis. The reversibility studies showed that the three most active 1-benzosuberone derivatives are reversible MAO-B inhibitors and that 6,7,8,9-tetrahydro-5*H*-benzo[7]annulen-5-yl acetate potentially exhibit tight binding to MAO-B. Lineweaver-Burk plots were constructed to investigate the mode of MAO-B inhibition of the three most active derivatives. The results showed that the 1-benzosuberone derivatives are competitive inhibitors of MAO-B and the K_i values were determined, which ranged from 8.40 to 17.7 µM. Docking studies were carried out to determine potential binding orientations and interactions of the 1-benzosuberone derivatives to the MAO enzymes. Although the docking yielded no conclusive conclusions, some insight into the binding orientations and interactions that are possible for the 1-benzosuberone derivatives were gained.

To conclude, 1-benzosuberone derivatives with moderately potent and specific MAO-B inhibition activities were discovered in this study. These 1-benzosuberone derivatives are reversible and competitive inhibitors of MAO-B and may represent new lead compounds for the future design of MAO-B inhibitors to be used in the treatment of PD.

Key Words:

Parkinson's disease; monoamine oxidase (MAO); MAO-A; MAO-B; 1-benzosuberone; α-tetralone; MAO-B inhibitors; inhibition potencies; reversibility; Lineweaver-Burk plots; competitive mode of inhibition; docking-studies.

TABLE OF CONTENTS

LIST OF ABBREVIATIONS

5-HT – 5-Hydroxytryptamine/serotonin

A

AD – Alzheimer's disease

AO – Amine oxidase

C

COMT – Catechol-O-methyltransferase

CNS – Central nervous system

D

DA – Dopamine

DMF – N,N-Dimethylformamide

F

FAD – Flavin adenine dinucleotide

H

HPLC – High pressure liquid chromatography

L

L-Dopa – Levodopa

LB – Lewy bodies

M

MAO – Monoamine oxidase

MAO-A – Monoamine oxidase A

MAO-B – Monoamine oxidase B

MPP^+ – 1-Methyl-phenylpyridinium

MPTP – 1-Methyl-4-phenyl-1,2,3,6-tetrahydropyridine

MS – Mass spectrometry

N

NA – Noradrenaline

NMR – Nuclear magnetic resonance

P

PD – Parkinson’s disease

R

RIMA – Reversible inhibitors of monoamine oxidase

ROS – Reactive oxygen species

S

SNpc – Substantia nigra pars compacta

SSAO - Semicarbazide-sensitive amine oxidase

SSRI – Selective serotonin reuptake inhibitor

T

TLC - Thin layer chromatography

TPQ - Topa-quinone

LIST OF TABLES

LIST OF FIGURES

CHAPTER 1: INTRODUCTION AND RATIONALE

1.1 Introduction and overview

Parkinson's disease (PD) is a disease characterised by the loss of dopaminergic neurons in the brain. These neurons are specifically located in the substantia nigra pars compacta (SNpc), and the loss of these neurons leads to a dopamine (DA) deficiency in the striatum. Levodopa (L-dopa) is a precursor of dopamine and is effective in alleviating most symptoms associated with PD. Although L-dopa is highly effective, adverse effects such as dyskinesias occur which have a negative impact on the quality of life of PD patients. All current treatment of PD are only symptomatic and none prevent the degradation of dopaminergic neurons and thus halt or slow the disease progression (Dauer & Przedborski, 2003).

Monoamine oxidase (MAO) has received much interest over the last decades as a target for the treatment of neurodegenerative disorders such as PD and Alzheimer's disease (AD). This is because the MAO iso-enzymes, MAO-A and MAO-B, metabolise neurotransmitters including DA in the brain and peripheral tissues (Edmondson *et al*., 2004). Two isoforms of MAO exist, MAO-A and MAO-B. These isoforms are encoded by two separate genes, which are approximately 70% identical at the amino acid level (Bach *et al*., 1988). MAO-A mainly metabolises serotonin (5-HT) and noradrenaline (NA) while MAO-B mainly metabolises phenylethylamine and benzylamine. Both isoforms metabolise DA and tyramine (Billett, 2004).

The structures of both MAO-A and MAO-B have only recently been elucidated (Youdim *et al*., 2006). Both isoforms contain a covalently attached flavin adenine dinucleotide (FAD) co-factor that is essential for catalysis (Edmondson *et al*., 2004). MAO-B crystalises as a dimer and each monomer contains three domains: a domain by which the enzyme binds to the mitochondrial membrane, a domain which binds to the FAD cofactor and the catalytic domain where the substrate binds (Binda *et al*., 2002).

The first MAO inhibitors have been developed more than 60 years ago as antidepressant agents (Youdim *et al*., 2006). These first inhibitors were non-selective and irreversible inhibitors of MAO and included phenelzine and tranylcypromine as examples. These drugs are potentially unsafe as they are capable of inducing the "cheese reaction" when ingested with tyramine containing food (Yamada & Yasuhara, 2004). Selective, MAO-B inhibitors (reversible and irreversible) such as selegiline and rasagiline do not cause the cheese reaction. Reversible inhibitors of MAO-A such as moclobemide are also not associated with the cheese reaction (Yamada & Yasuhara, 2004). It may thus be concluded that MAO-A inhibitors with an irreversible mode of inhibition possess a high risk of the cheese reaction compared to reversible and MAO-B selective inhibitors.

With regards to MAO inhibitors, the goal is to discover novel inhibitors that would be highly selective for the MAO-B isoform. Such compounds may be used for the treatment of PD. Inhibitors that act reversibly at the MAO-A isoform, in turn, may be used for the treatment of depression (Edmondson *et al*., 2004).

1.2 Rationale

The benzosuberone class of compounds has not previously been investigated as potential MAO inhibitors. 1-Benzosuberone bear some structural resemblance to rasagiline (Fig.1.1), a well-known MAO-B specific inhibitor. In contrast to rasagiline, however, 1-benzosuberone does not contain the propargylamine group and is expected to be a reversible inhibitor. Propargylamine compounds such as rasagiline and selegiline are irreversible MAO inhibitors since the propargylamine moiety is oxidised by the enzyme to a reactive intermediate that alkylates the FAD cofactor. 1-Benzosuberone also bear structural resemblance to 1-tetralone, which is reported to be a moderately potent MAO inhibitor with IC_{50} values of 14.8 µM and 18.6 µM for the inhibition of human MAO-A and MAO-B, respectively (Legoabe *et al*., 2014). 1-Benzosuberone can therefore be considered as the 7-membered ring analogue of 1-tetralone and 1-benzosuberone and 1-benzosuberone derivatives may thus act as MAO inhibitors.

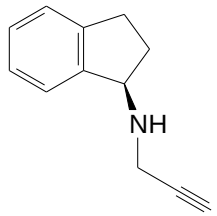

Figure 1-1 Structure of rasagiline

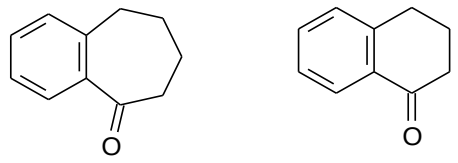

1-Benzosuberone 1-Tetralone

Figure 1-2 Structures of 1-benzosuberone and 1-tetralone

The goal of this dissertation is to investigate the MAO inhibition properties of 1-benzosuberone and 1-benzosuberone derivatives. Based on their structural similarities to rasagiline and 1-tetralone, 1-benzosuberone derivatives may possess interesting potency and selectivity profiles towards the MAOs, which may offer safer and more effective drugs for the treatment of PD.

1.3 Hypothesis of this study

Rasagiline is a selective, potent and irreversible inhibitor of MAO-B. Rasagiline contain a propargylamine functional group that is responsible for its irreversible mode of MAO-B inhibition. 1-Benzosuberone and the 1-benzosuberone derivatives of this study bear resemblance to rasagiline, but does not contain the propargylamine group. The assumption may thus be made that 1-benzosuberone and 1-benzosuberone derivatives may act as reversible MAO-B inhibitors. The proposal that 1-benzosuberone and 1-benzosuberone derivatives may act as MAO inhibitors is further supported by the observation that 1-tetralone is a moderately potent MAO-A and MAO-B inhibitor. This study will contribute to the design of new MAO inhibitors, and specifically will be the first investigation of the MAO inhibition properties of the 1-benzosuberone class of compounds. Good potency MAO-B inhibitors may act as new leads for the design of reversible MAO-B inhibitors for the treatment of PD.

1.4 Objectives of this study

The objectives of this study are:

- To attempt the syntheses of the 1-benzosuberone derivatives shown in Fig. 1.3 using 1-benzosuberone as starting reagent.

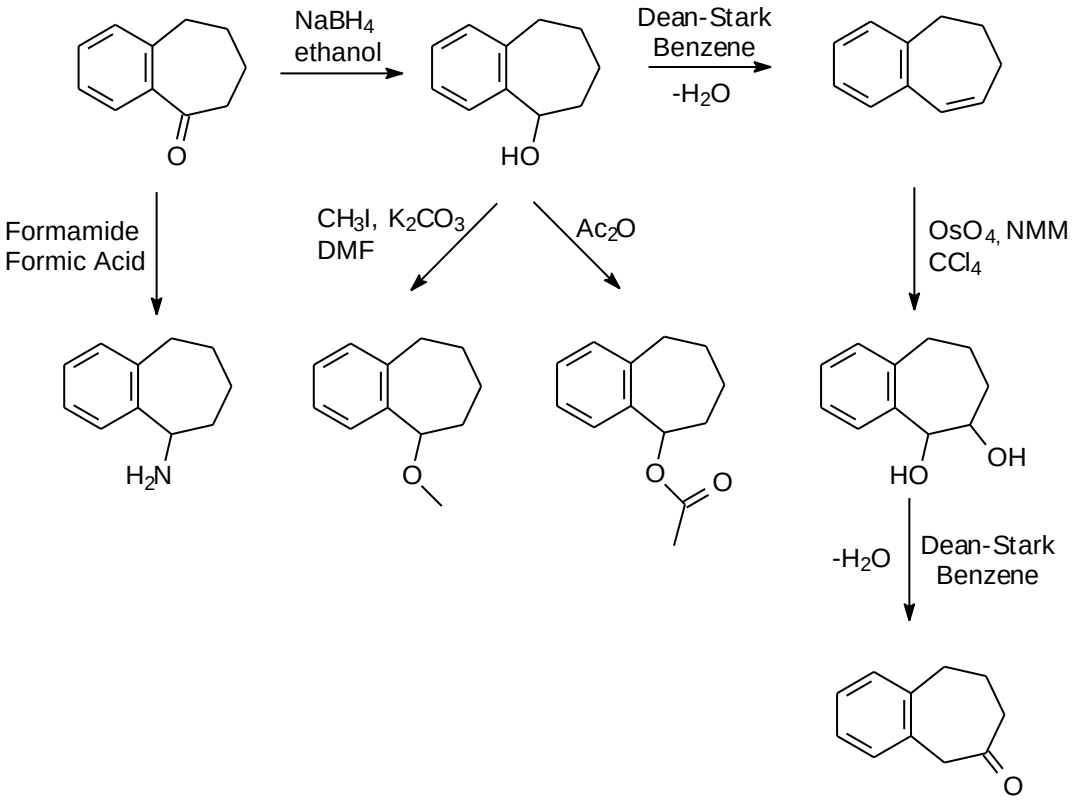

Figure 1-3 The synthesis route for the 1-benzosuberone derivatives that will be investigated in this study

- To evaluate 1-benzosuberone and the 1-benzosuberone derivatives as potential inhibitors of human MAO-A and MAO-B by measuring IC_{50} values as an index of the potency of the inhibition.
- The reversibility of the inhibition of the most potent inhibitors will be further investigated. Dialysis will be used to determine whether the inhibitors bind to MAO in a reversible or irreversible manner.
- The mode of inhibition will be investigated by constructing sets of Lineweaver-Burk plots the most potent inhibitors. This will give an indication whether the inhibitors bind competitively to MAO, and will also allow for the measurement of enzyme-inhibitor dissociation constants (K_i values).
- The binding of the most potent inhibitors to MAO-A and MAO-B will be investigated on the molecular level with molecular docking experiments.

CHAPTER 2: LITERATURE STUDY

2.1 Monoamine oxidase

2.1.1 General background

Since the discovery of MAO more than 85 years ago, a variety of inhibitors have been described. These include irreversible non-selective inhibitors, irreversible isoform-selective inhibitors and reversible isoform-selective inhibitors (Youdim & Bakhle, 2006). Iproniazid was the first MAO inhibitor used in the treatment of depression and during the past decades iproniazid as well as other MAO inhibitors have demonstrated excellent antidepressant effects in the clinic. In spite of this, many MAO inhibitors exhibit serious side effects and MAO inhibitors as a class have been replaced by other antidepressant agents (Youdim *et al*., 1988).

MAO is involved in the metabolism of several monoamine neurotransmitters such as 5-HT, DA, NA and adrenaline as seen in Fig. 2.1. Besides depression, MAO inhibitors are also used for the symptomatic treatment of neurodegenerative diseases such as PD and AD (Youdim *et al*, 2006). MAO is essential in brain development and research has shown that MAO activity influences certain personality traits (Youdim *et al.*, 2006).

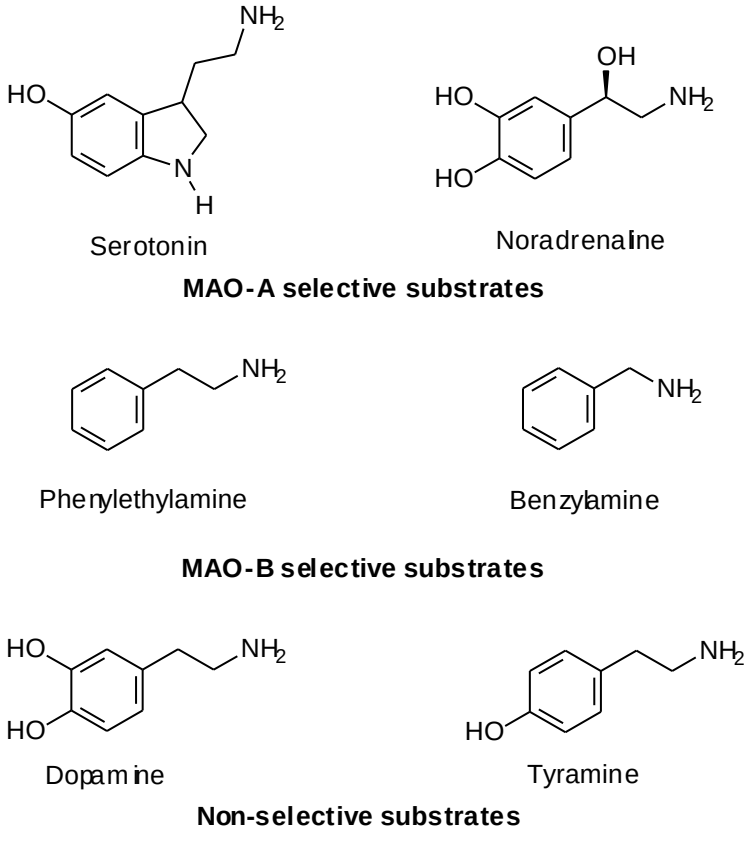

Figure 2-1 Structures of MAO substrates

Two different MAO isoforms have been identified, MAO-A and MAO-B. These isoforms possess different tissue distribution and substrate specificities. For example, MAO-A is involved in the metabolism of 5-HT and is inhibited by clorgyline, while MAO-B metabolises benzylamine and 2-phenylethylamine and is inhibited by selegiline. DA and tyramine are metabolised by both enzymes depending on the concentration of the substrate (Billett, 2004).

The MAOs are located on the outer membrane of mitochondria and are flavin proteins since they employ FAD as cofactor (Youdim *et al.,* 2005). In both enzymes, the FAD cofactor is covalently bound to the 8α-(S-cysteinyl)-riboflavin linkage (Walker *et al*., 1971).

Obtaining the purified MAO enzymes which are required for many research programs proved difficult because of the location of the enzymes on the outer membranes of mitochondria. For many years bovine liver mitochondria was used as source of MAO-B (Salach, 1979) while human placental mitochondria served as source for MAO-A (Weyler & Salach, 1985). The first recombinant MAO was produced by a *S. cerevisiae* expression system for MAO-A, but was not capable of expressing efficient quantities of MAO-B (Weyler *et al*., 1990). The *Pichia pastoris* expression system, however, yields recombinant MAO-A and MAO-B in high enough quantities to have allowed for X-ray crystallography studies (Newton-Vinson *et al*., 2000).

MAO-A and MAO-B have similar, and often shared, biological functions. The goal of the design of MAO inhibitors is to discover compounds with high specificity for either isoform, which may lead to reduced side-effects (Edmondson *et al*., 2004). This is especially true for the design of MAO-B inhibitors that are free form the adverse effects associated with MAO-A inhibition. It is interesting to note that MAO-B activity in the brain increases with age, an observation that makes inhibitors of this isoform of much relevance to the treatment of neurodegenerative diseases (Kumar *et al*., 2003).

2.1.2 Tissue distribution

MAO is associated with the outer membrane of mitochondria (Youdim *et al*., 2006). The MAO enzymes are abundant in both the central nervous system (CNS) and peripheral tissues. In this respect, the liver, gastrointestinal system and platelets contain MAO in high levels (Kopin, 1994; Tipton, 1980, 1986). In peripheral tissues, MAO-A can be considered the dominant isoform (Billett, 2004). The lungs contain both isoforms and is most likely responsible for the metabolism of locally released NA and circulatory amines (Bryan-Lluka & O'Donnell, 1992). In the CNS, the highest level of MAO activity exists in the basal ganglia and hypothalamus (O'Carroll *et al*., 1983).

2.1.2.1 The distribution of MAO-A

Most of the MAO-A in the brain is found in the catecholaminergic neurons of the locus coeruleus (Foley *et al*., 2000), substantia nigra and periventricular regions of the hypothalamus (Westlund *et al*., 1985). High levels of MAO-A in the duodenum are responsible for the deamination of tyramine and other dietary amines. MAO-A thus functions as a metabolic barrier at the gastrointestinal tract. MAO-A in smooth muscle, in turn, is responsible for the deamination of NA and adrenaline (Billet, 2004). Importantly, MAO-A is also found in cardiomyocytes where it metabolises NA and adrenaline (Babin & Gliese, 1995). DA, 5-HT and other amines that are synthesised in the kidney are also metabolised by renal MAO (Lee, 1982). Human placental tissue almost exclusively expresses MAO-A (Billet, 2004).

2.1.2.2 The distribution of MAO-B

The highest concentration of MAO-B in the brain is found in the dorsal raphe (serotonergic nerves) and posterior hypothalamus (Westlund *et al*., 1988). There are also high concentrations of MAO-B in the basal ganglia (Oreland *et al*., 1983). Astrocytes mainly contain MAO-B while platelets exclusively express MAO-B (Foley *et al*., 2000). There is a high concentration of MAO-A in the basal ganglia (Oreland *et al*., 1983), but MAO-B is the main isoform in this region (Youdim *et al*., 2006). The duodenum contains high levels of MAO-B, but in general MAO-A is responsible for the metabolism of dietary amines in the gastrointestinal tract (Billet, 2004). Smooth muscle contains low levels of MAO-B, but the function of MAO-B here is unknown (Billet, 2004).

2.1.3 The reaction and reaction pathways of MAO

MAO-A and MAO-B catalyse the metabolism of amine substrates through oxidative deamination (Edmondson *et al*., 2004). MAO-A and MAO-B transfer two electrons from the substrate amine to the FAD to yield an imine product. Molecular oxygen serves as final electron acceptor for the re-oxidation of the reduced FAD (Edmondson *et al*., 2009). The oxidative deamination of amines by MAO may be illustrated by the following reaction:

$RCH_2NH_2 + H_2O + O_2 \rightarrow RCHO + NH_3 + H_2O_2$ (Kopin, 1994).

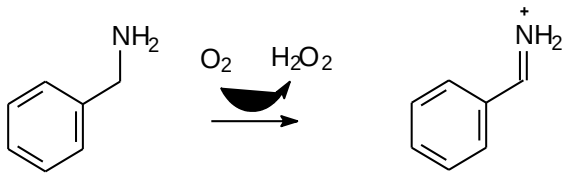

Figure 2-2 The deamination reaction of amines by MAO

There are two different reaction pathways which substrates may follow when oxidised by the MAOs. Most substrates follow the reaction pathway in which the enzyme-product complex reacts with oxygen prior to dissociation of the complex (figure 2.13 bottom). Fewer substrates follow the top pathway where the enzyme-product complex dissociates prior to reaction of the FAD with oxygen (Edmondson *et al*., 2009). For catalysis by MAO-B, benzylamine follows the bottom reaction pathway while phenylethylamine follows the top reaction pathway. Studies have shown that MAO-A catalysis follows the bottom reaction pathway (Edmondson *et al*., 2004).

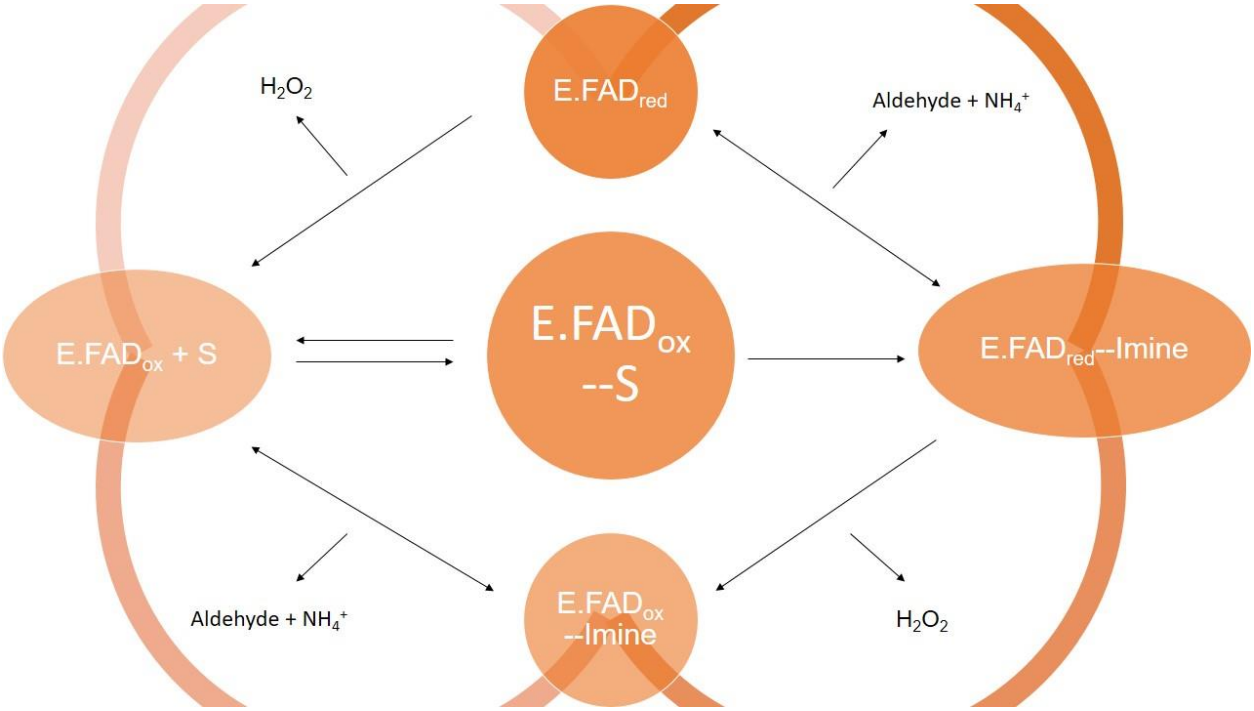

Figure 2-3 The reaction pathways for MAO catalysis (Adapted from Edmondson *et al*. 2004)

2.1.4 Genetics of MAO

The cloning and sequencing of the MAO enzyme demonstrated that two enzymes, MAO-A and MAO-B, exist. These enzymes exhibit a high degree of similarity and is approximately 70% identical on the amino acid level (Edmondson *et al*., 2004). MAO-A and MAO-B are thus encoded by separate genes, both located on the short leg of the X-chromosome. MAO-A is composed of 527 amino acids while MAO-B consists of 520 amino acids (Bach *et al*., 1988). Both enzymes consist of 15 exons and share a common ancestral gene as both enzymes have

the same intron-exon organisation. A flavin cofactor, the FAD, is required by both isoforms and binds with the same cysteine residue, which is part of a conserved pentapeptide sequence in both enzyme isoforms (Nagatsu, 2004).

2.1.5 Irreversible inhibitors of MAO, the first available inhibitors

The first MAO inhibitors to be discovered were irreversible acting inhibitors. Irreversible non-selective inhibitors of MAO such as phenelzine and tranylcypromine are known to cause the cheese reaction, which describes a hypertensive crisis when MAO-A is used in combination with food that contain tyramine (Yamada & Yasuhara, 2004). This adverse effect severely limits the clinical use of irreversible MAO inhibitors, and tranylcypromine is the only irreversible inhibitor still clinically used in the treatment of depression. Tranylcypromine is considered to be highly effective in patients that are compliant with a tyramine-restricted diet (Stewart, 2007; Adli *et al*., 2008; Gillman, 2011; Goldberg & Thase, 2013). Most irreversible inhibitors first bind reversibly to the MAO active site. After oxidation by MAO, the inhibitor binds to the N5 or C4a positions of the flavin ring. These are thus mechanism-based inhibitors and render the MAO enzymes permanently unavailable for further substrate oxidation. *De novo* synthesis of the MAO protein will be required for enzyme activity to be regained. A single dose of an irreversible inhibitor inhibits MAO completely and without a subsequent dose, enzyme activity will slowly recover (Youdim & Finberg, 1985; Youdim *et al.*, 1988).

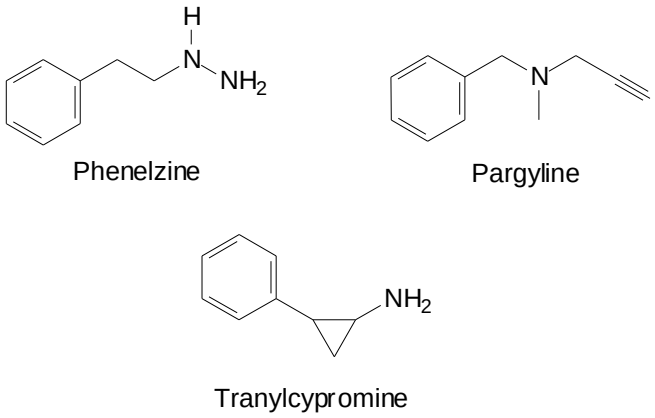

Figure 2-4 The structures of phenelzine, pargyline and tranylcypromine, examples of irreversible non-selective MAO inhibitors

2.2 MAO-A

2.2.1 Biological function of MAO-A

2.2.1.1 Substrate specificity

MAO-A in the human central nervous system is primarily responsible for the metabolism of 5-HT and NA. In the intestine, the MAO-A enzyme is responsible for the metabolism of tyramine (Foley *et al*., 2000). MAO-A is thus responsible for the metabolism of neurotransmitters that is considered important in disorders such as depression and anxiety (Yamada & Yasuhara, 2004). DA is a substrate for both MAO-A and MAO-B (Green *et al*, 1977). The differences in substrate specificity between MAO-A and MAO-B is mainly caused by Ile-335 and Phe-208 in MAO-A, and Tyr-326 and Ile-199 in MAO-B (Son *et al*., 2008). These residues restrict the binding of specific substrates and inhibitors to the respective MAO isoforms.

2.2.1.2 The cheese reaction

In the early 1960's the use of MAO inhibitors as antidepressants was limited due to severe adverse effects with irreversible non-selective MAO inhibitors. The most notable adverse effect was the cheese reaction, which occurs when irreversible MAO-A inhibitors are combined with tyramine which is found in fermented food that includes cheese. Normally tyramine is deaminated by MAO-A in the intestine, however, when MAO-A is inhibited, tyramine enters the systemic circulation and causes a release of NA, which in turn leads to severe hypertension (Youdim & Weinstock, 2004).

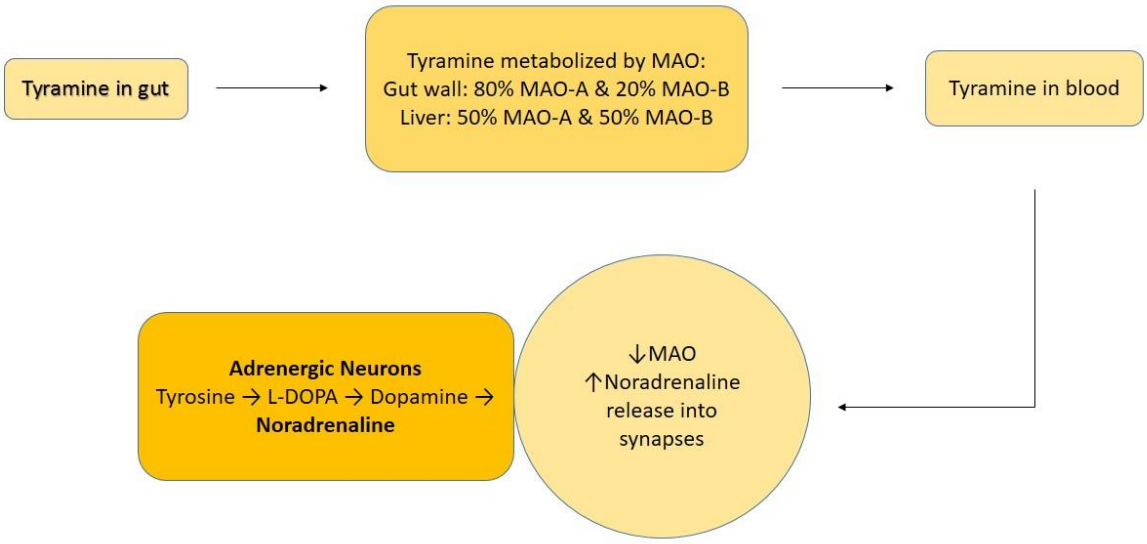

Figure 2-5 The metabolism of tyramine and its involvement in the cheese reaction (Youdim & Bakhle, 2006)

Tyramine and other dietary amines are extensively metabolised by MAO-A in the intestine and liver. When an inhibitor of MAO-A is administered, tyramine is not metabolised adequately and is absorbed into the bloodstream. Once in the systemic circulation, tyramine, being an indirectly acting sympathomimetic agent, induces the release of NA from peripheral adrenergic neurons. This causes severe hypertension which may be fatal, and is known as the cheese reaction (Finberg *et al*., 1981). Irreversible MAO-A inhibitors have a higher risk of causing the cheese reaction than reversible inhibitors since increasing concentrations of tyramine (as a result of the inhibition of its MAO-A-catalysed metabolism) will displace a reversible inhibitor from MAO-A and will thus be normally metabolised (Haefely *et al*., 1992).

Irreversible MAO-B inhibitors such as selegiline do not cause the cheese reaction with normal doses since tyramine is almost exclusively metabolised by the MAO-A isoform in the gastrointestinal tract (Knoll & Magyar, 1972; Youdim *et al*., 1988). At higher doses, irreversible MAO-B inhibitors may, however, inhibit MAO-A to some degree. In spite of this, irreversible MAO-B inhibitors such as selegiline are not associated with the cheese reaction (Finberg & Tenne, 1982). Reversible MAO-B specific inhibitors such as safinamide do not inhibit MAO-A even at high concentrations and thus have no risk of causing the cheese reaction (Youdim & Weinstock, 2004).

2.2.1.3 MAO and heart conditions

Aging is associated with an increase in MAO-A activity in the heart, which in turn leads to an increase in apoptosis and necrosis of cardiac cells. This is due to increased production of hydrogen peroxide (H_2O_2) by MAO-A (Edmondson *et al*., 2009). MAO metabolises monoamines to their corresponding aldehydes with ammonia and hydrogen peroxide as by-products. Aldehyde dehydrogenase metabolises the aldehydes to their corresponding acids, while hydrogen peroxide, if not cleared by cell buffering systems, may react in the Fenton reaction to yield the highly destructive hydroxyl radical. It should be noted that both MAO-A and MAO-B are present in human cardiomyocytes, but MAO-A is more dominant, and MAO-A inhibitors have thus been suggested to act as potential agents for protection against cardiac cellular degeneration (Sivasubramaniam *et al*., 2003; Saura *et al*., 1992). In theory, MAO-A inhibitors would reduce the formation of these injurious aldehydes and the hydroxyl radical.

2.2.2 Inhibitors of MAO-A

MAO-A inhibitors are mainly used in the treatment of depression (Leonard *et al*., 2004). The two monoamines that are implicated in depression are 5-HT and NA (Youdim & Bakhle, 2006). According to the monoamine hypothesis of depression, 5-HT and NA levels are decreased in the brain, which are primarily responsible for the symptoms of depression. MAO-A inhibition increases both 5-HT and NA levels, and MAO-A inhibitors have thus been used for decades as antidepressant agents (Colzi *et al*., 1992). The next section will give a brief overview of well-known MAO-A inhibitors.

2.2.2.1 Irreversible inhibitors of MAO-A

2.2.2.1.1 Non-selective Inhibitors of MAO-A and MAO-B

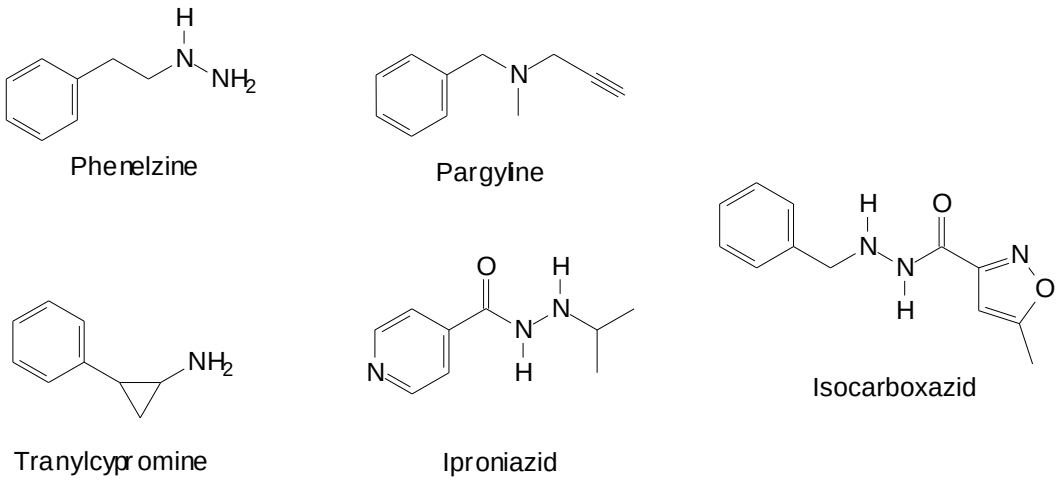

Figure 2-6 Structures of irreversible inhibitors of MAO-A and MAO-B

Iproniazid: Iproniazid was the first MAO inhibitor that was discovered following molecular modifications to isoniazid, an anti-tuberculosis drug. Further modifications lead to phenelzine which was clinically used in the treatment of depression (Finberg, 2014).

Phenelzine: Phenelzine is a non-selective inhibitor of MAO-A and MAO-B that is clinically used in depression resistant to other treatments as well anxiety disorders (Finberg, 2014). N-Acetylphenelzine is a metabolite that is generated by the MAO-B-catalysed metabolism of phenelzine, and is also a MAO inhibitor (Coutts *et al*., 1991).

Tranylcypromine: Tranylcypromine is a non-selective inhibitor of MAO still used in the treatment of depression and is highly effective inhibitor of both isoforms (Finberg, 2014). Tranylcypromine is also an irreversible inhibitor of lysine-specific histone demethylase type 1 (Lee *et al*, 2006; Schmidt & McCafferty, 2007; Yang *et al*., 2007), which may contribute to the effectiveness of tranylcypromine in the treatment of depression (Baker *et al*., 1992).

Isocarboxazid: Isocarboxazid is a hydrazine inhibitor of MAO that binds irreversibly to MAO and is currently used in the treatment of depression (Finberg, 2014). The hydrazine structure may lead to side-effects such as neurotoxicity and hepatotoxicity (Gillman, 2011).

Pargyline: Pargyline is a non-selective inhibitor of MAO which was used in the treatment of hypertension, but is not clinically used at present. Pargyline was discovered in the 1950's and has a propargylamine functional group that binds irreversibly to the FAD co-factor. Pargyline has a slight degree preference for MAO-B (Finberg, 2014).

2.2.2.1.2 Selective irreversible inhibitors of MAO-A

Clorgyline: Clorgyline is a potent MAO inhibitor that selectively inhibits MAO-A. Low doses of clorgyline increases levels of DA, NA and 5-HT in various tissues including the brain (Waldmeier *et al*., 1981). MAO inhibition by clorgyline is also reported to reduce oxidative stress by reducing the MAO-A-catalysed production of hydrogen peroxide (Aluf *et al*., 2013).

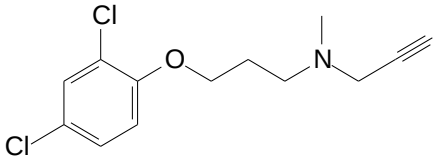

Figure 2-7 The structure of clorgyline

2.2.2.2 Selective reversible inhibitors of MAO-A (RIMAs)

Moclobemide: Moclobemide is a reversible inhibitor of MAO-A, which does not affect the synthesis, uptake or release of neurotransmitters (Fulton & Benfield, 1996). Moclobemide has been successfully used in the treatment of major depression and patients receiving this drug exhibit improvement in alertness, motor function and improvement in memory (Kerr *et al*., 1992; Allain *et al.*, 1993; Fairweather *et al*., 1993). Since moclobemide is a reversible MAO-A inhibitor, it does not cause the cheese reaction and is considered a safe drug as it is devoid of serious adverse effects (Bieck *et al*., 1993; Da Prada *et al.*, 1987; Haefely *et al.,* 1992; Korn *et al*., 1987).

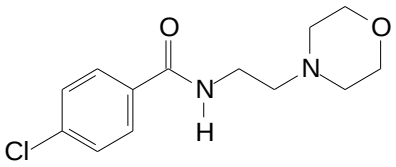

Figure 2-8 The structure of moclobemide

Other examples of RIMAs include: cimoxotone, befloxatone, brofaromine. None of these are currently clinically used (Finberg, 2014). Brofaromine is a RIMA and studies have shown that brofaromine is better tolerated then most other antidepressants such as imipramine and tranylcypromine. Furthermore, brofaromine is considered to be a very effective antidepressant (Lum & Stahl, 2012). Studies have shown that RIMAs are effective antidepressants, and although less effective than irreversible inhibitors of MAO they exhibit better side-effect profiles (Finberg, 2014).

2.2.3 The three-dimensional structure of MAO-A

The X-ray crystal structures of human and rat MAO-A have been reported and show that human MAO-A crystallises as a monomer. The human MAO-A structure has a 90% sequence identity to rat MAO-A, and the two crystal structures therefore have nearly identical structures (Son *et al*., 2008). The structure of human MAO-A is different from that of rat MAO-A in residues 108-118 and also in residues 210-216. These residues form the loop conformations that form an essential part of the active site (Edmondson *et al*., 2007). The C-terminus of MAO-A forms an α-helix transmembrane structure which is thought to be imbedded into the outer mitochondrial membrane. The 29-amino acid residues of the C-terminal have been shown to be responsible for the targeting and anchoring of the protein to the outer membrane of the mitochondrion (Son *et al*., 2008). In MAO-A, membrane anchoring affects the catalytic efficiency of the enzyme (Son *et al*., 2008). In this respect, membrane anchoring facilitates the entry of the substrate into the

active site, and membrane-anchored MAO-A thus exhibits higher catalytic activity than purified MAO-A.

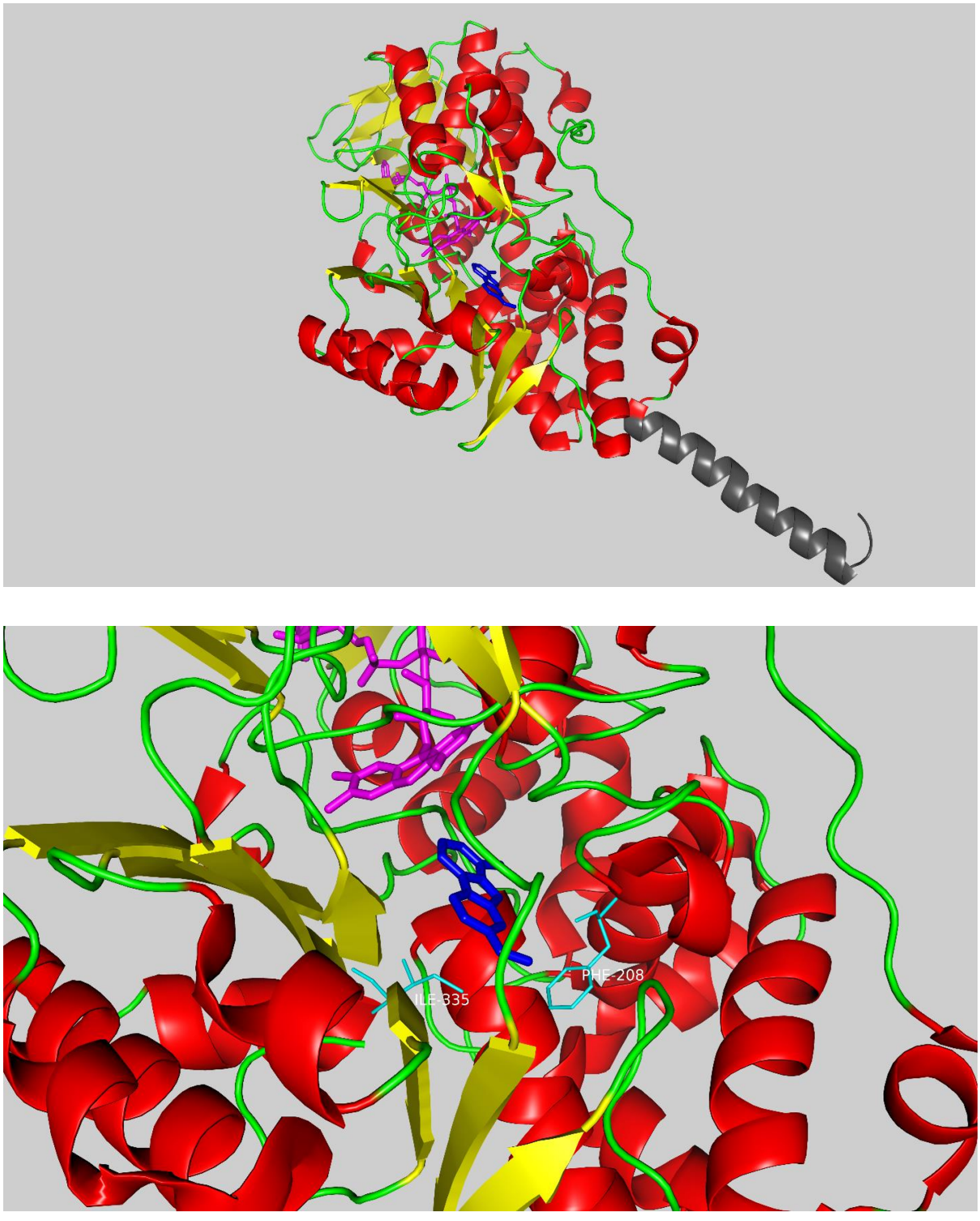

Figure 2-9 **The structure of MAO-A. The FAD cofactor is shown in magenta while harmine, the co-crystallised ligand, is shown in blue. The α-helix at the C-terminal is shown in grey. In the bottom figure, the key residues Phe-208 and Ile-335 are shown in cyan**

The MAO-A substrate cavity consists of a single chamber and is close to the surface of the mitochondrial membrane (Binda *et al*., 2002; Milczek *et al.*, 2011). There are 16 residues that surrounds the substrate cavity and only six of these residues differs between MAO-A and MAO-B. There are seven water molecules in the cavity and two of the water molecules form a bridge between the FAD and an inhibitor such as harmine, through hydrogen bonds (Son *et al.*, 2008). The Ile-335 and Phe-208 residues in MAO-A play important roles in substrate and inhibitor specificity between MAO-A and MAO-B (Son *et al*., 2008). The corresponding residues in MAO-B is Tyr-326 and Ile-199, respectively. The large size of Phe-208 restricts the binding of certain MAO-B specific inhibitors to MAO-A, while Tyr-326 in MAO-B restricts the binding of certain MAO-A specific inhibitors to MAO-B (Son *et al*., 2008).

2.3 MAO-B

2.3.1 Biological function of MAO-B

MAO-B catalyses the oxidative deamination of several substrates including phenylethylamine, DA and benzylamine. MAO-B does not catalyse the metabolism of 5-HT (Youdim & Bakhle, 2006). MAO-B metabolises primary, secondary and tertiary amines with hydrogen peroxide as a side product, which as mentioned, may lead to oxidative stress (Youdim & Bakhle, 2006). Patients with PD have been shown to have an aldehyde dehydrogenase deficiency and this may lead to a build-up of toxic aldehydes that form from DA metabolism by MAO (Grünblatt, 2004).

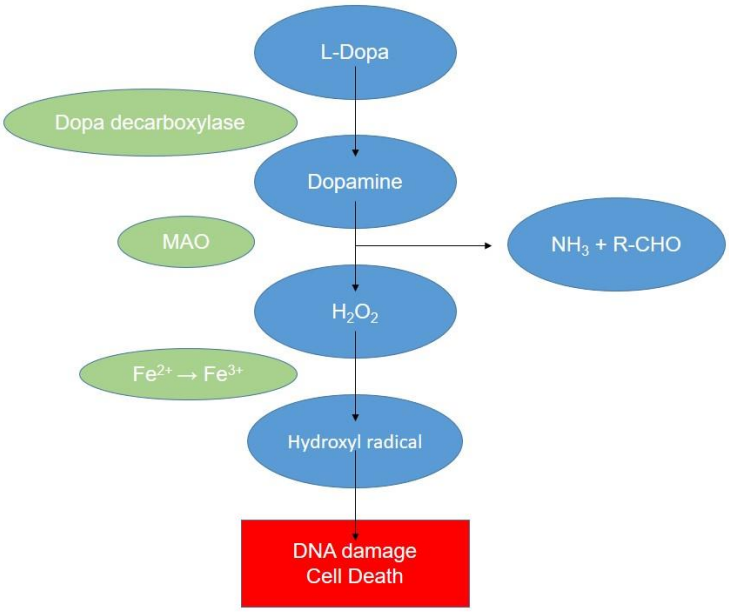

Figure 2-10 Flow diagram showing how MAO oxidation of DA leads to cell death (adapted from Riederer *et al*, 2004)

2.3.2 Inhibitors of MAO-B

Inhibitors of MAO-B are used in the treatment of PD (Leonard *et al*., 2004). MAO-B inhibitors such as rasagiline and selegiline contain an N-propargyl group that, after activation by the enzyme, binds covalently to the FAD-cofactor and deactivate the MAO enzyme. Propargylamine inhibitors such as rasagiline and selegiline bind to the N5 position of the FAD-cofactor (Weinreb *et al*., 2010). Inhibitors of MAO-B are thought to possess neuroprotective properties, which are mediated by the reduction of MAO-B-catalysed hydrogen peroxide formation in the brain (Weinreb *et al*., 2010).

2.3.2.1 Irreversible MAO-B inhibitors

Selegiline: Selegiline is a selective irreversible inhibitor of MAO-B. Although selegiline is used in the treatment of PD, recent transdermal formulations of selegiline have been approved for the treatment of depression. Since selegiline is a specific inhibitor of MAO-B it has a very low risk of causing the cheese reaction (Birkmayer *et al*., 1985). Selegiline thus has an excellent safety profile. As mentioned, selegiline is used in the symptomatic treatment of PD, particularly in combination with L-dopa (Youdim & Bakhle, 2006). In PD, selegiline reduces the MAO-B-catalysed metabolism of dopamine in the brain, and in this way enhances dopaminergic neurotransmission. A disadvantage of selegiline is that it is metabolised to amphetamine derivatives that can cause symphatomimetic effects (Youdim & Bakhle, 2006).

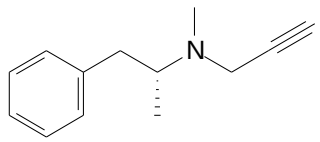

Figure 2-11 The structure of selegiline

Rasagiline: Rasagiline is also a selective irreversible inhibitor of MAO-B but display higher inhibition potency compared to selegiline (Youdim & Bakhle, 2006). Rasagiline does not have an amphetamine structure and is therefore not metabolised to amphetamine metabolites as is selegiline (Youdim & Bakhle, 2006). In addition to its MAO-inhibition properties, rasagiline also possesses anti-apoptotic and neuroprotective effects (Youdim & Bakhle, 2006). Rasagiline is 10-fold more potent than selegiline as an MAO-B inhibitor and is selective for MAO-B in the liver and brain. Rasagiline also results in high potency inhibition of MAO-B in human platelets (Weinreb *et al*., 2010). Similar to selegiline, at high doses of rasagiline both MAO-A and MAO-B may be inhibited which increases the risk of the cheese reaction (Weinreb *et al*, 2010).

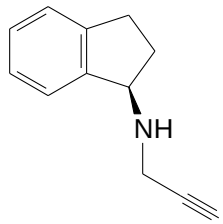

Figure 2-12 The structure of rasagiline

Mofegiline:

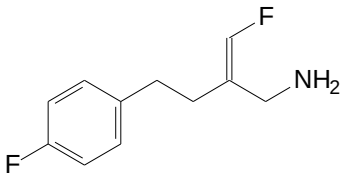

Figure 2-13 The structure of mofegiline

Mofegiline: Mofegiline is an irreversible and mechanism-based inhibitor of MAO-B (Zreika *et al.*, 1989). Mofegiline can also inhibit semicarbazide-sensitive amine oxidase (SSAO), although only the inhibition of MAO is clinically significant (Palfreyman *et al*., 1994). Mofegiline does not cause the cheese reaction (Hinze *et al*., 1994). Mofegiline has been discontinued and is not in clinical use (Bentue-Ferrer *et al*., 1996).

2.3.2.2 Reversible inhibitors of MAO-B

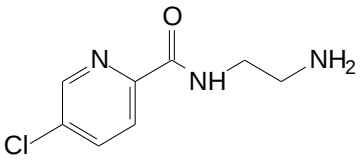

Figure 2-14 The structure of lazabemide

Lazabemide: Lazabemide is a derivative of moclobemide, a selective reversible MAO-A inhibitor (Da Prada *et al*., 1990). Lazabemide is a reversible inhibitor of MAO that is more selective towards MAO-B. Unlike selegiline, lazabemide does not contain a propargylamine group and is not metabolised to amphetamine. It also undergoes fast clearance once administration is

terminated (Lewitt *et al*., 1993). Doses of 100-350 mg twice a day inhibit platelet MAO-B for 16-36 hours (Guentert *et al*., 1994).

Safinamide: Safinamide is a recently discovered reversible MAO-B selective inhibitor. Safinamide also has dopamine modulator properties and cause a blockade of dopamine reuptake. Safinamide is a potent inhibitor of MAO-B with an IC_{50} of 0.08 μM (Caccia *et al*., 2006). According to X-ray crystallography studies, safinamide occupies both cavities of the MAO-B active site with the 3-fluorobenzyloxy moiety bound to the entrance cavity of the enzyme and the amide group bound to the substrate cavity. This cavity-spanning mode of binding is responsible for the high specificity of safinamide for MAO-B. The amide group of safinamide is orientated towards the flavin cofactor, but does not bind covalently to the FAD. Two hydrogen bonds form between the amide group of safinamide and the MAO-B enzyme, one with Gln206 and the other with a water molecule in the active site (Binda *et al*., 2007).

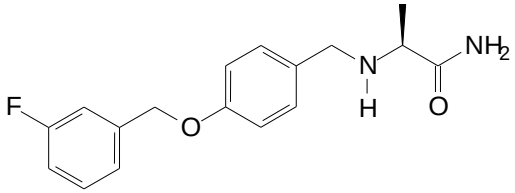

Figure 2-15 The structure of safinamide

2.3.3 The three-dimensional structure of MAO-B

MAO-B crystallises as a dimer while MAO-A crystallises as a monomer. The MAO-B enzyme consists of three domains: the flavin binding domain, the substrate binding domain and the membrane binding domain (Edmondson *et al*., 2004).The structure of MAO-B consists out of 520 amino acids arranged in a similar structure to that of MAO-A (Fraaije & Mattevi, 2000). The structure of MAO-B also closely resemble that of L-amino acid oxidase and polyamine oxidase (Binda *et al.*, 1999).

In the crystal structure of MAO-B, residues 461-520 are predicted to be the membrane-binding domain. (Edmondson *et al*., 2004). As in MAO-A, the 27-residue α-helix at the C-terminal is imbedded into the outer mitochondrial membrane and thus facilitates membrane attachment of MAO-B (Edmondson *et al*., 2004). The active site of MAO-B consists of two cavities, an entrance cavity and a larger substrate cavity. The entrance cavity has a volume of 290 $Å^3$ and the substrate cavity has a volume 420 $Å^3$. These substrate binding site connect via the entrance cavity to the opening of active site. A flexible loop is situated on the entry point of the cavities and is suggested to serve as a “gating switch” to the entrance cavity (Edmondson *et al*., 2004).

The substrate cavity is positioned in front of the flavin ring, and is the site where amine oxidation occurs (Binda *et al*, 2004).

In most crystal structures of MAO-B, the active site of MAO-B contains several active site water molecules. Two of these molecules can be found at the bottom of the substrate cavity in proximity to the FAD. Two other water molecules can be found on the lateral side of the cavity. These water molecules are an integral part of the binding site and interact with bound substrates and inhibitors (Binda *et al*, 2004).

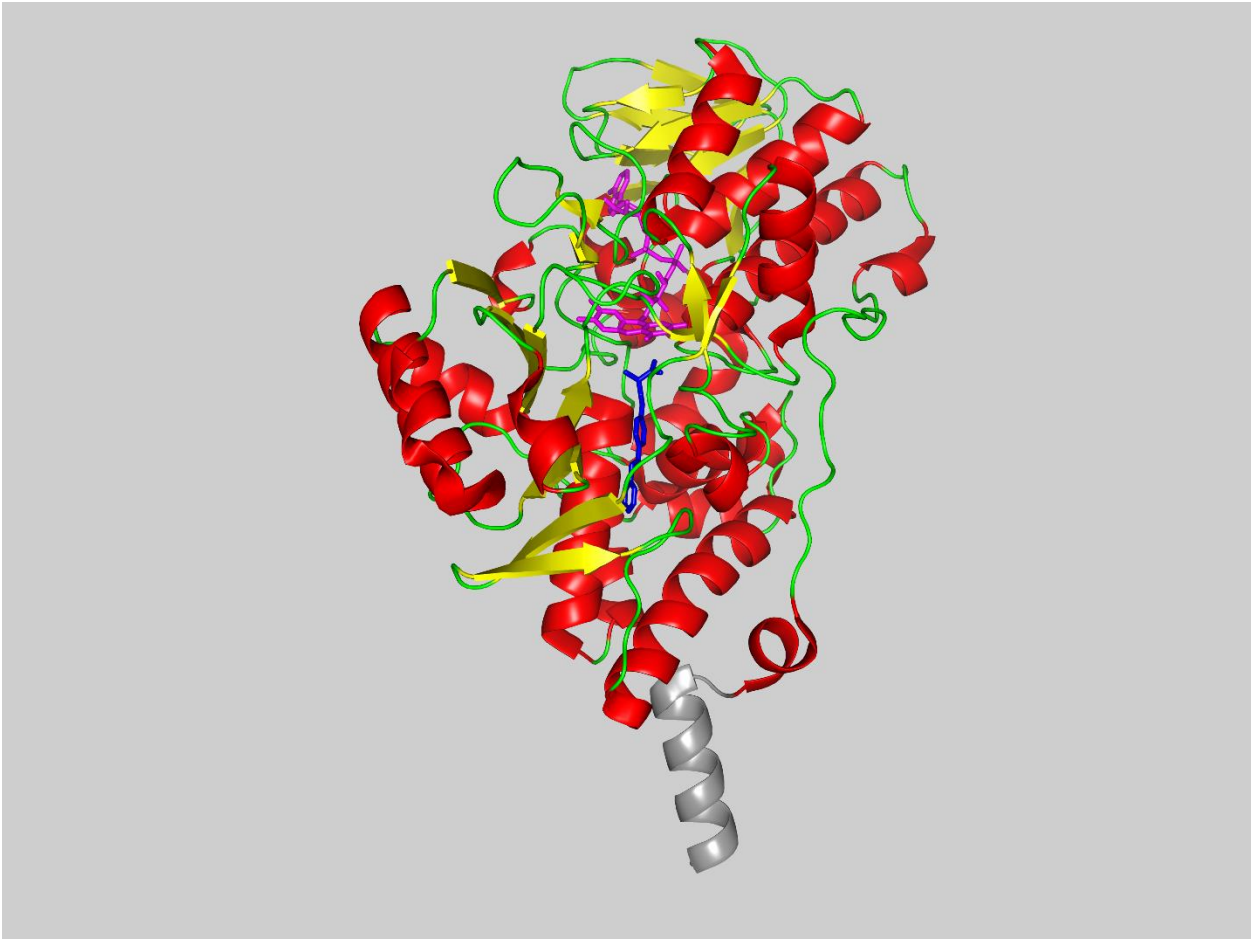

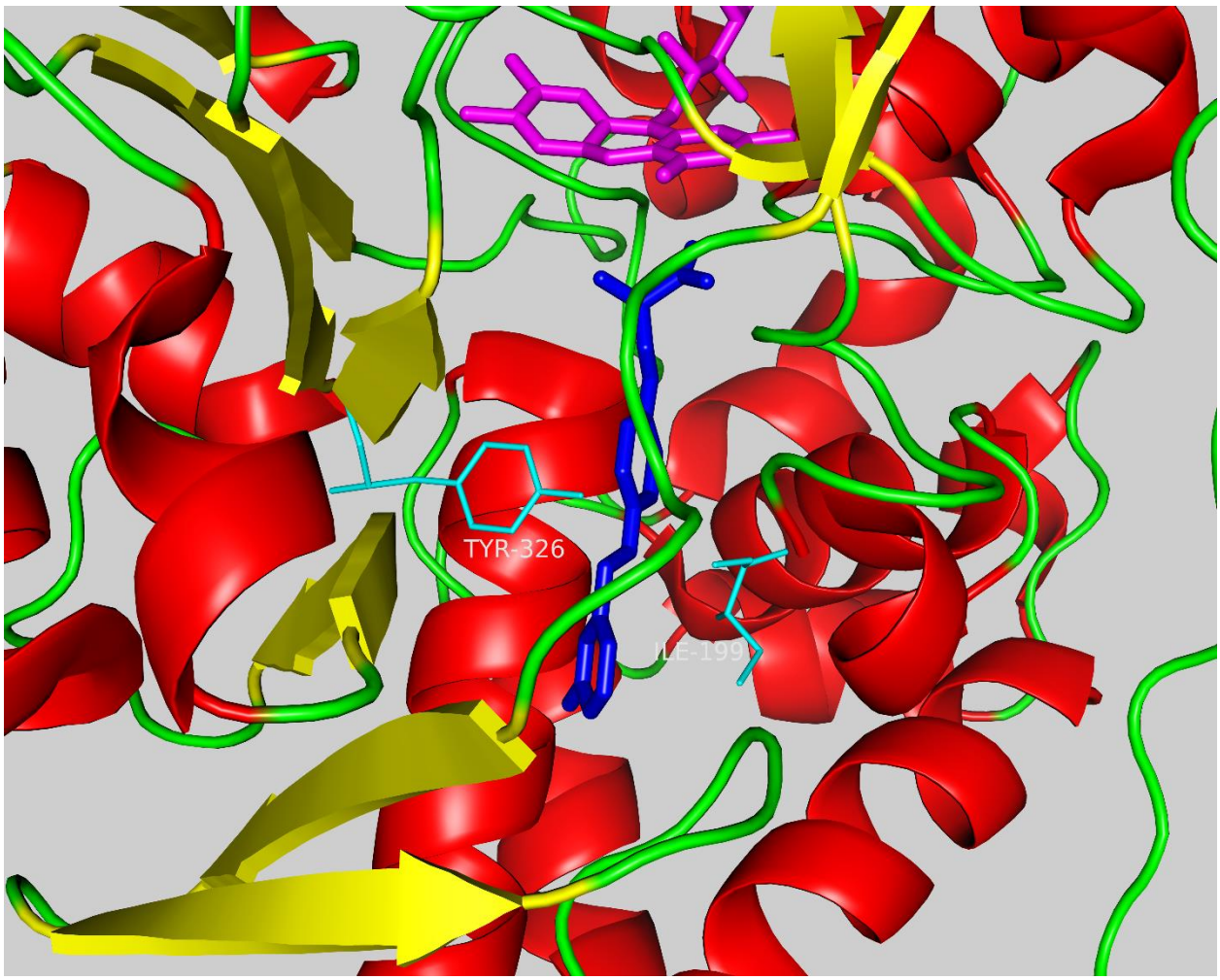

Figure 2-16 **The structure of MAO-B with the FAD cofactor shown in magenta and safinamide, the co-crystallized ligand, shown in blue. The α-helix at the C-terminal is shown in grey. In the bottom figure, the key residues Ile-199 and Tyr-326 are shown in cyan**

2.4 Role of MAO in neurodegenerative disorders

2.4.1 Parkinson's disease

2.4.1.1 General Background

PD occurs in approximately 0.3% of the overall population. The incidence of PD increases with age and is approximately 1% in the population older than 60, and approximately 4% in the population older than 80 (Agid, 1998). The most prominent pathological feature in PD is the loss of dopaminergic neurons in the SNpc. The loss of neurons in the SNpc leads to a DA deficiency in the striatum and is responsible for most of the symptoms of PD (Dauer & Przedborski, 2003). The motor symptoms of PD can thus be attributed to damage of the nigrostriatal pathway (Braak

et al., 2003). Another pathological characteristic of PD is the presence of Lewy bodies (LBs) in the affected brain regions (Burke, 1998). LBs mainly consists of an aggregated form of the protein, α-synuclein.

The most prominent clinical feature of PD is impaired motor function with bradykinesia (slowed body movements), rigidity, tremor and postural instability. At the onset of PD, the motor impairment is asymmetric, but becomes bilateral as the disease progresses (Jankovic, 2008). Since the motor symptoms such as akinesia, rigidity and tremor are the most debilitating aspects of PD, current treatment focuses on alleviating these symptoms. Dopaminergic treatment successfully reduces these symptoms (Pedrosa & Timmermann, 2013). Non-motor symptoms also occur with PD and include depression, sleep pattern changes, sensory abnormalities, autonomic dysfunction and cognitive changes (Langston, 2006).

1-Methyl-4-phenyl-1,2,3,6-tetrahydropyridine (MPTP) is a neurotoxin that also can cause parkinsonism in humans. MPTP selectively causes destruction of dopaminergic neurons in the substantia nigra of humans and animals, and can therefore be used to create animal models for testing PD drugs (Youdim & Bakhle, 2006). MAO-B is important to the action of MPTP since it catalyses the oxidation of MPTP to yield the active form, 1-methyl-4-phenylpyridinium (MPP^+). MPP^+ is toxic to dopaminergic neurons by inhibiting complex I of the mitochondrial electron transport chain, and thus causes a syndrome that is highly similar to PD. MAO-B inhibitors such as selegiline and rasagiline prevent the activation of MPTP and thus protect experimental animals against MPTP-induced neurotoxicity (Olanow *et al*., 1995).

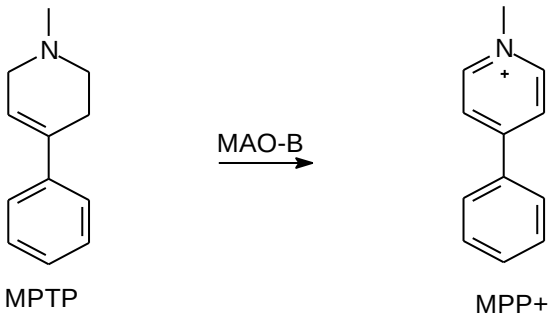

Figure 2-17 The MAO-B catalysed oxidation of MPTP to MPP^+

2.4.1.2 Drugs used in the symptomatic treatment of PD

The current treatment of PD is only symptomatic and does not slow down the degeneration of dopaminergic neurons (Dauer & Przedborski, 2003). The most effective symptomatic treatments are those that affect the dopaminergic system by either providing exogenous DA, increasing dopaminergic activity or decreasing DA catabolism (Robakis & Fahn, 2015). L-Dopa is the most

effective drug available for the treatment of PD and alleviates most of the motor symptoms and proves effective in nearly all patients (Hughes *et al*., 1992). Other drugs used in the therapy of PD include MAO inhibitors such as selegiline, DA receptor agonists (e.g. bromocriptine), amantadine, catechol-O-methyltransferase (COMT) inhibitors (e.g. entacapone) and anticholinergic drugs (e.g. benztropine) (Singh *et al*., 2007).

2.4.1.2.1 L-Dopa

L-Dopa was the first drug used in the treatment of PD in 1967 and it proved the most effective drug to date as it has been difficult to improve upon the effectiveness of L-dopa (LeWitt & Nyholm, 2004). After several years of treatment with L-dopa, patients develop dyskinesia, which are involuntary movements associated with long-term dopaminergic therapy (Dauer & Przedborski, 2003). Another disabling side effect of L-dopa is the unpredictable "on-off" phenomenon (Singh *et al*., 2007). To extend the efficacy of L-dopa, patients start with very low doses, which are eventually titrated up as higher doses are needed (Mercuri & Bernardi, 2005). L-Dopa is not effective in the treatment of the non-motor symptoms of PD such as dementia (Hubert *et al*., 2007).

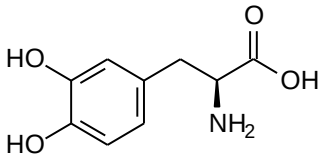

Figure 2-18 The structure of L-dopa

2.4.1.2.2 MAO inhibitors

As previously discussed, MAO inhibitors are used in the treatment of PD. MAO inhibitors can be used as monotherapy in the treatment of early PD or as adjunctive therapy in patients who are already receiving L-dopa but are experiencing motor fluctuations (Hubert *et al*., 2007). When used as monotherapy in the treatment of PD, MAO-B inhibitors may delay the introduction of L-dopa by 9 months (Lees, 2005). Later in the disease MAO-B inhibitors are used in combination with L-dopa to enhance the dopaminergic effects of L-dopa (Singh *et al*., 2007). Potential neuroprotective properties of MAO inhibitors in PD will be discussed later in this chapter.

2.4.1.2.3 COMT inhibitors

COMT inhibitors can be used as adjunct therapy to L-dopa in PD, and is particularly effective in decreasing the motor fluctuations caused by L-dopa. COMT inhibitors also allow for a reduction

in L-dopa dose, and in this manner further reduces the occurrence of the adverse effects of L-dopa (Olanow *et al*., 2001).

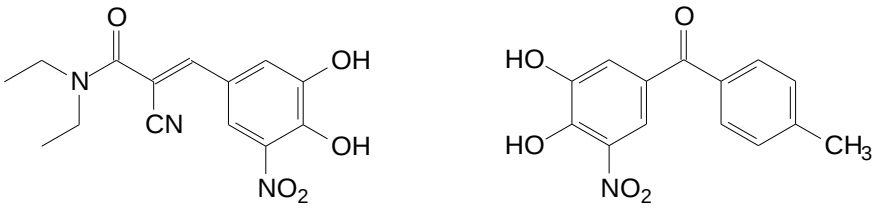

Entacapone Tolcapone

Figure 2-19 Structures of COMT inhibitors, entacapone and tolcapone.

Tolcapone, a nitrocatechol inhibitor of COMT, is effective in the treatment of motor symptoms (Rajput *et al*., 1997) but the side effects such as hepatotoxicity can be serious (Assal *et al*., 1998). Other side effects include sleep disturbances such as insomnia, dyskinesias, hypotension and confusion (Singh *et al*., 2007). Entacapone is less potent as a COMT inhibitor compared to tolcapone, but is free from hepatotoxicity and is thus more frequently used in the treatment of PD.

2.4.1.2.4 DA receptor agonists

DA agonists are effective drugs used in the treatment of PD, either as monotherapy in early PD or as adjunct therapy to L-dopa. DA agonists have a longer half-life than L-dopa and thus provide more sustained dopaminergic stimulation at DA receptors in the striatum (Olanow *et al*., 2001).

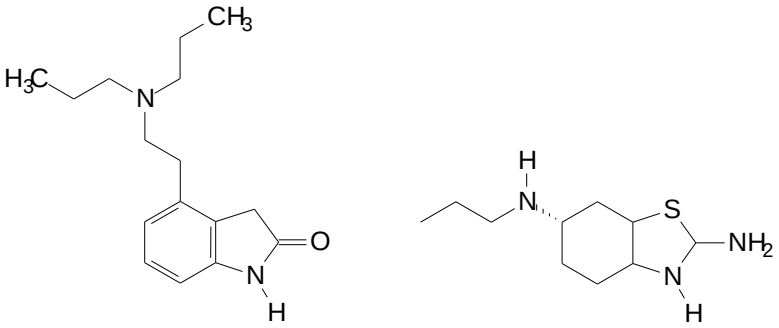

Ropinirole Pramipexole

Figure 2-20 Examples of dopamine agonists, ropinirole and pramipexole

Although DA agonists can delay L-dopa induced motor fluctuations, DA agonists are less potent and not effective in the treatment of all PD symptoms. DA agonists can also cause severe adverse effects such as hallucinations and psychosis (Shapiro *et al*., 2007). DA agonists can be used as monotherapy in newly diagnosed patients but eventually L-dopa will have to be added to the treatment regime (Silver & Ruggieri, 1998).

2.4.1.2.5 Anticholinergic Drugs

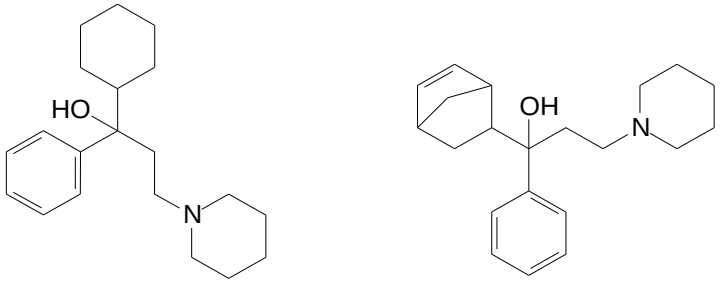

Trihexyphenidal Biperiden

Figure 2-21 Examples of anticholinergic drugs, trihexyphenidyl and biperiden

Anticholinergics are highly effective for the treatment of tremors in PD, but have little effect on reducing bradikinesia or akinesia (Comella & Tanner, 1995). Adverse effects such as hallucinations, confusion and drowsiness limit the dosing of anticholinergic drugs (Katzung, 2001).

2.4.1.2.6 Amantadine

Amantadine is an antiviral drug that can be used to treat PD. It is most effective in the treatment of dyskinesias and it is suggested that amantadine acts in this respect as an antiglutamatergic agent (Stoof *et al*., 1992). The exact mechanism by which amantadine is effective in PD is still unknown but adverse effects such as cardiovascular side-effects make the drug intolerable, especially for elderly patients (Katzung, 2001).

2.4.1.3 The role of MAO in PD

MAO-B levels increase with age in the human brain, while DA levels in the basal ganglia decrease (Kumar *et al*., 2003). An increase in MAO activity leads to an increase in oxidative stress since MAO produces hydrogen peroxide as by-product of catalysis. The increased oxidative stress associated with MAO activity in the brain, in turn, contribute to the vulnerability

of neuronal tissue to neurodegeneration in PD (Cohen, 1990). Because the MAO-catalysed formation of hydrogen peroxide may be increase in the aged parkinsonian brain, it has been suggested that MAO inhibitors may be useful as potential neuroprotective agents in the treatment of neurodegenerative diseases (Youdim *et al*., 2006). In this respect, MAO-B inhibitors may reduce the formation of hydrogen peroxide in the brain and thus reduce oxidative damage and neurodegeneration.

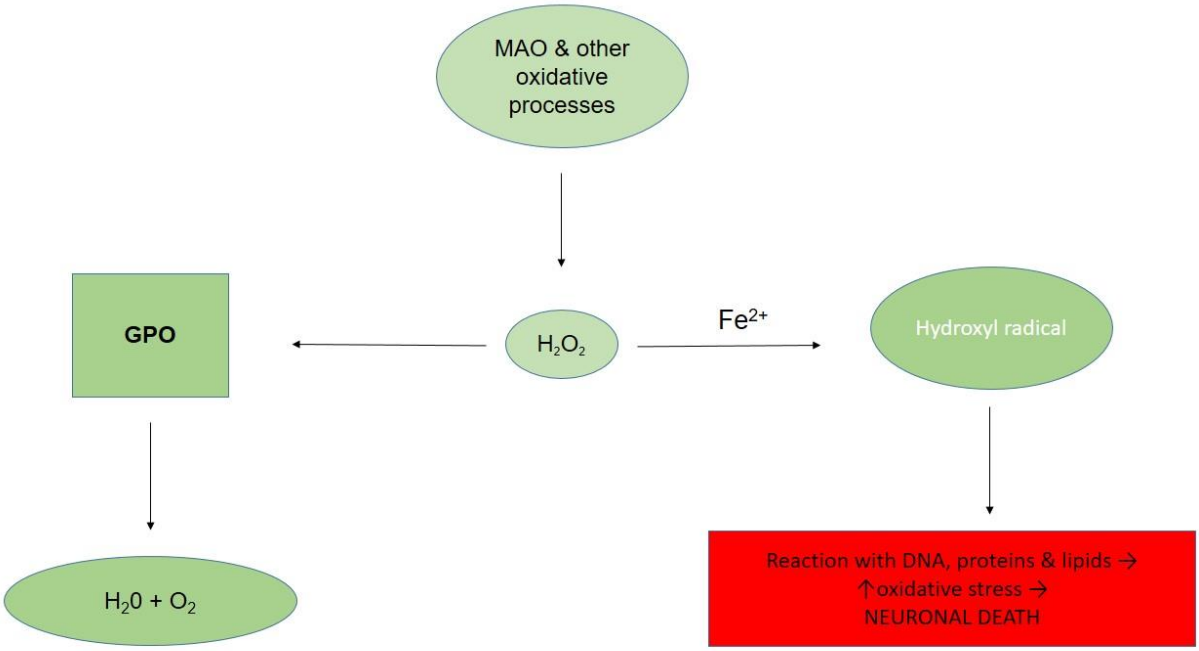

Figure 2-22 **The formation of hydrogen peroxide from MAO and subsequent oxidative damage initiated by hydrogen peroxide (Youdim & Bakhle, 2006)**

As mentioned, increased MAO activity in PD leads to higher hydrogen peroxide levels in the brain (Mandel *et al.*, 2005). Hydrogen peroxide is normally inactivated by glutathione peroxidase with glutathione serving as cofactor for this reaction. In PD, glutathione levels are however low and therefore hydrogen peroxide may accumulate in the brain (Riederer *et al.,* 1989). Hydrogen peroxide is subsequently available for the Fenton reaction, in which it reacts with iron to generate the hydroxyl radical. The hydroxyl radical is a highly reactive free radical that depletes cellular anti-oxidants, and reacts with lipids, proteins and DNA to contribute to further neuronal damage (Youdim & Bakhle, 2006).

A second role for MAO-B inhibitors in PD is to preserve the central DA supply. In PD, MAO-B inhibitors block the MAO-B-catalysed metabolism of DA in the brain and thus enhance dopaminergic neurotransmission. This provides relief of the motor symptoms of PD. MAO-B

inhibitors are frequently combined with L-dopa in PD therapy. MAO-B inhibitors enhances DA levels in the brain derived from L-dopa and allows for a reduction of the effective L-dopa dose.

2.4.1.4 Neuroprotection in PD

Currently there are two MAO-B selective inhibitors for use in PD, rasagiline and selegiline (Youdim *et al*., 2001). Rasagiline and selegiline are propargylamines that, after activation by the MAO enzyme, bind covalently to the flavin cofactor. These inhibitors are mechanism-based or suicide inhibitors. *De novo* synthesis of the MAO protein is the only way in which MAO activity can be restored (Youdim, 1978). Both drugs are thought to possess neuroprotective properties although rasagiline is a more potent MAO-B inhibitor than selegiline (Mandel *et al.*, 2005). The principal metabolite of rasagiline, 1-(R)-aminoindan, also exhibits neuroprotective properties and may contribute to the neuroprotective effects of rasagiline (Weinreb *et al*., 2010). As mentioned, MAO-B inhibitors are considered to be neuroprotective drugs in the treatment of PD as they lower hydrogen peroxide and aldehyde levels in the brain (Youdim & Bakhle, 2006).

More cases of PD are recorded in metamphetamine addicts and thus either the drug or the metabolites are neurotoxic (Callaghan *et al*., 2012). Selegiline is metabolised to R-metamphetamine, which may compromise the putative neuroprotective effects of selegiline (Bar Am *et al.,* 2004). Nicotine also may have neuroprotective properties and studies have shown a lower incidence of PD with regular nicotine consumption (Quik, 2004). Nicotine was also shown to protect against the neurotoxic action of MPTP in both mice and non-human primates, as well as to improve motor function (Quik *et al*., 2007).

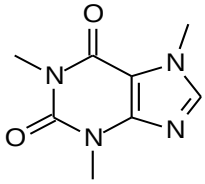

Figure 2-23 The structure of caffeine

Research has shown that the intake of caffeine reduces the risk of developing PD (Meissner *et al*., 2011; Prediger, 2010). Caffeine antagonises both the A_1 and A_2 adenosine receptors (Meissner *et al*., 2011), but it is the antagonism of the A_{2A} receptor that is considered important in PD (Postuma *et al*., 2012). The human striatum contains high concentrations of A_{2A} receptors and antagonism of these receptors not only may be neuroprotective in preventing neurodegeneration in PD, but also enhance dopaminergic neurotransmission to alleviate the

motor symptoms in PD (Xu *et al.,* 2005). A lesser known effect of caffeine is low potency inhibition of MAO-A and MAO-B. Whether the inhibition of MAO by caffeine contributes to its observed neuroprotective effects is still unclear.

2.4.2 Depression

2.4.2.1 The role of MAO in depression

The monoamine hypothesis states that a decrease or imbalance of monoamine neurotransmitters in the brain is responsible for the symptoms of depression. Decreased levels of specifically 5-HT, NE and DA are hypothesised to be the cause of the symptoms characterised as depression (Stahl, 2008). All the current treatments for depression focus on increasing the levels of 5-HT, NE and DA, either by blocking the reuptake systems or by inhibiting the enzymes responsible for the breakdown of these monoamine neurotransmitters (Lum & Stahl, 2012).

Recent studies have shown that the central levels of MAO-A may be higher in patients with depression compared to normal subjects, which implies that overactive MAO-A activity may be the cause of many subtypes of depression (Meyer *et al*., 2006). MAO metabolises all three neurotransmitters implicated in the symptoms of depression (Lum & Stahl, 2012). To further support the role of MAO-A in depression, studies have shown that patients with depression who were treated with selective serotonin reuptake inhibitors (SSRIs), have higher levels of MAO-A than untreated depressed patients and patients in remission (Ioannidis, 2008).

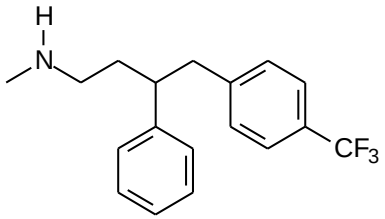

Figure 2-24 The structure of fluoxetine, a well-known SSRI

It has been proposed that even though SSRIs increase the levels of 5-HT in synapses, 5-HT levels will remain low because of the high levels of MAO-A (Lum & Stahl, 2012). MAO inhibitors may thus be useful in the treatment in depression by lowering MAO activity and thus increasing the levels of monoamine neurotransmitters in synapses (Lum & Stahl, 2012).

2.4.2.2 Treatment of depression with RIMAs

The antidepressant effects of MAO inhibitors were first discovered in the 1950's but because of adverse effects, most notably the cheese reaction, these drugs fell out of favour with clinicians (Yamada & Yashuhara, 2004). Moclobemide, however, proved to be effective for the treatment of major depression without causing this serious adverse effect (Amrein *et al*., 1993; Tiller, 1993). RIMAs can be used in the treatment of depression, and block the metabolism of neurotransmitters rather than targeting reuptake of neurotransmitters (Meyer *et al*., 2006). RIMAs have the advantage over irreversible inhibitors by displaying better safety profiles, particularly with respect to the cheese reaction (Lum & Stahl, 2012).

2.4.3 Alzheimer's disease

Age is the most important risk factor in developing AD (von Strauss *et al*., 1999). AD is recognised as a progressive cognitive decline. Other neuropsychiatric symptoms can include depression, anxiety and psychosis (Garcia-Alberca *et al*., 2008).

The aetiology of AD is still uncertain but studies suggest multiple causes such as genetic factors (e.g. mutations of susceptible genes) as well as environmental factors (Yokel *et al*., 2000). Oxidative damage by reactive oxygen species (ROS) also play a prominent role in the pathology of AD (Christen, 2000). ROS causes cellular and tissue degeneration when the cell buffering systems responsible for clearing ROS are deficient (Christen, 2000). Oxidative stress is suggested to play a role in AD as neurons are more susceptible to damage by ROS (Cooper, 1997). As mentioned, MAO produces hydrogen peroxide as a by-product in the metabolism of amines (Weyler *et al*., 1990). Hydrogen peroxide produced by MAO may thus contribute to oxidative stress in AD (Ciccone, 1998; Gotz *et al*., 1994; Riederer & Youdim, 1993). Furthermore, MAO-B activity increases with age and MAO-B activity is reported to be high in senile plaques in AD. By reducing MAO-catalysed hydrogen peroxide formation, selegiline or rasagiline may therefore suppress the progression of AD (Knoll, 2000; Thomas, 2000). Moclobemide has also been reported to be effective in AD and there is evidence of cognition-enhancing effects with the use of this drug (Amrein *et al*., 1993).

2.5 Copper containing amine oxidase

Two groups of amine oxidase (AO) have been identified and are divided according to the cofactor attached to the enzyme. MAO-A, MAO-B and polyamine oxidases contain FAD as a cofactor and are classified as the first class (Shih *et al*., 1999). The other class contains enzymes such as diamine oxidases and lysyl oxidase which possess a cofactor that contains one or more carbonyl groups, usually topa-quinone (TPQ) (Klinman & Mu, 1994; Klinman, 1996; Lyles, 1996). The second class are known as SSAOs (Shih *et al*., 1999).

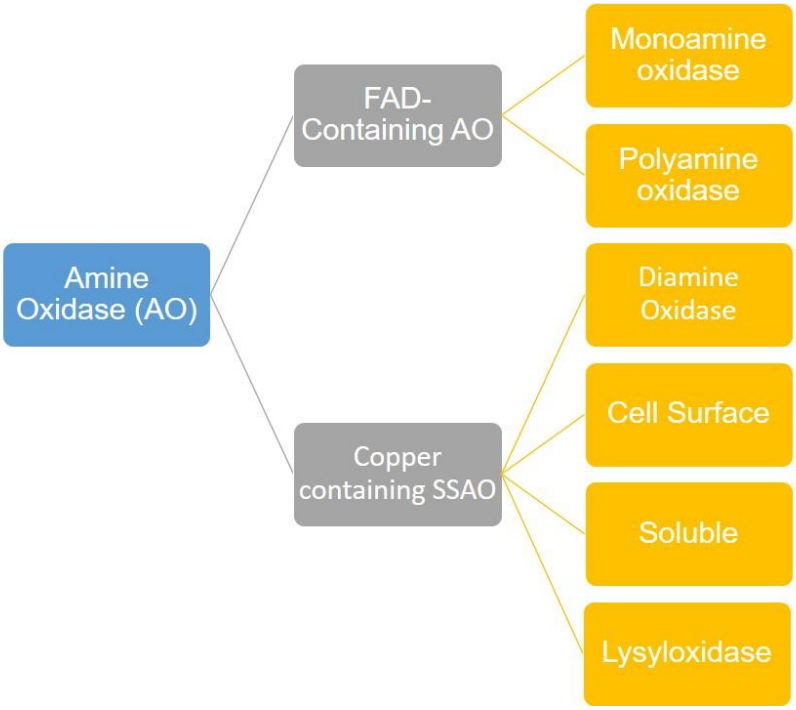

Figure 2-25 Summary of the amine oxidase classification (adapted from Jalkanen & Salmi, 2001)

These two classes differ in distribution, substrates they metabolise, inhibitor specificity and biological function (Shih *et al*., 1999). MAO metabolises neurotransmitters while polyamine oxidase metabolises spermine and spermidine, and is therefore essential for cell growth (Seiler, 1990). TPQ-containing diamine oxidase metabolises diamines and histamine and is therefore essential in inflammation and allergic reactions (Buffoni, 1966; Robinson-White *et al*., 1985; Barbry *et al*., 1990). SSAOs metabolise different substrates than MAO, and are weakly or totally insensitive to MAO inhibitors (Lyles, 1996). SSAOs are defined as enzymes that are inhibited by carbonyl-reactive compounds such as semicarbazide (Tabor *et al*., 1954). Semicarbazide is the most selective and potent SSAO inhibitor. Other non-specific inhibitors include propargylamine, aminoguanidine, carbidopa and procarbazine (Jalkanen & Salmi, 2001).

2.6 Summary of this chapter

Two isoforms of MAO exist namely MAO-A and MAO-B. These enzymes differ in tissue distribution, substrate and inhibitor specificities, and their physiological actions. MAO activity produces hydrogen peroxide as by-product which may contribute to neurodegeneration in progressive neurodegenerative diseases such as PD and AD. Since MAO also metabolises dopamine, they play prominent roles in disorders such as depression and PD where DA levels are deficient. Inhibitors of MAO-B such as selegiline and rasagiline are effective in the treatment of PD and may also be neuroprotective. Non-selective irreversible MAO inhibitors and selective irreversible inhibitors of MAO-A may cause the cheese reaction, which is a potentially fatal hypertensive crisis when these drugs are ingested with tyramine containing food. RIMAs do not cause the cheese reaction and are safer alternatives to irreversible MAO-A inhibitors. MAO-A inhibitors are important drugs for the treatment of depression. New MAO inhibitors that are highly potent and selective are expected to exhibit less adverse effects and may be of enhanced value in the treatment of neurodegenerative disorders.

CHAPTER 3: CHEMICAL SYNTHESIS OF THE TARGET 1-BENZOSUBERONE DERIVATIVES

3.1 Introduction

In this study 1-benzosuberone and derivatives of 1-benzosuberone will be evaluated as potential inhibitors of MAO-A and MAO-B. This chapter describes the syntheses and characterisations of four 1-benzosuberone derivatives. Compounds containing a benzosuberone structure have been reported to possess a broad-spectrum of biological properties such as anti-pyretic, anti-ulcer, CNS stimulation and depression, and anti-cancer activities (Sajja *et al*., 2016). 1-Benzosuberone and 1-benzosuberone derivatives have not yet been evaluated as potential MAO inhibitors, and it is in this regard that this study will contribute. The structure of 1-benzosuberone resembles the structure of rasagiline, a well-known MAO-B inhibitor, and 1-benzosuberone derivatives may therefore also possess MAO inhibition activity. Rasagiline is an irreversible and specific MAO-B inhibitor, and possesses the propargylamine functional group. Propargylamine compounds are classified as mechanism-based inhibitors and are activated by MAO to form irreversible adducts with the enzyme. 1-Benzosuberone and the 1-benzosuberone derivatives, however, do not possess functional groups that are associated with irreversible MAO inhibition, and it is therefore anticipated that the study compounds will interact reversibly with MAO should inhibition be observed. As discussed, 1-benzosuberone also bear structural resemblance to 1-tetralone, which is reported to be a moderately potent and nonspecific MAO inhibitor (Legoabe *et al*., 2014).The structures of the 1-benzosuberone derivatives that were synthesised in this study are shown in table 3.1. As will be discussed, difficulties with the chemical syntheses of the 1-benzosuberone derivatives limited the number of derivatives that could be successfully synthesised in this study.

Table 3-1 The structures of 1-benzosuberone and the 1-benzosuberone derivatives that were synthesised

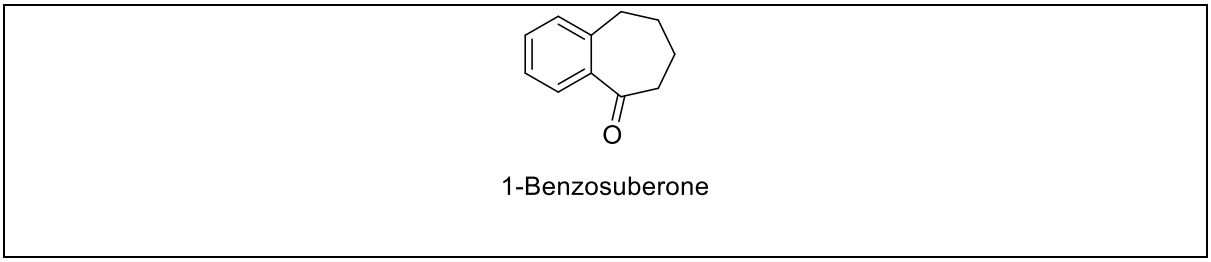

1-Benzosuberone

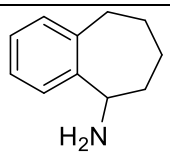 **1a**	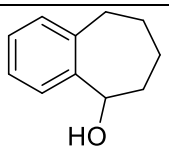 **1b**
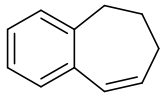 **1c**	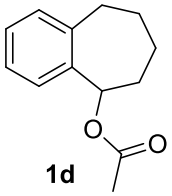 **1d**

3.2 Materials and instrumentation

Materials

In this study all reagents and solvents was obtained from Sigma-Aldrich. No further purification of the reagents were necessary.

Thin layer chromatography (TLC)

Progress of reactions was monitored by TLC employing silica gel sheets with UV_{254} fluorescent indicator. A mixture of ethyl acetate and petroleum ether in a ratio of 1:1 was used as mobile phase. A UV light with a wavelength of 254 nm was used to examine the TLC sheets in order to visualise the migrated compounds.

Melting points

A Büchi B-545 melting point apparatus was used to determine melting points, which are given uncorrected.

Mass spectrometry (MS)

To determine the high resolution mass spectra (HRMS) and the nominal mass spectra (MS) of the 1-benzosuberone derivatives, a Burker micrOTOF-Q II mass spectrometer functioning in atmospheric-pressure chemical ionisation (APCI) mode was used to determine the mass spectra of the synthesised compounds.

Nuclear magnetic resonance (NMR)

To record proton (^{1}H) and carbon (^{13}C) NMR spectra, a Bruker Avance III 600 spectrometer was used. ^{1}H NMR was recorded at 600 MHz while ^{13}C NMR was recorded at 150 MHz. Deuterated chloroform ($CDCl_3$) served as NMR solvent and chemical shifts are reported in parts per million (δ), and were referenced to the residual solvent signal.

High pressure liquid chromatography (HPLC)

The degree of purity of the 1-benzosuberone derivatives was determined by HPLC. For this purpose, HPLC grade acetonitrile (Merck) and Milli-Q water (Millipore) were used to prepare the mobile phase. An Agilent 1100 HPLC system equipped with a quaternary pump and a diode array detector served as chromatographic system. Separation was carried out with a Venusil XBP C18 column (4.60 x 150 mm, 5 µm) and the mobile phase consisted at the start of each run of acetonitrile 30% and Milli-Q water 70%. The flow rate was set to 1 ml/min. After each run was started, a solvent gradient program was initiated and the composition of acetonitrile in the mobile phase was increased linearly to 80% over a period of 5 min. Each run lasted 15 min, with a 5 min equilibration period between runs. 20 µl of each test compound, dissolved in acetonitrile (1 mM), was injected into the HPLC system and the eluent was monitored at a wavelength of 254 nm.

3.3 Methods for synthesis of 1-benzosuberone derivatives 1a-d

3.3.1 Synthesis of 6,7,8,9-tetrahydro-5*H*-benzo[7]annulen-5-amine (1a)

1-Benzosuberone (10 mmol) was dissolved in formamide (20 ml) and formic acid (10 ml) in a round-bottom flask. The solution was heated under reflux for 1 h at 210 °C to obtain a light yellow solution. The solution was cooled to ambient temperature and quenched with the addition of distilled water (30 ml). The mixture was extracted to diethyl ether (3 x 30 ml), the combined organic phases were washed with brine and dried over anhydrous $MgSO_4$. The organic phase was evaporated under reduced pressure.

30 ml hydrochloric acid (33%) was added to the crude product from the first step and the resulting solution was heated under reflux for 2 h at 120 °C. The solution was quenched with the addition of water (20 ml) and cooled to ambient temperature. An aqueous solution of sodium hydroxide (33%) was added to adjust the pH to 10. The mixture was extracted to diethyl ether (3 x 30 ml), the combined organic phases were washed with brine and dried over anhydrous $MgSO_4$. The organic phase was evaporated under reduced pressure to obtain a light yellow oil. The product was purified by distillation followed by column chromatography. Distillation was

carried out under reduced pressure using a quick-distillation setup (Aldrich). The distillate was further purified by silica gel column chromatography using ethyl acetate as mobile phase.

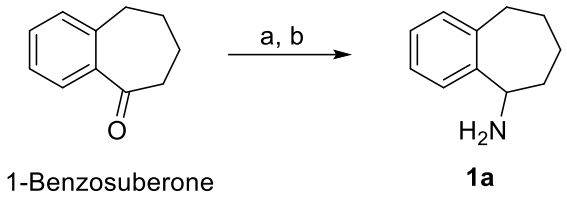

Figure 3-1 Reaction pathway for the synthesis of 1a. Key: (a) formamide, formic acid, 210 °C, 1 h. (b) HCl, reflux, 2 h.

3.3.2 Synthesis of 6,7,8,9-tertahydro-5*H*-benzo[7]annulen-5-ol (1b)

1-Benzosuberone (7 mmol) was dissolved in methanol (20 ml) in a round bottom flask and cooled to 0 °C in an ice bath. Sodium borohydride (14 mmol) was added portion-wise to the reaction. The reaction was stirred at room temperature for 6 h, and the solvent was evaporated under reduced pressure. The reaction was subsequently quenched with the addition of water (20 ml) and extracted to dichloromethane (3 x 30 ml). The combined organic phases were washed with brine and dried over $MgSO_4$. After the organic phase was evaporated under reduced pressure, the crude product was purified by recrystallisation from cyclohexane.

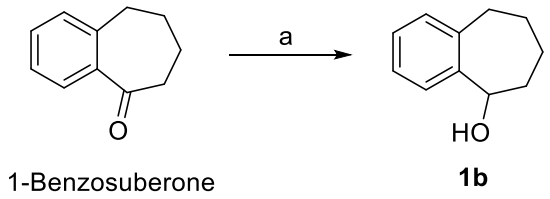

Figure 3-2 Reaction pathway for the synthesis of 1b. Key: (a) $NaBH_4$, methanol, 6 h.

3.3.3 Synthesis of 6,7-dihydro-5*H*-benzo[7]annulene (1c)

Alcohol derivative **1b** (1.5 mmol) and p-tolenesulfonic acid (5 mg) was dissolved in 100 ml benzene in a round bottom flask and heated under reflux with the azeotropic removal of water. For this purpose the Dean-Stark reaction setup was employed. TLC was used to monitor the

progress of the reaction. After 24 h the reaction was complete. The reaction was washed with 50 ml of an aqueous solution of sodium carbonate (5%) and dried over anhydrous $MgSO_4$. The organic phase was evaporated under reduced pressure and the crude product was purified with silica gel column chromatography with petroleum ether as mobile phase.

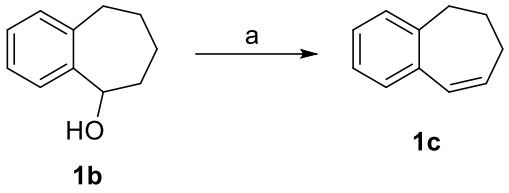

Figure 3-3 **Reaction pathway for the synthesis of 1c. Key: (a) Dean-Stark, benzene, p-tolenesulfonic acid, 24 h.**

3.3.4 Synthesis of 6,7,8,9-tetrahydro-5*H*-benzo[7]annulen-5-yl acetate (1d)

A mixture of alcohol derivative **1b** (1.4 mmol), acetic anhydride (0.2 ml), trimethylamine (0.23 ml) and N,N-dimethylaminopyridine (0.017 g) in a round-bottom flask was stirred for 24 h at room temperature. After 24 h the reaction was not complete as indicated by TLC and further portions of acetic anhydride (0.2 ml), trimethylamine (0.23 ml) and N,N-dimethylaminopyridine (0.017 g) were added, and stirring was continued for another 24 h. TLC indicated that the reaction was complete and methanol (20 ml) was added to the reaction. The reaction was subsequently evaporated under reduced pressure and distilled water (30 ml) was added. The mixture was extracted to ethyl acetate (3 x 30 ml) and the combined organic fractions were washed with brine and dried over anhydrous $MgSO_4$. The organic phase was evaporated under reduced pressure and the crude was purified by silica gel column chromatography using petroleum ether as mobile phase.

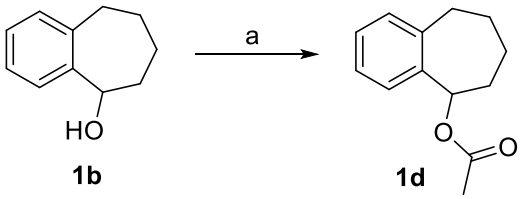

Figure 3-4 **Reaction pathway for the synthesis of 1d. Key: (a) acetic anhydride, triethylamine, N,N-dimethylaminopyridine, 24 h.**

3.4 Physical characterisation

This section provides the characterisation of the synthesised 1-benzosuberone derivatives. ^{1}H and ^{13}C NMR spectra as well as mass spectrometry was used to determine and verify the structures of the derivatives. Melting points were recorded where the products were solids at room temperature. HPLC was used to determine the purity of the compounds, while TLC was used to monitor the progress of the reactions and to obtain an estimate of product purity. For TLC the retention factors (R_f values) are listed.

3.4.1 Interpretation of NMR spectra

NMR spectra for compounds are given in Annexure A. MS spectra are given in Annexure B. HPLC traces are given in Annexure C.

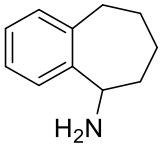 **1a**	**Melting point**: Oil **Purity**: 97.6% **R_f**: 0.13 **Yield (final step)**: 31%
^{1}H NMR:	**^{13}C NMR:**
^{1}H NMR (600 MHz, Chloroform-*d*) δ 7.40 (d, *J* = 7.6 Hz, 1H), 7.19 (td, *J* = 7.5, 1.6 Hz, 1H), 7.11 (td, *J* = 7.3, 1.4 Hz, 1H), 7.08 (dd, *J* = 7.4, 1.5 Hz, 1H), 4.20 (dd, *J* = 9.2, 1.7 Hz, 1H), 2.90 – 2.74 (m, 2H), 2.02 – 1.90 (m, 1H), 1.89 – 1.74 (m, 3H), 1.63 – 1.50 (m, 1H), 1.49 – 1.35 (m, 1H).	^{13}C NMR (151 MHz, $CDCl_3$) δ 145.59, 141.36, 129.39, 126.30, 126.10, 124.04, 54.69, 37.16, 35.77, 28.80, 27.50.
APCI-HRMS m/z calcd for $C_{11}H_{16}N$ (MH^+), 162.1277, found 162.1270	

On the ^{13}C NMR spectrum of **1a**, 6 signals are observed in the aromatic region (δ>110 ppm) which corresponds to the 6 types of aromatic C atoms of this compound. In the aliphatic region (δ<76 ppm), 5 signals are observed, which correspond to the five aliphatic carbons of this compound, including the carbon alpha of the secondary amine. The absence of a signal for a carbonyl carbon indicates the successful transformation of the carbonyl to the amine. On the ^{1}H NMR spectrum, the aromatic protons (δ>6 ppm) integrate for 4 protons as expected for this compound. Unfortunately the multiplets for aromatic protons are not clearly seen. The four CH_2

groups of the aliphatic ring are observed as multiplets at 2.90–1.35 ppm (8H), while the aliphatic proton at C1 of the ring corresponds to the doublet of doublets at 4.20 ppm (1H). The multiplicity of signal is the result of coupling with two protons on C2, which are not equivalent due to the chiral center at C1. Since this compound is chiral and represents two enantiomers, the multiplicities of the aliphatic signals is rather complex, indicating non-equivalence of protons attached to the same carbons and complex splitting patterns.

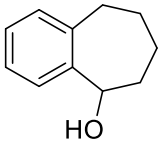 **1b**	**Melting point**: 101.3-103.1 °C **Purity**: 100% **R_f**: 0.51 **Yield (final step)**: 92%
^{1}H NMR:	**^{13}C NMR:**
^{1}H NMR (600 MHz, Chloroform-*d*) δ 7.36 (d, *J* = 7.5 Hz, 1H), 7.13 (td, *J* = 7.5, 1.5 Hz, 1H), 7.08 (td, *J* = 7.4, 1.5 Hz, 1H), 7.02 (dd, *J* = 7.4, 1.4 Hz, 1H), 4.90 – 4.80 (m, 1H), 2.84 (dd, *J* = 14.3, 8.3 Hz, 1H), 2.64 (ddd, *J* = 14.3, 10.6, 1.7 Hz, 1H), 2.04 – 1.93 (m, 1H), 1.92 – 1.78 (m, 2H), 1.77 – 1.63 (m, 3H), 1.46 – 1.32 (m, 1H).	^{13}C NMR (151 MHz, $CDCl_3$) δ 144.27, 140.80, 129.50, 126.98, 126.11, 124.59, 74.00, 36.60, 35.76, 27.82, 27.62.
APCI-HRMS m/z calcd for $C_{11}H_{13}O$ (M^+–H), 161.0961, found 161.0983	

On the ^{13}C NMR spectrum of **1b**, 6 signals are observed in the aromatic region (δ>110 ppm) which correspond to the 6 carbon atoms of the phenyl ring. In the aliphatic region (δ<76 ppm), 5 signals are observed, which corresponds to the five aliphatic carbons, including the carbon alpha of the secondary alcohol. As with the amine compound **1a**, the absence of a signal for a carbonyl carbon indicates the successful reduction of the carbonyl to the alcohol. On the ^{1}H NMR spectrum, the aromatic protons (δ>6 ppm) integrate for 4 protons as expected for this compound. All four signals are complex and include a doublet, a doublet of doublets and triplet of doublets. This complexity is due to *meta* coupling of the protons of the phenyl ring. The four CH_2 groups of the aliphatic ring are observed as multiplets at 2.84–1.32 ppm (9H). The additional proton observed may be from the OH. The aliphatic proton at C1 of the ring corresponds to the multiplet at 4.90–4.80 ppm (1H). The multiplicity of signal is the result of

coupling with two protons on C2, which are not equivalent due to the chiral center at C1. This compound is also chiral and represents two enantiomers. As with the amine compound **1a**, the multiplicities of the aliphatic signals is rather complex, indicating non-equivalence of protons attached to the same carbons and complex splitting patterns.

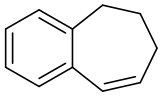 **1c**	**Melting point**: Oil **Purity**: 91.2% **R_f**: 0.66 **Yield (final step)**: 56%
^{1}H NMR:	**^{13}C NMR:**
^{1}H NMR (600 MHz, Chloroform-*d*) δ 7.10 – 7.04 (m, 2H), 7.03 – 6.98 (m, 2H), 6.32 (dt, *J* = 12.3, 2.1 Hz, 1H), 5.81 (dt, *J* = 12.2, 4.5 Hz, 1H), 2.82 – 2.71 (m, 2H), 2.34 (tdd, *J* = 6.6, 4.4, 2.1 Hz, 2H), 1.94 – 1.81 (m, 2H).	^{13}C NMR (151 MHz, $CDCl_3$) δ 141.71, 136.31, 132.30, 130.88, 129.82, 129.00, 126.60, 125.89, 36.17, 32.55, 26.97.
APCI-HRMS m/z calcd for $C_{11}H_{13}$ (MH^+), 145.1012, found 145.1000	

On the ^{13}C NMR spectrum of **1c**, 8 signals are observed in the aromatic region (δ>110 ppm) which correspond to the 6 types of aromatic C atoms of phenyl ring and the 2 vinilyc carbons. In the aliphatic region (δ<76 ppm), 3 signals are observed, which corresponds to the three aliphatic carbons of this compound. On the ^{1}H NMR spectrum, the aromatic protons (δ>6 ppm) of the fused phenyl ring are represented by two multiplets at 7.10–6.98 ppm which integrate for 2 protons each. The protons of the vinilyc groups are represented by the signals at 6.32 and 5.81 ppm, each integrating for 1 proton. The three CH_2 groups of the aliphatic ring are observed as signals at 2.34–1.81 ppm (6H).

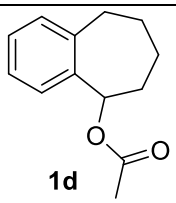 **1d**	**Melting point**: Oil **R_f**: 0.88 **Yield (final step)**: 29%
^{1}H NMR:	**^{13}C NMR:**
^{1}H NMR (600 MHz, Chloroform-*d*) δ 7.24 – 7.19 (m, 1H), 7.11 – 7.05 (m, 2H), 7.05 – 7.00 (m, 1H), 5.87 (dd, *J* = 8.4, 1.8 Hz, 1H), 2.96 – 2.84 (m, 1H), 2.74 – 2.62 (m, 1H), 2.06 (s, 3H), 1.98 – 1.71 (m, 3H), 1.70 – 1.57 (m, 1H), 1.56 – 1.45 (m, 1H).	^{13}C NMR (151 MHz, $CDCl_3$) δ 170.01, 141.39, 140.23, 129.76, 127.57, 126.04, 76.03, 35.73, 33.48, 27.68, 27.26, 21.30.

On the ^{13}C NMR spectrum of **1d**, 5 signals are observed in the aromatic region (δ>110 ppm) which corresponds to the 6 carbons of the phenyl ring. It is speculated that 2 carbon signals overlap. The carbonyl carbon of the acetyloxy group is represented by the signal at 170.01 ppm. In the aliphatic region (δ<40 ppm), 5 signals are observed, which correspond to the five aliphatic carbons of this compound. The CH_3 carbon of the acetyloxy group is represented by the signal at 76.03 ppm. On the ^{1}H NMR spectrum, the aromatic protons (δ>6 ppm) integrate for 4 protons as expected for this compound. As for **1b**, all four signals are complex multiplets. This complexity is due to *meta* coupling of the protons of the phenyl ring. The four CH_2 groups of the aliphatic ring are observed as multiplets at 2.96–1.45 ppm (7H). The signal of one proton is not observed since it may partly overlap with the singlet at 2.06 ppm. The aliphatic proton at C1 of the ring corresponds to the doublet of doublets at 5.87 ppm (1H). Again the multiplicity of signal is the result of coupling with two protons on C2, which are not equivalent due to the chiral center at C1. Since this compound is chiral and represents two enantiomers, the multiplicities of the aliphatic signals is rather complex, indicating non-equivalence of protons attached to the same carbons and complex splitting patterns. The CH_3 protons are represented by the singlet at 2.06 ppm (3H).

3.4.2 Interpretation of TLC

To determine when the reactions have proceeded to completion, TLC was used. Silica gel 60 with UV_{254} fluorescent indicator was employed for this purpose. The mobile phase consisted of a mixture of petroleum ether and ethyl acetate in a 1:1 ratio. The developed plates were visualised under a UV light at 254 nm.

Equation in 3.1 was used to calculate the R_f values of the 1-benzosuberone derivatives, which are given in table 3.2. Since only one spot is visible for each 1-benzosuberone derivative it may be concluded that the compounds are pure as judged by TLC.

$$Rf = \frac{[Analyte]_{Distance\ of\ migration}}{[Solvent]_{Distance\ of\ migration}}$$

Equation 3.1. The equation for the calculation of R_f values.

Table 3-2 The R_f values of the 1-benzosuberone derivatives

Compound	R_f	Compound	R_f
1a	0.13	**1b**	0.51
1c	0.66	**1d**	0.88

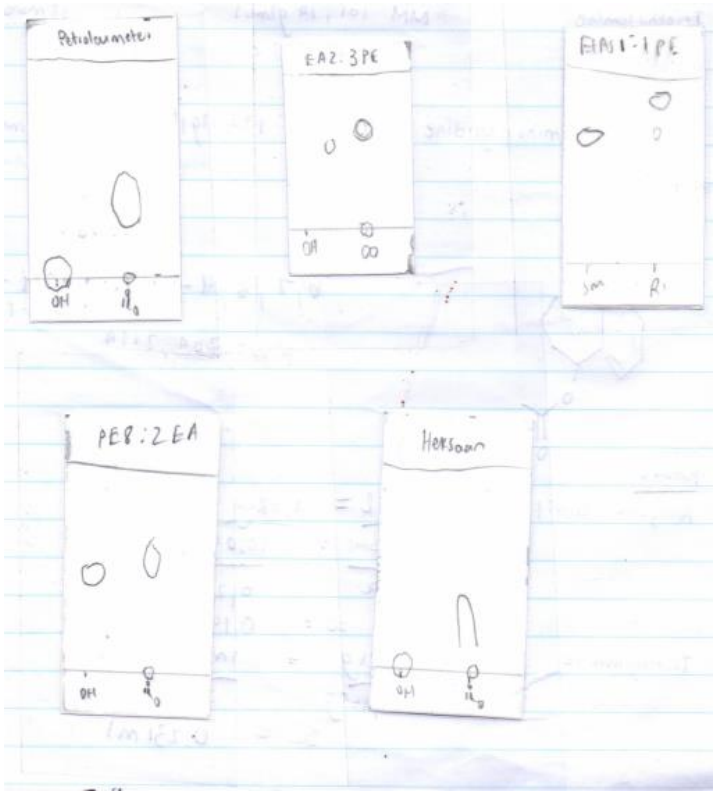

Figure 3-5 Examples of TLC plates obtained during the syntheses of 1a-d

3.4.3 Interpretation of mass spectra

The 1-benzosuberone derivatives were characterised by high resolution mass spectrometry. The estimated and experimentally determined molecular weights of the derivatives are given in table 3.3. The difference between the calculated and experimentally determined molecular weights are expressed in parts per million (ppm) and were calculated according to equation 3.2. A ppm difference of <5 is regarded as acceptable and indicates that the calculated and experimental masses are in agreement. An examination of the calculated and experimentally determined molecular weights of the derivatives show that, for all derivatives, the calculated and experimental values correspond well. Note that for **1d**, a mass spectrum could not be recorded in APCI mode, presumably because the compound does not ionise under the conditions used. Other ionisation techniques should thus be explored in order to record a mass spectrum for this compound.

$$ppm = \frac{[Found\ -Calculated]}{[Calculated]} \times 10^6$$

Equation 3.2. The equation for the calculation of ppm values as an indication of the difference between calculated and experimentally determined molecular weights.

Table 3-3 The calculated and experimentally determined high resolution masses of the 1-benzosuberone derivatives

	Calculated	**Found**	**Formula**	**ppm**
1a	162.1277	162.1270	$C_{11}H_{16}N$ (MH^+)	–4.32
1b	161.0961	161.0983	$C_{11}H_{13}O$ (M^+–H)	13.66
1c	145.1012	145.1000	$C_{11}H_{13}$ (MH^+)	-8.27

3.4.4 Purity by HPLC

The purities of the 1-benzosuberone derivatives were estimated by HPLC analyses. The 1-benzosuberone derivatives were dissolved in acetonitrile at a concentration of 1 mM and analysed by HPLC. For this purpose, the eluent was monitored at a wavelength of 254 nm. The results of the HPLC analyses are given in table 3.3 with the purity of each compound given as

the percentage. For **1d**, we failed to obtain satisfactorily conditions for the elution and detection, and the purity thus was not estimated.

It should be noted that purity determination by HPLC is only an estimate of purity since different organic compounds (e.g. 1-benzosuberone derivatives and potential impurities) possess different molar extinction coefficients at 254 nm, and thus will yield peaks of different sizes (areas and heights) even when present in the exact same molar concentration.

Table 3-4 The percentage purities of the 1-benzosuberone derivatives

	Purity		**Purity**
1a	97.6	**1b**	100
1c	91.2		

3.5 Conclusion

Using several methods, 4 derivatives of 1-benzosuberone have been successfully synthesised in this study. These compounds have been characterised by NMR and MS and the proposed structures correspond with the physicochemical data. In particular, the NMR data such as the integration values, multiplicities, chemical shifts and the number of signals correlated with the proposed structures. This study attempted to synthesise several additional derivatives of 1-benzosuberone but complex mixtures that could not be separated were obtained, while in other instances the desired products were not obtained due to side reactions occurring under the experimental conditions. The following is a list of the structures of derivatives of 1-benzosuberone for which the syntheses were attempted, but failed. The reaction pathways by which the syntheses of these derivatives were attempted are shown in fig. 3.6.

Table 3-5 **The structures of derivatives of 1-benzosuberone for which the syntheses were attempted, but failed**

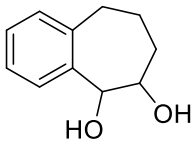 6,7,8,9-Tertahydro-5*H*-benzo[7]annulene-5,6-diol	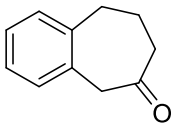 6,7,8,9-Tertahydro-5*H*-benzo[7]annulen-6-one	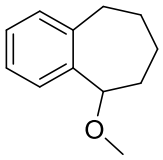 5-Methoxy-6,7,8,9-tertahydro-5*H*-benzo[7]annulene

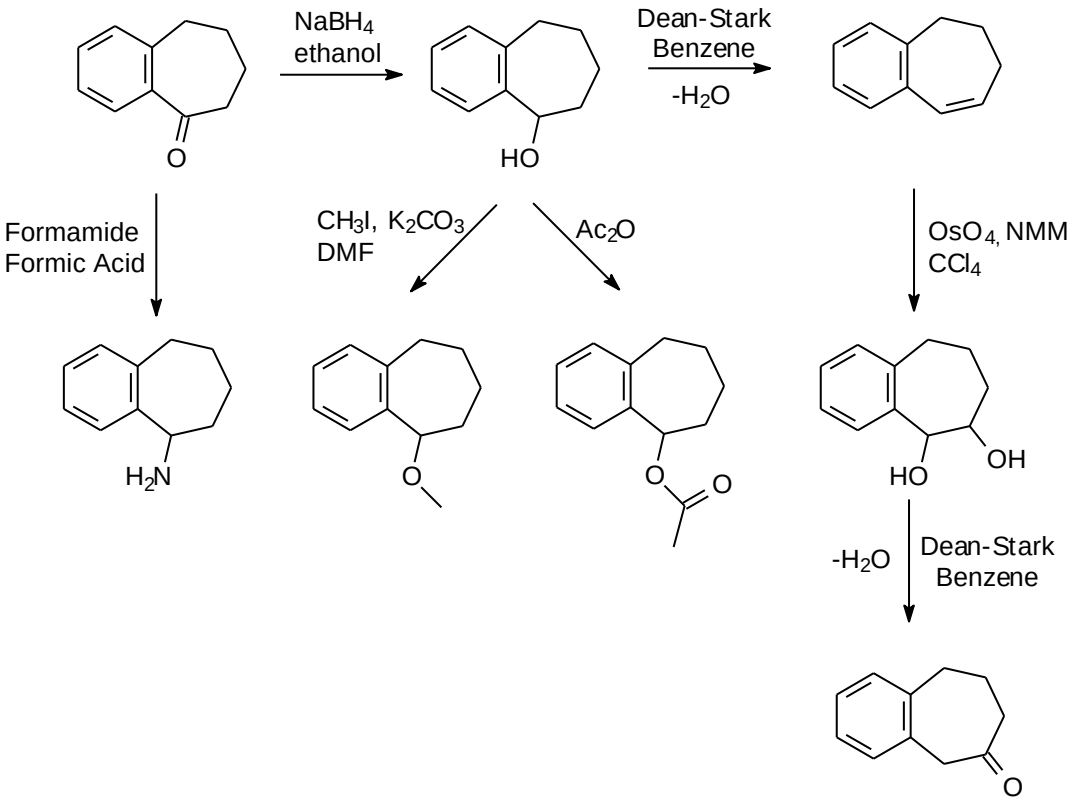

Figure 3-6 **The synthesis route for the 1-benzosuberone derivatives of this study**

CHAPTER 4: ENZYMOLOGY

4.1 Introduction

In this chapter 1-benzosuberone and the 1-benzosuberone derivatives that were synthesised in chapter 3 were investigated for potential inhibitors of human MAO-A and MAO-B. Several different methods for measuring MAO activity have been reported. The method that was used in this study is described by Strydom *et al*. (2010). The synthesised compounds were tested as potential inhibitors of human MAO-A and MAO-B by measuring IC_{50} values, which were determined by constructing sigmoidal curves of enzyme activity versus the logarithm of inhibitor concentration. In this study, kynuramine is used as MAO substrate. 4-Hydroxyquinoline is the metabolite that forms when kynuramine is oxidised by MAO-A and MAO-B. 4-Hydroxyquinoline fluoresces at an excitation wavelength of 310 nm and an emission wavelength of 400 nm when dissolved an alkaline media. Fluorescence spectrophotometry was thus used to measure the extent by which kynuramine is oxidised by the MAO enzymes, both in the absence and presence of various concentrations of the test inhibitors. When performing the MAO activity measurements, it was established that 1-benzosuberone and the 1-benzosuberone derivatives do not fluoresce under the conditions under which the assay is employed, and thus do not interfere with the quantitation of 4-hydroxyquinoline by fluorescence spectrophotometry.

4.2 MAO activity measurements

4.2.1 Kynuramine as MAO substrate

Kynuramine was used as substrate for both MAO-A and MAO-B in this study. MAO metabolises kynuramine to yield 4-hydroxyquinoline, a metabolite that fluoresces. As mentioned, when dissolved in alkaline media, 4-hydroxyquinoline fluoresces and can thus be quantitated by a fluorescence spectrophotometer.

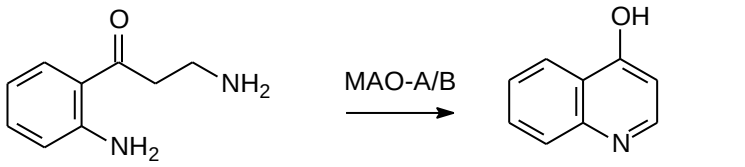

Kynuramine 4-Hydroxyquinoline

Figure 4-1 Oxidation of kynuramine by MAO-A and MAO-B to yield 4-hydroxyquinoline

4.2.2 Enzyme kinetics

Enzymes may undergo modifications during the enzyme-catalysed reaction, but after the reaction always remains unchanged. An enzyme-catalysed reaction can be expressed as follows:

$$A + B + Enz \leftrightharpoons P + Q + Enz$$

When the rate at which substrates are converted to products is equal to the rate at which products are converted to substrates, the reaction is in equilibrium and this equilibrium is described by the equilibrium constant (K_{eq}). Enzymes have no effect on the K_{eq} value.

Biological evaluations, however, take place over a short period of time when the rate of the reverse reaction is negligible. The rate of the forward reaction is thus measured and is known as the initial velocity (v_i), when very little of the substrate has been converted to product. In a typical enzyme activity assay, v_i increases as the substrate concentration increases until a maximum v_i value is reached. This maximum value is known as V_{max}. At this point the enzyme is saturated. The Michaelis constant (K_m) is the substrate concentration where the v_i value is half of the V_{max} value for a particular enzyme. To determine the K_m value of a substrate for a specific enzyme, Lineweaver and Burke method of plotting is used.

Kinetic studies play an important role in the determination of the potency of potential enzyme inhibitors. As mentioned, enzyme-catalysed reactions will reach equilibrium with the formation of an equilibrium enzyme-substrate (ES) intermediate when an enzyme (E) reacts with its substrate (S). This can be illustrated as:

$$E + S \leftrightarrow ES$$

For this reaction, the dissociation constant (K_d) is given as:

$$\mathrm{K_d} = \frac{(\mathrm{E}) \times (\mathrm{S})}{(\mathrm{ES})}$$

Equation 4.1

K_d represents the dissociation of the ES complex, while the affinity of an enzyme for its substrate is represented by the inverse of K_d.

The dissociation constant for the reversible combination of an enzyme and its substrate can, with certain assumptions, be equal to the Michaelis constant (K_m) (Dixon, 1952). The K_m value

for the interaction between as substrate and enzyme can be easily determined by constructing either hyperbolic plots of v_i versus S (equation 4.2, the Michaelis equation) or by Lineweaver and Burk's method of plotting where a straight line is obtained when $1/v_i$ is plotted against 1/S (equation 4.3.) (Dixon, 1952).

$$V_i = \frac{\mathrm{V_{max}} \times \mathrm{S}}{\mathrm{K_m} + \mathrm{S}}$$

Equation 4.2.

In this equation the substrate concentration is represented by *S*, while V_{max} is the maximum velocity obtained at high substrate concentrations. As mentioned, K_m can also be determined from the line on the Lineweaver-Burk plot and its intercept on the vertical axis. By manipulating the equation above, the following equation is yielded:

$$\frac{1}{V_i} = \frac{\mathrm{K_m}}{\mathrm{V_{max}}} \times \frac{1}{\mathrm{S}} + \frac{1}{\mathrm{V_{max}}}$$

Equation 4.3

When $1/v_i$ is plotted on the y-axis and 1/S on the x-axis, a Lineweaver-Burk plot is generated where the slope of the line is determined by K_m/V_{max}. The intercept on the x-axis represents $1/K_m$ while the y-axis intercept as $1/V_{max}$.

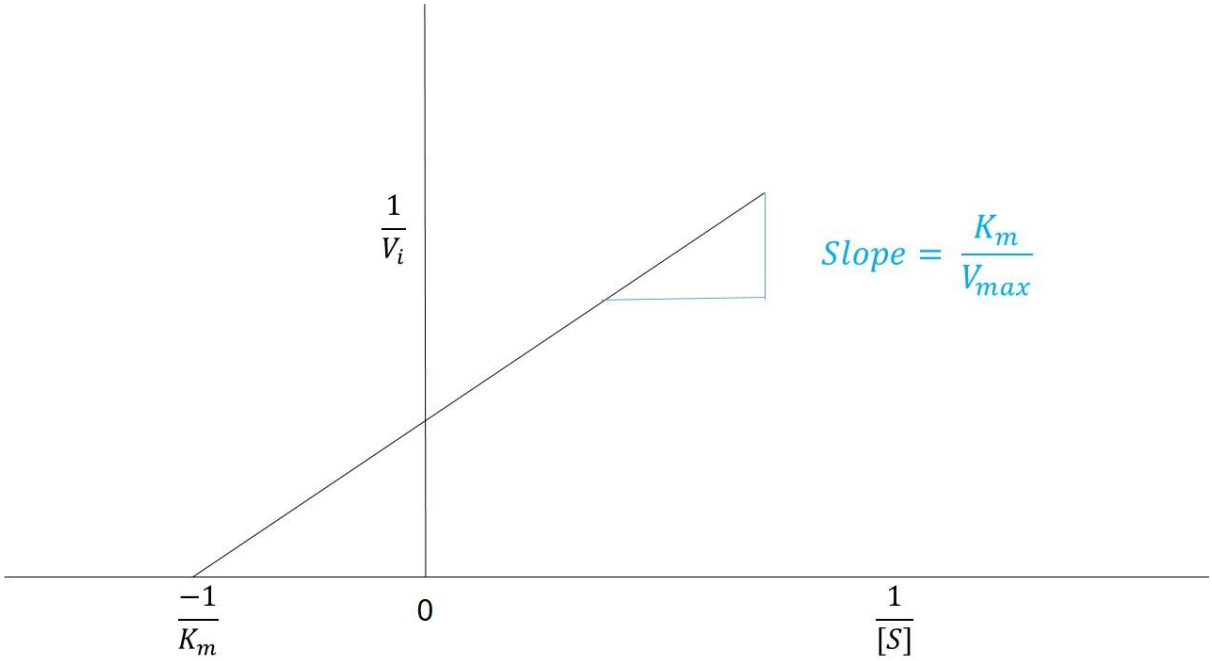

Figure 4-2 **An illustration of a Lineweaver-Burk plot, which may be used to determine K_m and V_{max}**

For competitive inhibition, the enzyme-inhibitor dissociation constant (K_i) can also be described by the Michaelis equation where i is the inhibitor concentration. K_i represents the equilibrium constant of the reversible combination of the enzyme with a competitive inhibitor.

$$V_i = \frac{\mathrm{V_{max}} \times \mathrm{S}}{\mathrm{K_m}\left(1 + \frac{\mathrm{i}}{\mathrm{K_i}}\right) + \mathrm{S}}$$

Equation 4.4

A simple graphical method for the determination of K_i can be done by plotting $1/v_i$ against i while S is kept constant to produce a straight line. When two different substrate concentrations is used, S_1 and S_2, the lines will intersect one another at a point left of the y-axis. This intersection point represents $-K_i$. Since the inhibition is competitive, $1/v_i$, I and V_{max} will be identical for both lines obtained at the intersection point (Dixon, 1952).

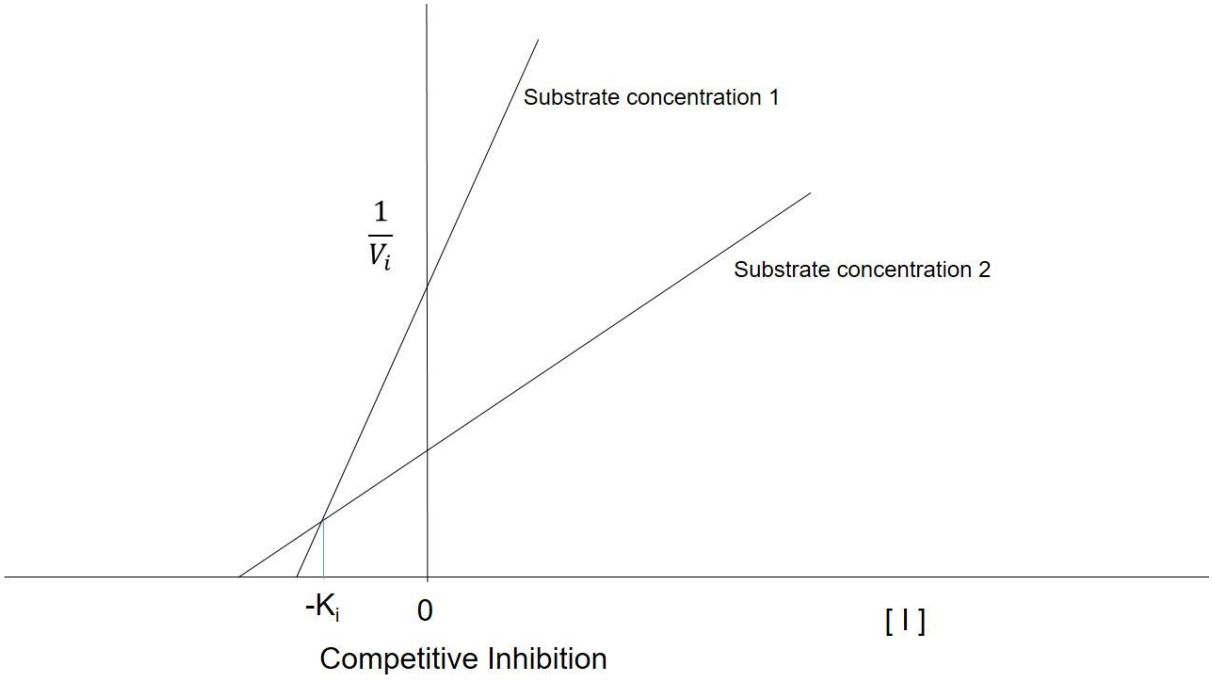

Figure 4-3 Graphical illustration of competitive Lineweaver-Burk plots for the determination of K_i using Dixon's method

4.2.3 Materials and instrumentation

The following materials and instrumentation were used in this chapter:

- Fluorescence spectrophotometry was carried out with a Varian Cary Eclipse fluorescence spectrophotometer.
- The following materials were obtained from Sigma-Aldrich: recombinant human MAO-A and MAO-B expressed in insect cell microsomes (5 mg protein/ml), kynuramine dihydrobromide, selegiline and 4-hyrdroxyquinoline.
- The Prism 5 software package (Graphpad) was used to construct sigmoidal curves of enzyme catalytic rate versus the logarithm of inhibitor concentration. Form these curves, IC_{50} values were determined.
- The following materials were obtained from Merck: polypropylene 96-well microtiter plates, potassium phosphate (mono- and dibasic), potassium chloride, sucrose, sodium hydroxide and dimethyl sulfoxide (DMSO).
- Milli-Q deionised water was used to prepare all buffers and aqueous solutions.
- The following were obtained from Thermo Scientific: Slide-A-Lyzer dialysis cassettes with a molecular weight cut-off of 10000 and a volume capacity of 0.5-3 ml.

4.2.4 Experimental method for IC_{50} determination

4.2.4.1 Method

- The test inhibitors were 1-benzosuberone and the 1-benzosuberone derivatives **1a**-**d**.
- Recombinant human MAO-A and MAO-B (5 mg protein/ml) were pre-aliquoted and stored at -70°C.
- Potassium phosphate buffer was prepared at a concentration of 100 mM and a pH of 7.4. The buffer was made isotonic with the addition of 20.2 mM KCl.
- All the enzyme reactions were carried out in white polypropylene 96-well microtiter plates.
    - A volume of 92 µl of the potassium phosphate buffer was added to each reaction.
    - A volume of 50 µl kynaramine was subsequently added to each reaction to yield a kynuramine concentration of 50 µM.
    - The test inhibitors was added to the reactions to yield a concentration range of 0.003 to 100 µM. The test inhibitors were dissolved in DMSO and added in a volume of 8 µl to the reactions. This yielded a final DMSO concentration of 4% in the enzyme reactions.
    - As controls, reactions were also carried out in the absence of the test inhibitors but contained 4% DMSO.
- The reactions were pre-incubated at 37 °C for 20 min.
- A volume of 50 µl of the MAO enzymes was added to each reaction to yield a final concentration of MAO-A of 0.0075 mg protein/ml, and 0.015 mg protein/ml of MAO-B.

- The reactions were incubated for 20 min at 37 °C, and subsequently terminated with the addition of 80 µl NaOH (2 N).
- 4-Hydroxyquinoline formed from the action of MAO on kynuramine was measured by fluorescence spectrophotometry. For this purpose an excitation wavelength of 310 nm and an emission wavelength of 400 nm was used. The PMT voltage of the spectrophotometer was set to medium. The excitation slit width was 5 nm and the emission slit width was 10 nm.
- A calibration curve was constructed to make quantitative estimations of 4-hydroxyquinoline. For this purpose, 4-hydroxyquinoline at concentrations ranging from 0.047 to 1.50 µM was dissolved in potassium buffer (200 µl) and 80 µl NaOH (2 N) was also added to each standard. The fluorescence of the calibration standards were subsequently measured as above.
- Control samples were also included in this study to confirm that the tested inhibitors doesn't fluorescence of quench the fluorescence of 4-hydroxyquinoline. The control samples contained 4-hydoxyquinoline (1.5 µM), test inhibitor (100 µM) and 80 µl NaOH.

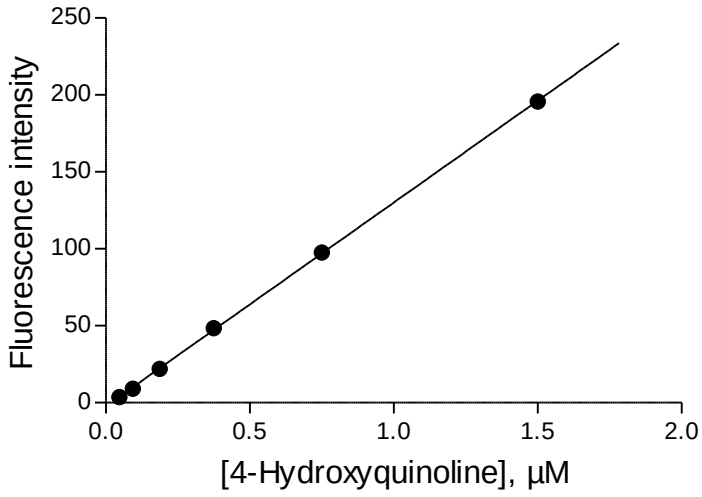

Figure 4-4 **An example of a calibration curve constructed in this study to make quantitative estimations of 4-hydroxyquinoline. The graph shows the fluorescence of 4-hydroxyquinoline versus the concentration of the 4-hydroxyquinoline. The graph should form a linear line and have a linearity of 0.999 to be acceptable for the study**

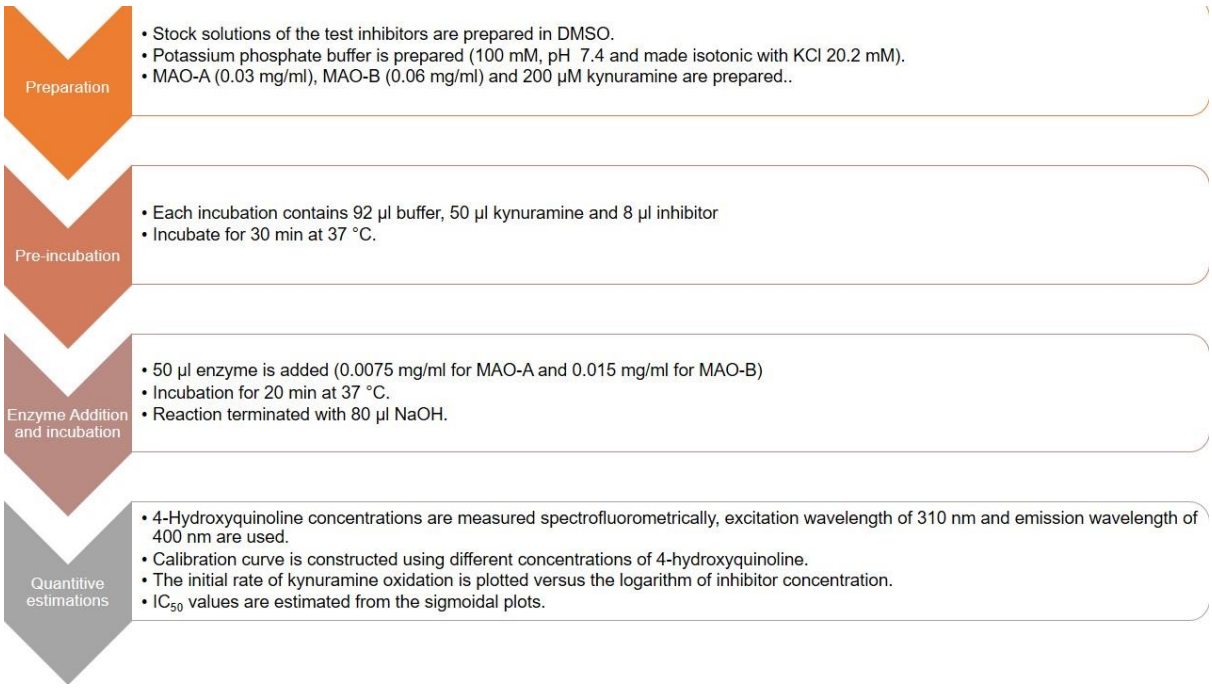

Figure 4-5 **A flow diagram illustrating the protocol followed for the determination of IC_{50} values**

4.2.4.2 Results

Table 4-1 **IC_{50} values for inhibition of human MAO-A and MAO-B by 1-benzosuberone and the 1-benzosuberone derivatives 1a-d**

Compound		IC_{50} MAO-A (µM)	IC_{50} MAO-B (µM)	SI[a]
1a	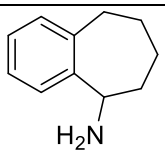	No Inhibition[b]	16.3 ± 2.06	>6.1
1b	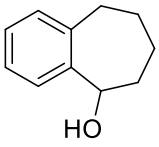	No Inhibition[b]	No Inhibition[b]	-
1c	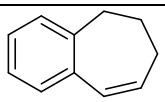	71.7 ± 4.18	14.0 ± 1.30	5.1

1d	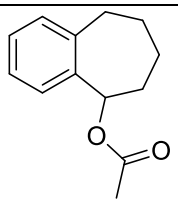	No inhibition[b]	8.31 ± 0.85	>12.0
1-Benzosuberone	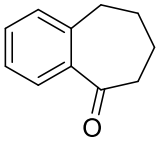	No inhibition[b]	71.6 ± 20.1	>1.4

* All values are expressed as the mean ± standard deviation (SD) of triplicate determinations.

[a] Selectivity index (SI) = IC_{50} of MAO-A/ IC_{50} of MAO-B. The value indicates the specificity of inhibition of MAO-B.

[b] No inhibition observed at maximum tested concentration of 100 µM.

The IC_{50} values for the inhibition of human MAO-A and MAO-B by 1-benzosuberone and the 1-benzosuberone derivatives are given in table 4-1. As mentioned, the IC_{50} value is an indication of how potent MAO is inhibited by a test inhibitor. The values are given in the mean ± SD. From the table it is evident that some compounds exhibited no inhibition, even at a maximum concentration of 100 µM. The SI value indicates the specificity of inhibition of MAO-B. When no inhibition of MAO-A occurred, the assumption was made that the lowest possible IC_{50} value is 100 µM, and the SI values were accordingly calculated. As mentioned IC_{50} values were estimated from sigmoidal curves of enzyme activity versus the logarithm of inhibitor concentration. For the inhibition of MAO-B by **1a**, **1c** and **1d**, these curves are shown in figure 4.4 as examples.

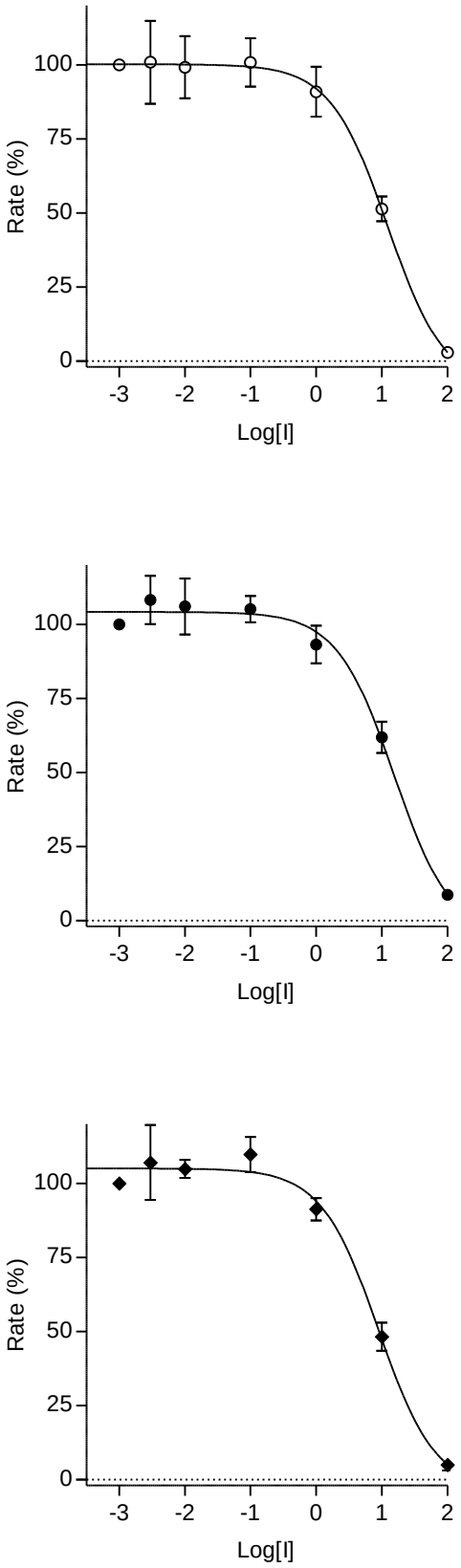

Figure 4-6 **The sigmoidal curves of enzyme catalytic rate versus the logarithm of inhibitor concentration for the inhibition of MAO-B by 1a (top), 1c (middle) and 1d (bottom)**

The following observations from the inhibition data can be made:

- Three 1-benzosuberone derivatives, compounds **1a**, **1c** and **1d**, display moderately potent inhibition of MAO-B. Among these **1d** is the most potent MAO-B inhibitor with an IC_{50} value of 8.31 µM.
- 1-Benzosuberone is a weak inhibitor of MAO-B with an IC_{50} value of 71.6 µM.
- Only one compound exhibited inhibition towards MAO-A. This is compound **1c** with an IC_{50} value of 71.7 µM. It may this be concluded that 1-benzosuberone and the 1-benzosuberone derivatives are weak MAO-A inhibitors.
- Compound **1d**, the most potent MAO-B inhibitor of the series, is also the most isoform-specific inhibitor with an SI value of >12.0. It noteworthy that **1d** did not inhibit MAO-A, even at a maximum tested concentration of 100 µM. Compound **1d** thus represent an MAO-B specific inhibitor with moderate inhibition potency.
- Compared to the well-known MAO-B inhibitors, lazabemide and safinamide, the 1-benzosuberone derivatives of the current study may be viewed as relatively weak MAO-B inhibitors. Under the same experimental conditions, lazabemide and safinamide exhibit IC_{50} values of 0.091 µM and 0.048 µM, respectively, for the inhibition of MAO-B (Petzer *et al*., 2013a).

The MAO inhibition potencies of the 1-benzosuberone and the 1-benzosuberone derivatives may be compared to those of other small molecule MAO inhibitors.

1-Tetralone: As mentioned, 1-benzosuberone bears structural resemblance to 1-tetralone, which is reported to be a moderately potent MAO inhibitor with IC_{50} values of 14.8 µM and 18.6 µM for the inhibition of human MAO-A and MAO-B, respectively (Legoabe *et al*., 2014). This study show that the active MAO inhibitors, compounds **1a**, **1c** and **1d**, display MAO-B inhibition potencies (8.31 to 16.3 µM) that are in a similar range to 1-tetralone. It is however noteworthy that the 1-benzosuberone derivatives are, in contrast to 1-tetralone, specific inhibitors of MAO-B.

Caffeine: Caffeine is reported to be a weak MAO inhibitor with IC_{50} values of 0.761 mM and 5.08 mM for the inhibition of human MAO-A and MAO-B, respectively (Petzer *et al*., 2013b). This study show that the active MAO inhibitors, compounds **1a**, **1c** and **1d**, display MAO-B inhibition potencies (8.31 to 16.3 µM) that are much more potent than that recorded for caffeine. In contrast to the 1-benzosuberone derivatives, caffeine is a more potent MAO-A inhibitor compared to MAO-B.

Isatin: Isatin is reported to be a moderately potent MAO inhibitor with IC_{50} values of 31.8 µM and 12.4 µM for the inhibition of human MAO-A and MAO-B, respectively (Manley-King *et al*., 2011). This study show that the active MAO inhibitors, compounds **1a**, **1c** and **1d**, display MAO-B inhibition potencies (8.31 to 16.3 µM) that are in a similar range to isatin. It is however noteworthy that the 1-benzosuberone derivatives, in contrast to isatin, do not inhibit MAO-A.

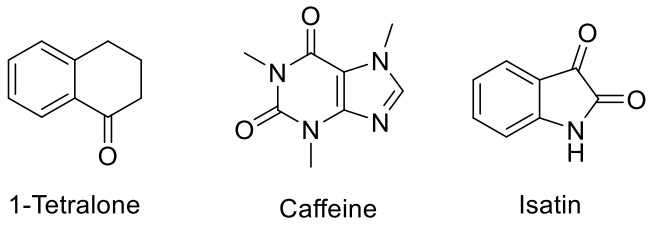

Figure 4-7 The structures of 1-tetralone, caffeine and isatin

4.2.5 Experimental method for the determination of the reversibility of inhibition

To determine whether an inhibitor is a reversible or irreversible inhibitor of an enzyme, the recovery of enzyme activity after dialysis is examined. The reversibility of the MAO-B inhibition by 1-benzosuberone derivatives **1a**, **1c** and **1d** were examined by dialysis. Slide-A-Lyzer dialysis cassettes (Thermo Scientific) with a molecular weight cut-off of 10 000 and a sample volume capacity of 0.5-3 ml were used for these studies.

4.2.5.1 Method.

- Three compounds were selected for the reversibility studies, **1a**, **1c** and **1d**.
- Potassium phosphate buffer was prepared at a concentration of 100 mM and a pH of 7.4. The buffer was made isotonic with the addition of 20.2 mM KCl and sucrose was added to a concentration of 5%.
- Dialysis was carried out to a volume of 0.8 ml in the above buffer and the dialysis incubations contained the following:
    - 0.03 mg/ml MAO-B were added to each incubation.
    - The test inhibitor was added at a concentration of 4 x IC_{50}.

- Control incubations were also conducted with the negative control conducted in the absence of an inhibitor and the positive control conducted in the presence of selegiline (an irreversible MAO-B inhibitor) at a concentration of 4 x IC_{50}.

- The dialysis mixtures were pre-incubated at 37 °C for 15 min.
- The dialysis cassettes were hydrated for 2 min in buffer and the reactions were placed into dialysis cassettes.
- The reactions were dialysed for 20-25 h at 4 °C in 80 ml outer buffer.
- The buffer was replaced after 3 h and 7 h after the dialysis was started.
- For comparison, non-dialysed enzyme-inhibitor reactions were also maintained at 4 °C for 20-25 h.
- After the dialysis, 250 µl of the dialysis sample was removed from the cassette and 250 µl kynuramine were added to each sample. This yielded a concentration of 50 µl kynuramine.
- These reactions were incubated for 20 min at 37 °C.
- The reactions were terminated with the addition of 400 µl NaOH (2 N) and 1000 µl deionised water.
- 4-hydroxyquinoline formation were measured spectrofluorometrically. For this purpose an excitation wavelength of 310 nm and an emission wavelength of 400 nm was used. The PMT voltage of the spectrophotometer was set to medium. The excitation slit width was 5 nm and the emission slit width was 10 nm.
- A calibration curve was constructed to make quantitative estimations of 4-hydroxyquinoline. For this purpose, 4-hydroxyquinoline at concentrations ranging from 0.047 to 1.50 µM was dissolved in potassium buffer (200 µl) and 80 µl NaOH (2 N) was also added to each standard. The fluorescence of the calibration standards were subsequently measured as above.

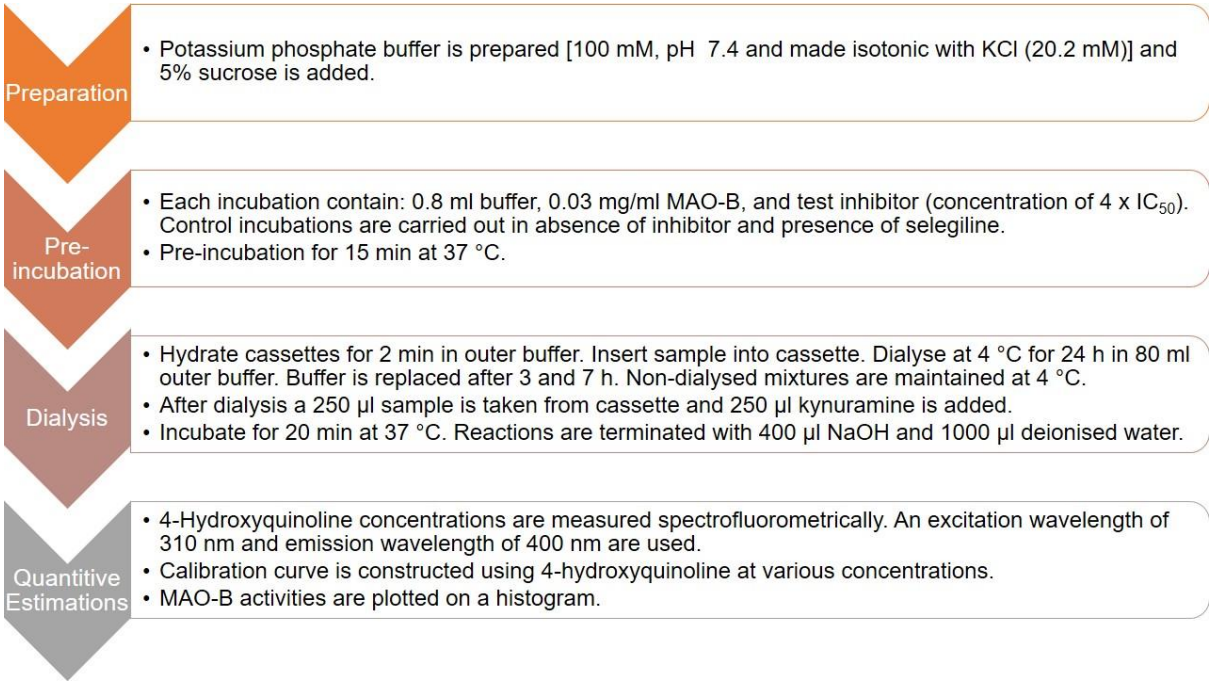

Figure 4-8 **A flow diagram illustrating the protocol followed for the determining reversibility of inhibition by dialysis**

4.2.5.2 Results.

Compounds **1a**, **1c** and **1d** were selected to determine the reversibility of MAO-B inhibition by dialysis. These compounds are the most potent MAO inhibitors among the 1-benzosuberone derivatives. The results of the dialysis studies are given in figures 4.9 to 4.11. As seen in the figures below, after dialysis of mixtures of compounds **1a** and **1c** and MAO-B, respectively for 24 h, almost complete recovery of MAO-B activity could be observed. Inhibition of MAO-B by compounds **1a** and **1c** is therefore completely reversible with the catalytic activity of MAO-B recovering to 96% and 87%, respectively, of the control value (recorded without the presence of the inhibitor). For compound **1d**, MAO-B activity is not completely recovered after 24 h of dialysis which indicate that inhibition by **1d** is not fully reversible. After dialysis, the enzyme activity only recovers to 53%. Since **1d** does not contain any functional groups that may result in irreversible inhibition and covalent modification of the MAO-B enzyme, it is speculated that **1d** exhibits tight-binding to MAO-B. In this case, inhibition may not be reversed by dialysis. Non-dialysed mixtures of MAO-B and the test inhibitors yielded residual activities of 57%, 52% and 36%, respectively. Since these values are lower than the activities after dialysis, it may be concluded that inhibition persists if the inhibitor is not removed and diluted by dialysis. This is further support for a reversible interaction between the test inhibitors and MAO-B. Dialysis of mixtures of MAO-B and selegiline (an irreversible MAO-B inhibitor) resulted in almost no recovery of MAO-B activity, with residual enzyme activity at only 3.5% of the control value. The

conclusion may be made that **1a** and **1c** are reversible MAO-B inhibitors while **1d** exhibits tight-binding, although is also interacts reversibly.

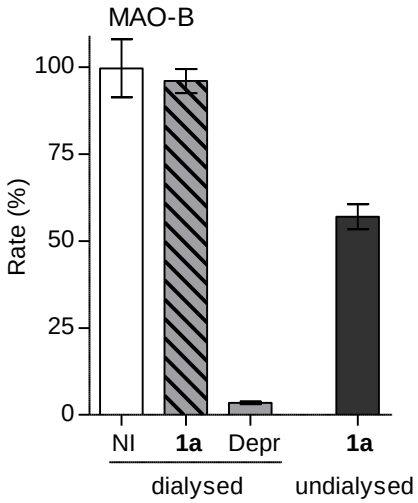

Figure 4-9 **Histogram depicting the reversibility of MAO-B inhibition by 1a. MAO-B was pre-incubated in the absence of inhibitor (NI-dialysed) and presence of 1a (1a-dialysed) and selegiline (Depr-dialysed). After dialysis, the residual enzyme activities were measured. For comparison, the MAO-B activity of undialysed mixtures of MAO-B and 1a were also measured (1a-undialysed)**

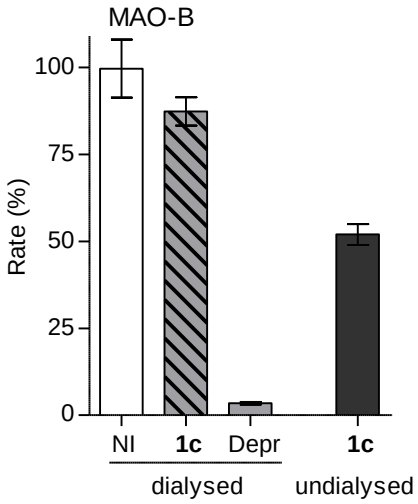

Figure 4-10 **Histogram depicting the reversibility of MAO-B inhibition by 1c. MAO-B was pre-incubated in the absence of inhibitor (NI-dialysed) and presence of 1c (1c-dialysed) and selegiline (Depr-dialysed). After dialysis, the residual enzyme activities were measured. For comparison, the MAO-B activity of undialysed mixtures of MAO-B and 1c were also measured (1c-undialysed)**

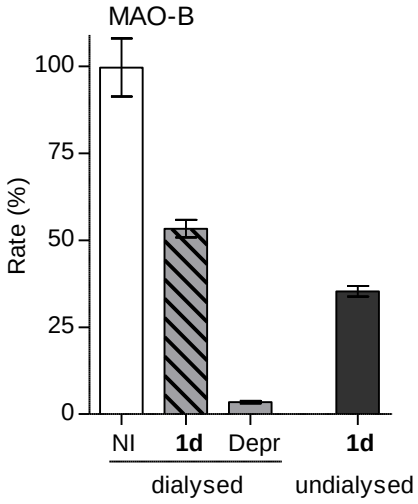

Figure 4-11 **Histogram depicting the reversibility of MAO-B inhibition by 1c. MAO-B was pre-incubated in the absence of inhibitor (NI-dialysed) and presence of 1c (1c-dialysed) and selegiline (Depr-dialysed). After dialysis, the residual enzyme activities were measured. For comparison, the MAO-B activity of undialysed mixtures of MAO-B and 1c were also measured (1c-undialysed)**

4.2.6 Experimental method for construction of Lineweaver-Burk plots

To determine the mode of inhibition of the 1-benzosuberone and derivatives, Lineweaver-Burk plots are constructed. Compounds **1a**, **1c** and **1d** were used in this study to determine whether the compounds are competitive or noncompetitive inhibitors of MAO-B. Compounds **1a**, **1c** and **1d** were selected since they are the most potent MAO inhibitors of this study. To construct each Lineweaver-Burk plots, eight different concentrations of kynuramine were used ranging from 15-250 µM. For each test inhibitor six Lineweaver-Burk plots were constructed, in the presence of five different inhibitor concentrations and the absence of an inhibitor. The different concentrations used for the test inhibitors were ¼ x IC_{50}, ½ x IC_{50}, ¾ x IC_{50}, 1 x IC_{50} and 1¼ x IC_{50}.

4.2.6.1 Method

- Recombinant human MAO-B (5 mg protein/ml) was pre-aliquoted and stored at -70°C.
- Potassium phosphate buffer was prepared at a concentration of 100 mM and a pH of 7.4. The buffer was made isotonic with the addition of 20.2 mM KCl.
- The enzyme reactions were carried out to volume of 500 µl, and each reaction contained:
    - kynuramine as substrate at eight different concentrations ranging from 15-250 µM)
    - MAO-B (0.015 mg protein/ml)
    - Test inhibitor in various concentrations (¼ x IC_{50}, ½ x IC_{50}, ¾ x IC_{50}, 1 x IC_{50} and $1^1/_4$ x IC_{50} of each inhibitor).
- The reactions were initiated with the addition of MAO-B, and were subsequently incubated for 20 min at 37 °C.
- 4-Hydroxyquinoline formation were measured spectrofluorometrically. For this purpose an excitation wavelength of 310 nm and an emission wavelength of 400 nm was used. The PMT voltage of the spectrophotometer was set to medium. The excitation slit width was 5 nm and the emission slit width was 10 nm.

  A calibration curve was constructed to make quantitative estimations of 4-hydroxyquinoline. For this purpose, 4-hydroxyquinoline at concentrations ranging from 0.047 to 1.50 µM was dissolved in potassium buffer (200 µl) and 80 µl NaOH (2 N) was also added to each standard. The fluorescence of the calibration standards were subsequently measured as above.

- Lineweaver plots were constructed from the inhibition data obtained. The inverse of the rate of kynuramine oxidation was plotted against the inverse of the substrate concentration.

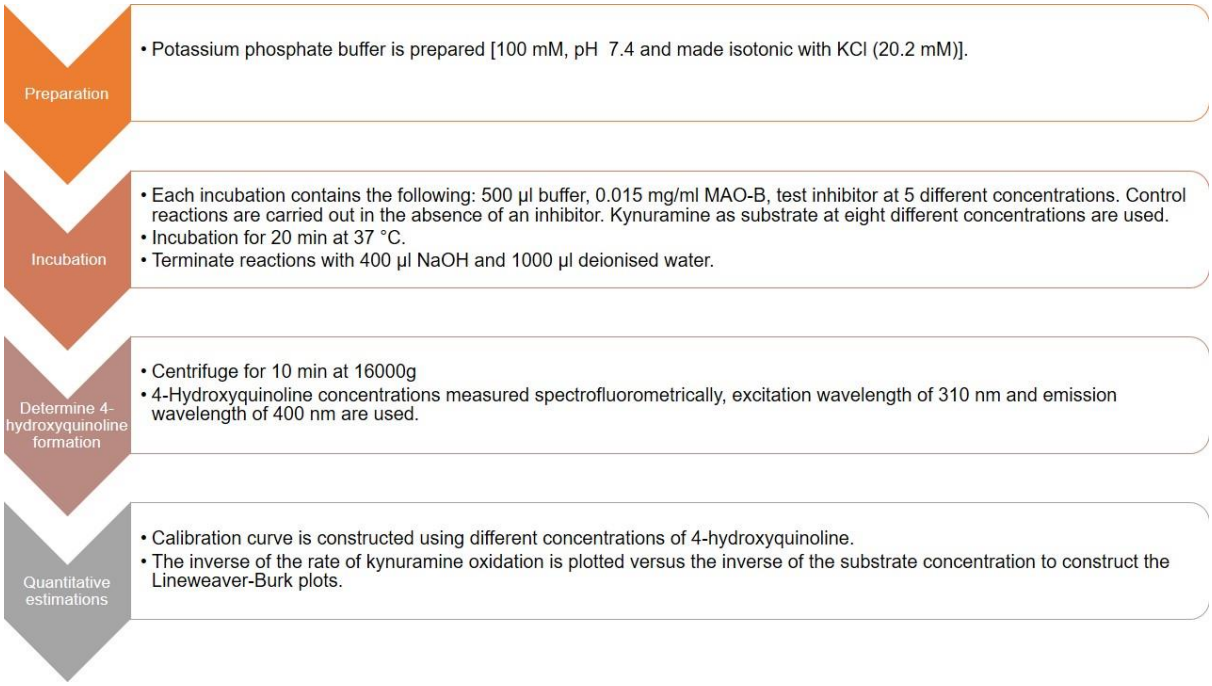

Figure 4-12 A flow diagram illustrating the protocol followed to determine the mode of inhibition by constructing Lineweaver-Burk plots

4.2.6.2 Results

Three 1-benzosuberone and derivatives, compounds **1a**, **1c** and **1d**, were selected for the construction of Lineweaver-Burk plots. These compounds showed the most potent MAO inhibition in this study. Lineweaver-Burk plots were constructed by plotting the inverse of the initial rate of kynuramine oxidation against the inverse of the substrate concentration. Five different inhibitor concentrations were used to construct Lineweaver-Burk plots. For each inhibitor, a Lineweaver-Burk plot was also constructed in the absence of inhibitor.

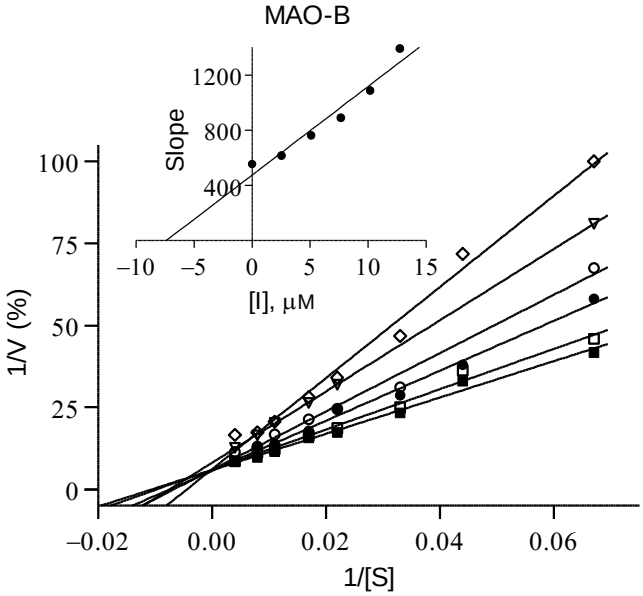

Figure 4-13 **Lineweaver-Burk plots of MAO-B activity in the absence and presence of 1a. MAO-B activity was recorded in the absence of inhibitor and presence of various concentrations of compound 1a. The concentrations of the inhibitor used are ¼ x IC_{50}, ½ x IC_{50}, ¾ x IC_{50}, 1 x IC_{50} and 1¼ x IC_{50} of 1a (IC_{50} = 16.3 μM). The inset is a graph of the slopes of the Lineweaver-Burk plots versus inhibitor concentration from which a K_i value of 7.40 μM is estimated**

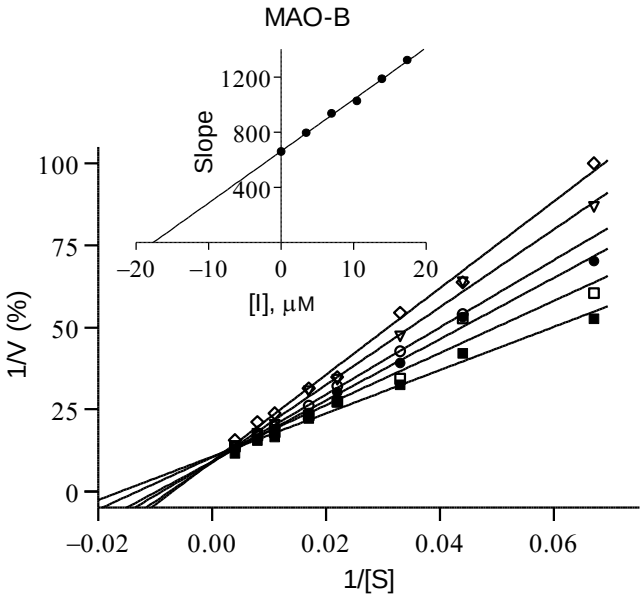

Figure 4-14 **Lineweaver-Burk plots of MAO-B activity in the absence and presence of 1c. MAO-B activity was recorded in the absence of inhibitor and presence of various concentrations of compound 1c. The concentrations of the inhibitor used are ¼ x IC_{50}, ½ x IC_{50}, ¾ x IC_{50}, 1 x IC_{50} and 1¼ x IC_{50} of 1c (IC_{50} = 14.0 μM). The inset is a graph of the slopes of the Lineweaver-Burk plots versus inhibitor concentration from which a K_i value of 17.7 μM is estimated**

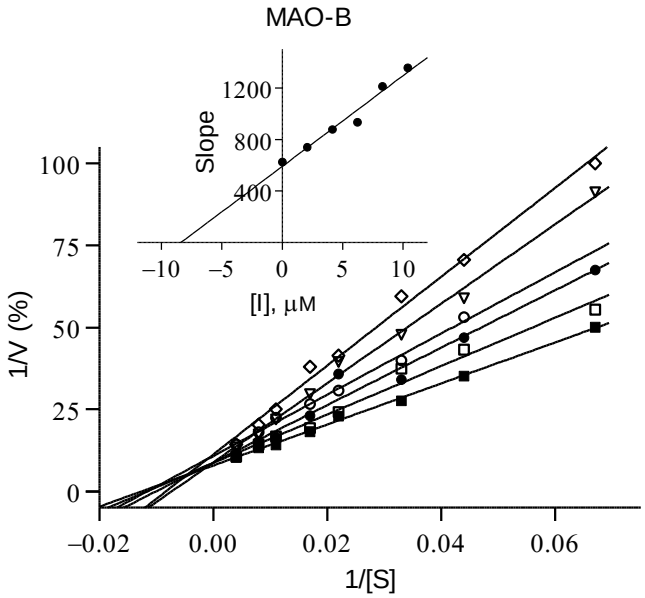

Figure 4-15 **Lineweaver-Burk plots of MAO-B activity in the absence and presence of 1d. MAO-B activity was recorded in the absence of inhibitor and presence of various concentrations of compound 1d. The concentrations of the inhibitor used are ¼ x IC_{50}, ½ x IC_{50}, ¾ x IC_{50}, 1 x IC_{50} and 1¼ x IC_{50} of 1d (IC_{50} = 8.31 µM). The inset is a graph of the slopes of the Lineweaver-Burk plots versus inhibitor concentration from which a K_i value of 8.40 µM is estimated**

The observation can be made from figure 4.13 to 4.15 that the Lineweaver-Burk plots constructed for the inhibition of MAO-B by compounds **1a**, **1c** and **1d** are linear and intersect on the y-axis. Such Lineweaver-Burk plots are typical for compounds that exhibit a competitive mode of inhibition. The conclusion may therefore be made that compounds **1a**, **1c** and **1d** are competitive inhibitors of MAO-B. This further supports the findings of the dialysis studies that these inhibitors are reversible inhibitors of MAO-B.

A Lineweaver-Burk plot may be used to estimate the enzyme-inhibitor dissociation constant (K_i). From a replot of the slopes of the Lineweaver-Burk plots versus inhibitor concentration, the negative of the x-axis intercept equals the K_i value. For compounds **1a**, **1c** and **1d**, K_i values of 7.40 µM, 17.7 µM and 8.40 µM for the inhibition of MAO-B, respectively, were measured. As for IC_{50} values, the potency of the inhibitor increases with lower K_i values. The conclusion may be made that when K_i values are considered, **1a** is the most potent and promising inhibitor among the 1-benzosuberone derivatives.

4.3 Molecular modelling

In this chapter it was shown that the 1-benzosuberone derivatives **1a**, **1c** and **1d** are moderately potent MAO-B inhibitors, while possessing no or very weak MAO-A inhibition potencies. To provide more insight into this findings, this section explores possible binding orientations of **1a**-**d** as well as of 1-benzosuberone in MAO-A and MAO-B by using molecular modelling. Firstly, the co-crystallised ligands, harmine (MAO-A) and safinamide (MAO-B) were redocked into protein models of these enzymes to determine the accuracy of the docking procedure.

4.3.1 Materials and instrumentation

- For the docking studies, the Windows-based Discovery Studio 3.1 software package (Accelrys, San Diego, CA, USA) was used, applying the default values and conditions (unless otherwise specified).
- The reported X-ray crystal structures of human MAO-A (PDB code 2Z5X) (Son *et al*., 2008) and human MAO-B (PDB code 2V5Z) (Binda *et al*., 2007) served as protein models. These models were obtained from the Brookhaven Protein Data Bank. In these structures MAO-A is complexed with harmine while safinamide serves as co-crystallised ligand for MAO-B.
- The illustrations were prepared with Discovery Studio 3.1.

4.3.2 Docking procedure

Docking of a structure into a receptor model involves three steps namely, (a) protein preparation, (b) construction of the ligands and (c) docking of the ligands into the receptor model. These steps are illustrated in Figure 4.16 and detailed below.

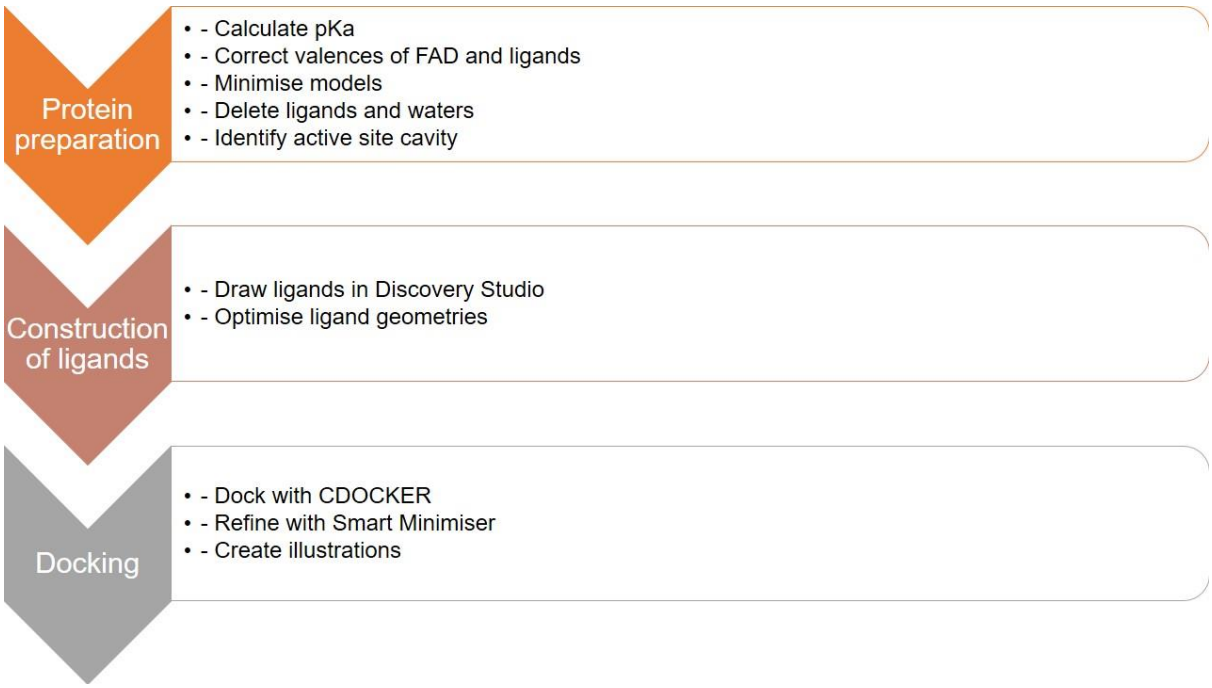

Figure 4-16 An illustration of the docking procedure

Protein preparation:

- The models were prepared for the docking simulations by firstly calculating the pKa values and protonation states (at pH 7.4) of the ionisable amino acids. Based on these calculations hydrogen atoms were added.
- The FAD cofactors were set to the oxidised state and after verifying that the valences of the FAD cofactors and co-crystallised ligands (harmine and safinamide) are correct, the Momany and Rone CHARMm forcefield was applied to the models.
- A fixed atom constraint was applied to the peptide backbone and employing the Smart Minimizer algorithm (maximum steps, 5000), the models were energy minimised. For this procedure the implicit generalized Born solvation model with molecular volume was used.
- The backbone constraints as well as co-crystallised ligands were removed and the active site cavities were identified by analysing the cavities present in the proteins.
- All waters were subsequently removed from the protein models, with the exception of HOH 710, 718 and 739 in MAO-A, and HOH 1155, 1170 and 1351 in the A-chain of MAO-B. These waters are located in the active sites of the MAOs and are considered to be conserved.

Construction of ligands

- The structures of the ligands were drawn in Discovery Studio and their geometries were briefly optimised using a Dreiding-like forcefield (5000 iterations). For the purpose of this step, the ligands were harmine, safinamide, compounds **1a**-**d** and 1-benzosuberone.
- After submitting the inhibitor structures to the Prepare Ligands protocol, atom potential types and partial charges were assigned with the Momany and Rone CHARMm forcefield.

Docking

- The ligands were docked into the MAO models with the CDOCKER algorithm, allowing for ten random conformations for each inhibitor. For the docking procedure, the heating target temperature was set to 700 K and full potential mode was used.
- Finally, the docking orientations were refined using *in situ* ligand minimisation with the Smart Minimizer algorithm.

4.3.3 Results of the docking study

Harmine docked into MAO-A

As shown in Figure 4.17, harmine docks into the MAO-A active site with a similar orientation to that observed in the X-ray crystal structure. The docked orientation of harmine exhibits a root-mean-square deviation (RMSD) value of only 1.20 Å from the orientation of the co-crystallised ligand. Based on the relatively small RMSD, it may be concluded that the docking protocol is suitable for docking ligands into an active site model of MAO-A.

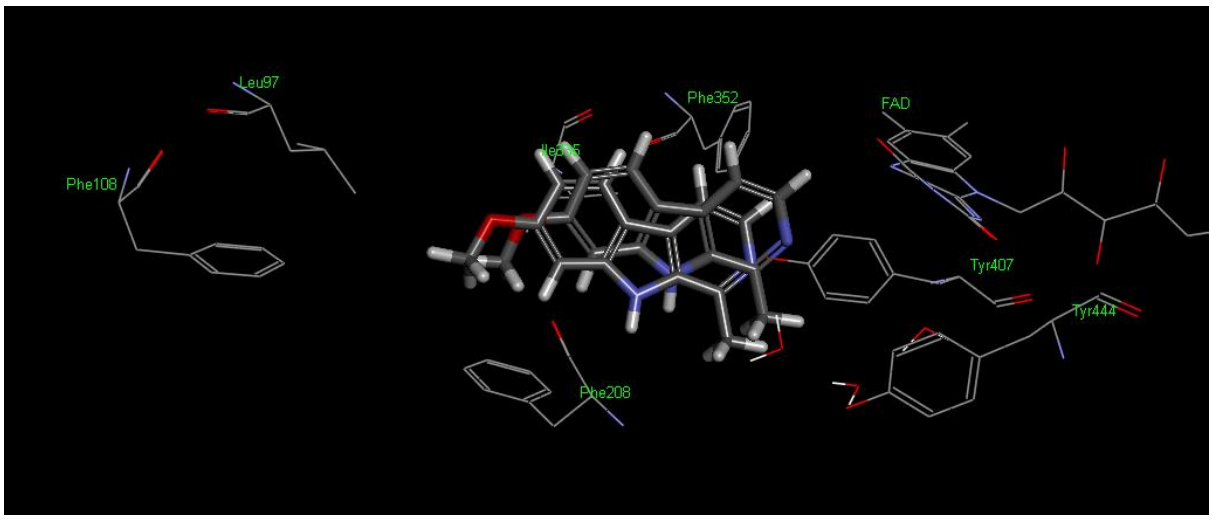

Figure 4-17 **The docked binding orientation of harmine in MAO-A compared to the orientation of harmine in the X-ray crystal structure**

Safinamide docked into MAO-B

As shown in Figure 4.18, the orientation by which safinamide docks into the MAO-B active site is virtually superimposable on the orientation observed in the X-ray crystal structure. The docked orientation of safinamide exhibits a RMSD value of only 0.44 Å from the orientation of the co-crystallised ligand. Based on the small RMSD, it may be concluded that the docking protocol is suitable for docking ligands into an active site model of MAO-B.

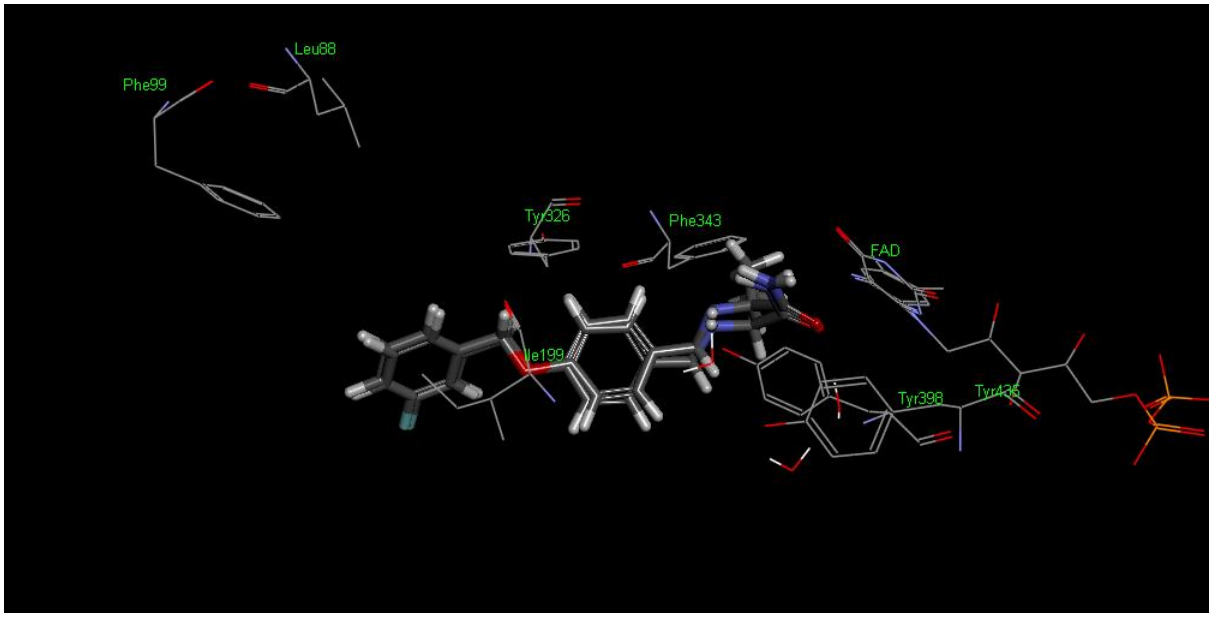

Figure 4-18 **The docked binding orientation of safinamide in MAO-A compared to the orientation of safinamide in the X-ray crystal structure**

1-Benzosuberone derivatives docked into MAO-A:

The docking results show that the 1-benzosuberone as well as the 1-benzosuberone derivatives **1a**-**d** dock in close proximity to the FAD cofactor. The inhibitors undergo in some instances hydrogen bonding within the MAO-A active site. For example (S)-**1a** is hydrogen bonded to the N5 of the FAD cofactor, while the hydroxyl group of (R)-**1b** is hydrogen bonded to a water molecule. Compound **1c**, in turn, forms a pi-pi interaction with Tyr407, while (R)-**1d** forms a pi-pi interaction with Tyr444. For these two compounds pi-pi interactions are possible since their phenyl rings are orientated towards the FAD cofactor. Although these observations show that the inhibitors are able to bind and interact with the MAO-A active site, a molecular explanation for the weak MAO-A inhibition potencies of the 1-benzosuberone derivatives is not apparent. As examples of the docking study, the orientations and interactions of (S)-**1a** and (R)-**1b** are presented in the figures below.

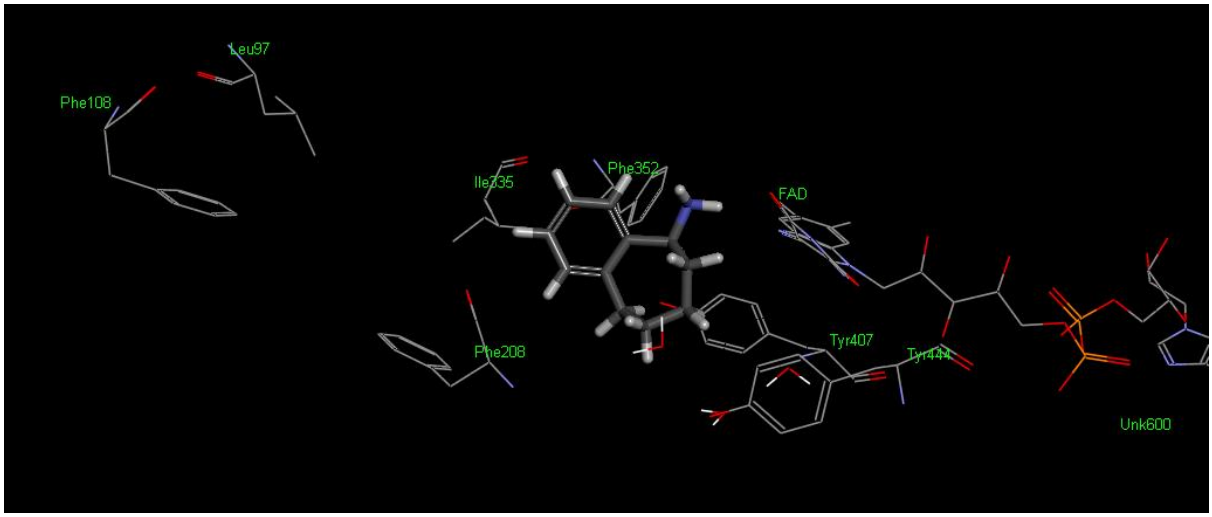

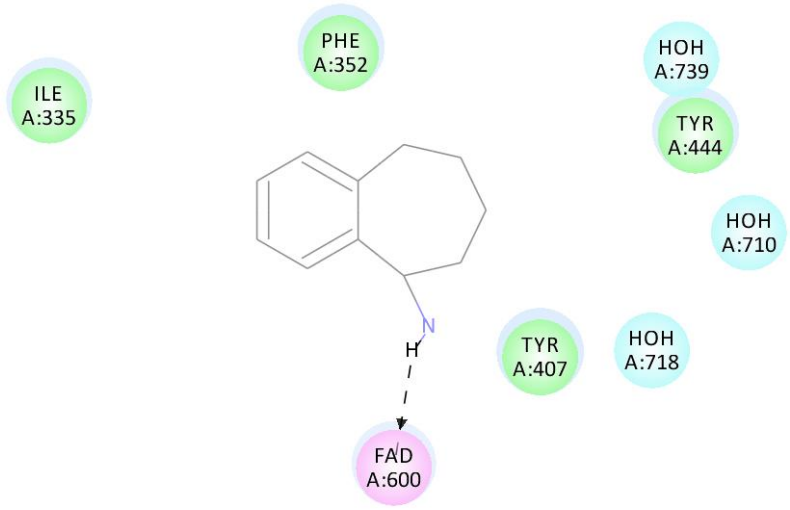

Figure 4-19 **The docked binding orientation of (S)-1a in MAO-A (top) with a 2D-diagram showing the key interactions (bottom). The dash line indicates hydrogen bonding while the blue shadow depicts van der Waals interactions**

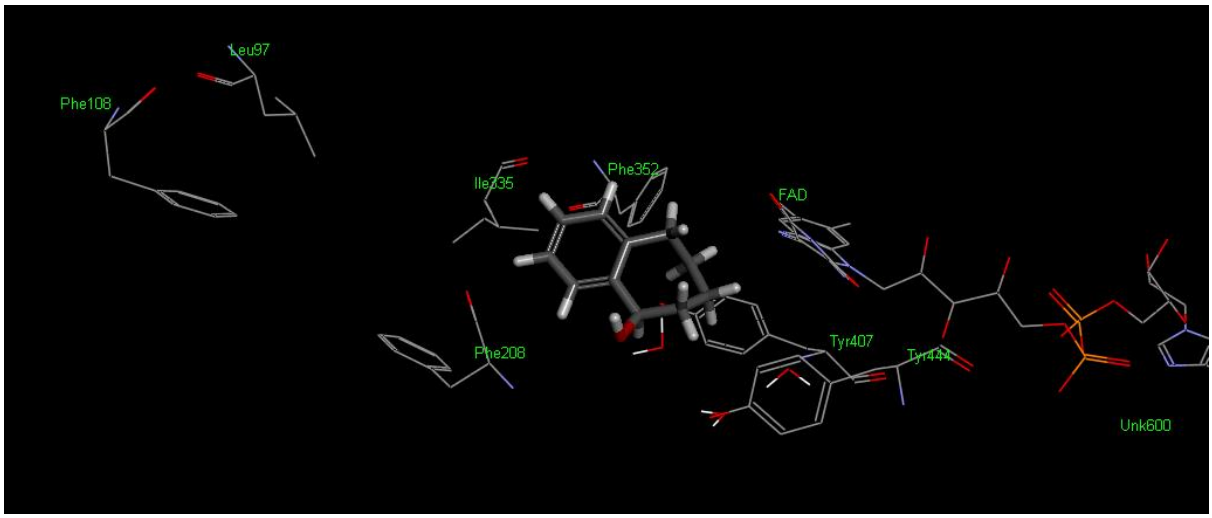

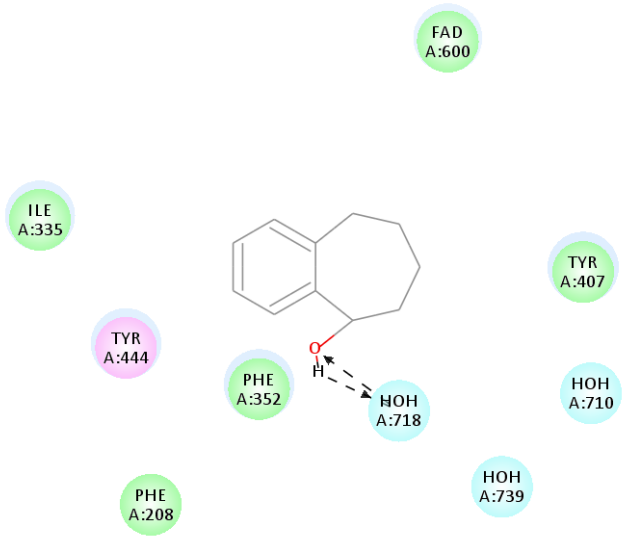

Figure 4-20 **The docked binding orientation of (R)-1b in MAO-A (top) with a 2D-diagram showing the key interactions (bottom). The dash line indicates hydrogen bonding while the blue shadow depicts van der Waals interactions**

1-Benzosuberone derivatives docked into MAO-B:

The docking results show that 1-benzosuberone and the 1-benzosuberone derivatives **1a**-**c** dock within the substrate cavity of MAO-B, in close proximity to the FAD cofactor. Interestingly, **1d** docks in the region between the entrance and substrate cavities. This mid-cavity mode of binding enables (S)-**1d** to form a hydrogen bond interaction with Tyr-326. For both enantiomers van der Waals interactions with Ile-199 are observed, which may be expected since **1d** binds in the cavity space lined by the gating residues Tyr-326 and Ile-199. This unusual mode of binding of **1d** may be responsible for the relatively good MAO-B inhibition potency observed for this compound in this study. It is interesting to note that (R)-**1a** and (R)-**1b** bind with the aliphatic ring directed towards the FAD, while (S)-**1a** and (S)-**1b** binds with the phenyl ring directed towards the FAD. (R)-**1a,** (R)-**1b** and (S)-**1b** established hydrogen bonding to Tyr-398 while (S)-**1a** forms a hydrogen bond interaction with Tyr-435 and a water molecule. (S)-**1a** also undergoes pi-pi interactions with Tyr-435. It may be speculated that, based on the numerous polar interactions of (S)-**1a** with MAO-B, this enantiomer may be responsible for the relatively good MAO-B inhibition potency observed for **1a**. As expected, compound **1c** does not undergo any polar interactions with MAO-B while 1-benzosuberone is stabilised by a pi-pi interaction with Tyr-398. In this respect, 1-benzosuberone binds with the phenyl wing directed towards the FAD. As for MAO-A, a definitive molecular explanation for the inhibition studies is not provided by the

docking studies. The docking study, however, gives some insight into the binding orientations and interactions that are possible for the 1-benzosuberone derivatives. As examples of the docking study, the orientations and interactions of (S)-**1d** and (S)-**1a** are presented in the figures below.

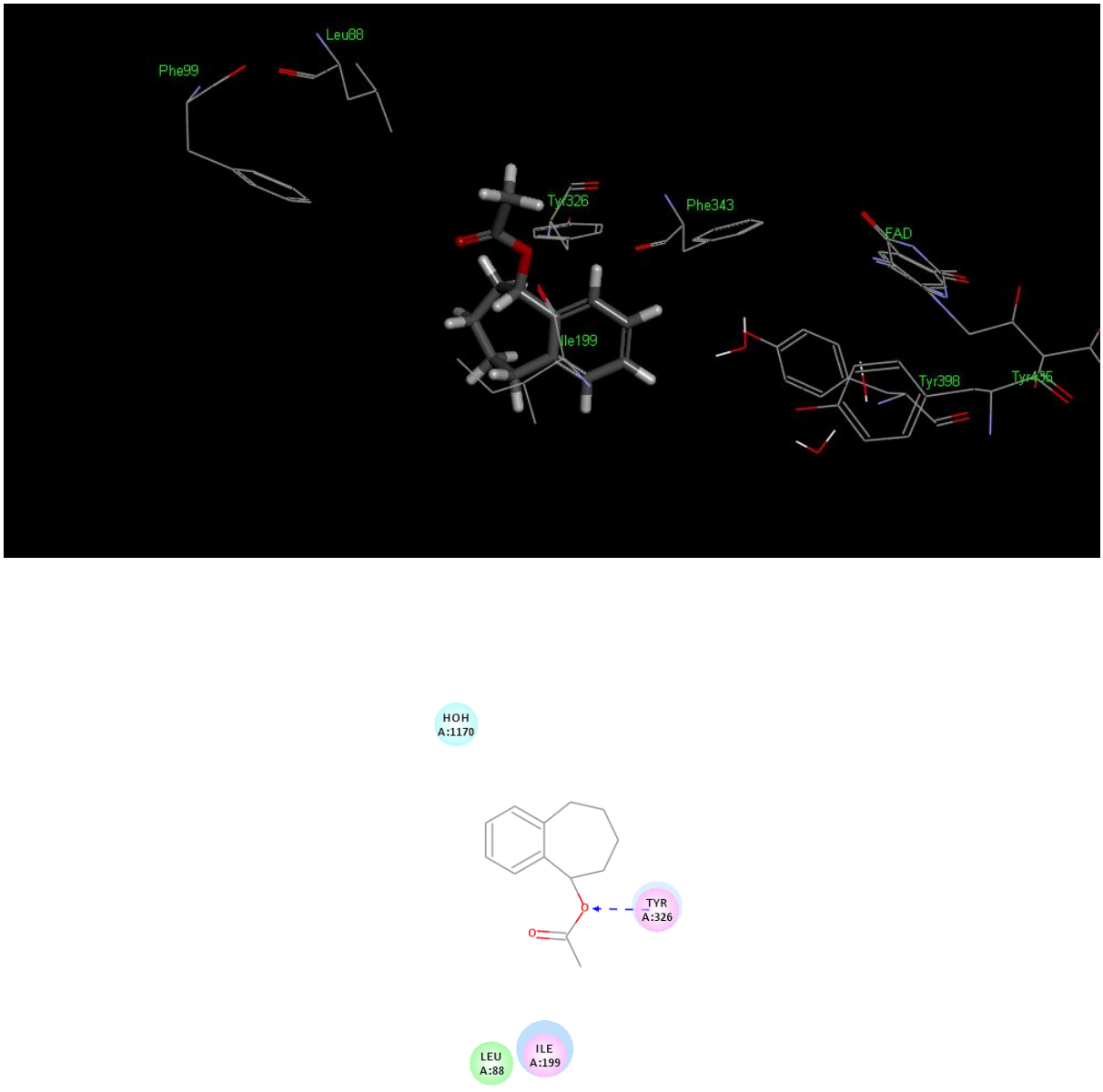

Figure 4-21 **The docked binding orientation of (S)-1d in MAO-B (top) with a 2D-diagram showing the key interactions (bottom). The dash line indicates hydrogen bonding while the blue shadow depicts van der Waals interactions**

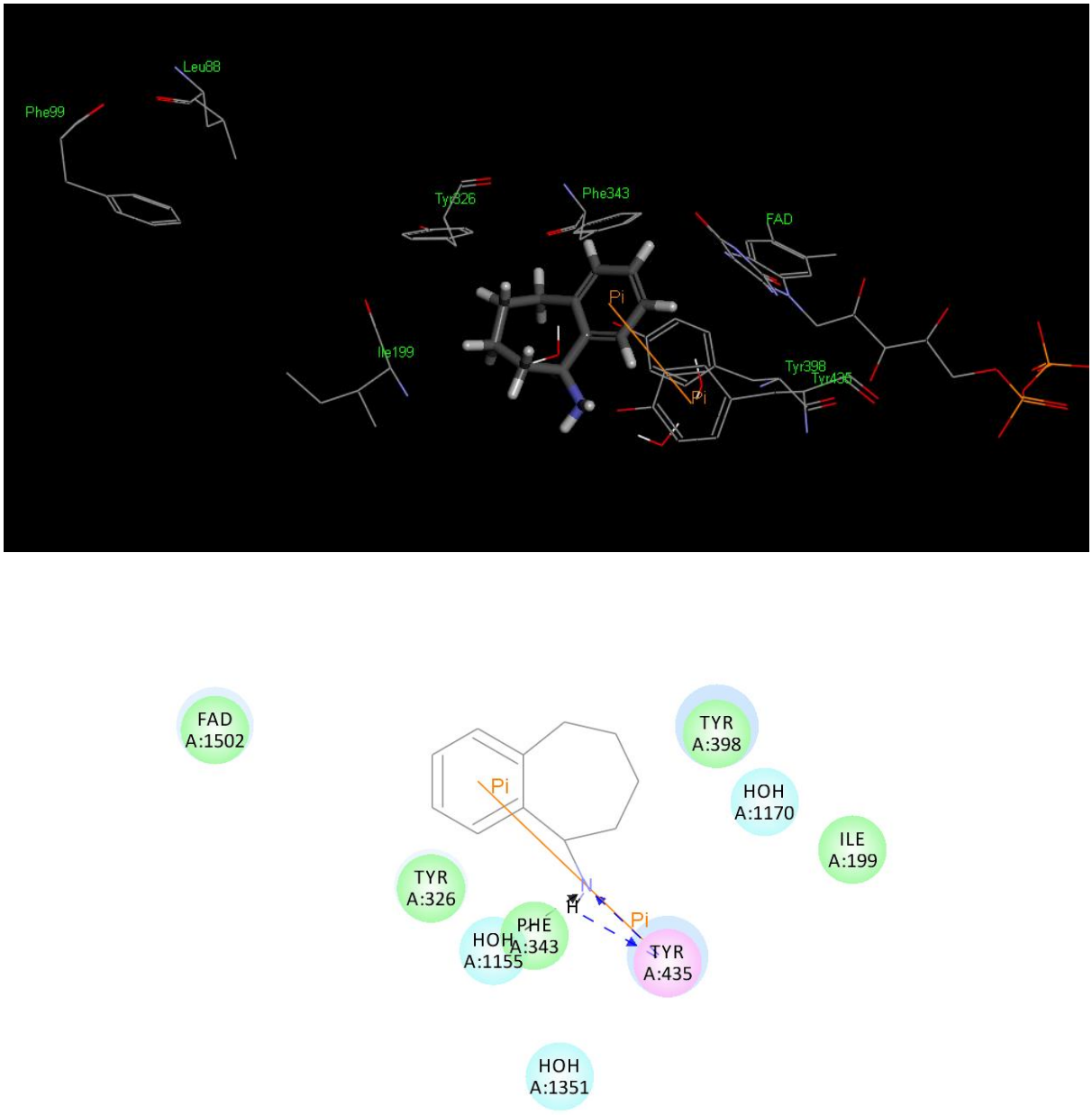

Figure 4-22 **The docked binding orientation of (S)-1a in MAO-B (top) with a 2D-diagram showing the key interactions (bottom). The dash line indicates hydrogen bonding while the blue shadow depicts van der Waals interactions**

4.4 Conclusion

In this chapter, the MAO inhibition properties of 1-benzosuberone and the 1-benzosuberone derivatives were measured and discussed. The inhibition potencies of the inhibitors were evaluated and given as the IC_{50} values. Recombinant human MAO-A and MAO-B were used as enzyme sources and kynuramine served as enzyme substrate. 4-Hydroxyquinoline formation from the oxidation of kynyramine by the MAOs were measured by fluorescence spectrophotometry. This provided a measure of enzyme activity. Sigmoidal curves of enzyme activity versus the logarithm of inhibitor concentration were constructed and the IC_{50} values were determined from these curves. From the results it was concluded that three 1-benzosuberone derivatives, compounds **1a**, **1c** and **1d**, display moderately potent inhibition of MAO-B. Among these **1d** is the most potent MAO-B inhibitor with an IC_{50} value of 8.31 µM. Weak or no inhibition of MAO-A was observed for the derivatives.

Reversibility studies found that, for the inhibition of MAO-B by **1a** and **1c**, dialysis almost completely recovers MAO-B activity which shows that these inhibitors are reversible MAO-B inhibitors. For the inhibition of MAO-B by **1d**, dialysis does not completely recover MAO-B activity which shows that this inhibitor may exhibit tight-binding to MAO-B. This chapter also shows that Lineweaver-Burk plots constructed for the inhibition of MAO-B by compounds **1a**, **1c** and **1d** are linear and intersect on the y-axis. Such Lineweaver-Burk plots are typical of competitive inhibition. For compounds **1a**, **1c** and **1d**, K_i values of 7.40 µM, 17.7 µM and 8.40 µM for the inhibition of MAO-B, respectively, were measured.

CHAPTER 5: CONCLUSION

5.1 Conclusion

PD is a neurodegenerative disorder associated with ageing. Degeneration in PD is progressive and with time the negative impact that PD has on the quality of life worsens. PD is characterised by the loss of dopaminergic neurons in the SNpc, which leads to the well-known motor symptoms of bradykinesia, tremor at rest, involuntarily movements and rigidity. L-Dopa is the most effective drug for the treatment of PD. All current treatments are symptomatic and none stop or halt the progress of the disease. The MAO catalytic cycle produces hydrogen peroxide which may form reactive oxygen radicals. By producing these potentially harmful oxygen species, the metabolism of neurotransmitters by MAO may contribute to the degeneration of dopaminergic neurons. MAO inhibitors is a unique class of drugs used in PD as they may possess neuroprotective properties and thus slow in the progress of the disease. MAO inhibitors also block the MAO-catalysed metabolism of dopamine and thus offer symptomatic relief of the motor symptoms of PD. The aim of this study was to discover novel MAO inhibitors that are potent and selective inhibitors of MAO-B.

The lead compound in this study, 1-benzosuberone, has not previously been evaluated as a potential MAO inhibitor. 1-Benzosuberone is structurally similar to rasagiline, a well-known MAO-B inhibitor. Rasagiline contains a propargylamine functional group that, after activation by the enzyme, binds irreversibly to the FAD cofactor. 1-Benzosuberone and the 1-benzosuberone derivatives of this study do not contain the propargylamine group or other functional groups that are associated with irreversible inhibition of MAO, and are thus expected to act as reversible MAO inhibitors. Furthermore, 1-benzosuberone is also structurally similar to 1-tetralone, a known inhibitor of MAO-A and MAO-B, which further supports the notion that 1-benzosuberone and the 1-benzosuberone derivatives may act as MAO inhibitors.

Four derivatives of 1-benzosuberone were synthesised employing different synthetic routes. The derivatives were characterised by NMR and MS. 1-Benzosuberone and the 1-benzosuberone derivatives were evaluated *in vitro* as inhibitors of both isoforms of MAO and the results are shown in table 5.1.

Table 5-1 **IC_{50} values for inhibition of human MAO-A and MAO-B by 1-benzosuberone and the 1-benzosuberone derivatives 1a-d**

Compound		IC_{50} MAO-A (µM)	IC_{50} MAO-B (µM)	SI
1a	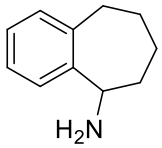	No Inhibition	16.3	>6.1
1b	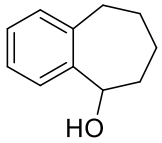	No Inhibition	No Inhibition	-
1c	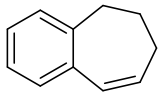	71.7	14.0	5.1
1d	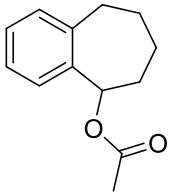	No inhibition	8.31	>12.0
1-Benzosuberone	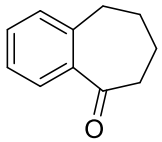	No inhibition	71.6	>1.4

Recombinant human MAO-A and MAO-B were used as enzyme sources and kynuramine served as enzyme source. To measure the activities of MAO-A and MAO-B, 4-hydroxyquinoline (the metabolite formed from the oxidation of kynuramine by MAO) was measured by fluorescence spectrophotometry. Sigmoidal curves of enzyme catalytic rate versus the logarithm of inhibitor concentration were constructed from which the IC_{50} values were estimated. From the results it was concluded that three 1-benzosuberone derivatives, compounds **1a**, **1c** and **1d**, display moderately potent inhibition of MAO-B. Among these **1d** is the most potent MAO-B inhibitor with an IC_{50} value of 8.31 µM. Weak or no inhibition of MAO-A was observed for the derivatives. 1-Benzosuberone showed no MAO-A inhibition and only weak inhibition of MAO-B.

The reversibility of MAO inhibition by **1a**, **1c** and **1d** was investigated by dialysis. The reversibility studies show that **1a** and **1c** are reversible MAO-B inhibitors and that **1d** potentially

exhibit tight binding to MAO-B. The mode of MAO-B inhibition (e.g. competitive or non-competitive) of these derivatives were also investigated by constructing Lineweaver-Burk plots. For **1a**, **1c** and **1d** the Lineweaver-Burk plots are linear and intersect on the y-axis. This shows that these derivatives are competitive inhibitors of MAO-B. For compounds **1a**, **1c** and **1d**, K_i values of 7.40 µM, 17.7 µM and 8.40 µM for the inhibition of MAO-B, respectively, were measured.

Based on the results of this study, 1-benzosuberone derivatives such as **1a** and **1d** may represent promising lead compounds for the design of new MAO-B inhibitors. Such compounds may find application in the future treatment of PD. The observation that **1a** and **1d** are reversible MAO-B inhibitors reduces the liability of the cheese reaction, which is associated with irreversible MAO inhibition. Considering the hypothesis of this study, it may be stated that some of the 1-benzosuberone derivatives (e.g. **1a**, **1c** and **1d**) of this study are moderately potent and specific MAO-B inhibitors, and interact in a reversible manner with MAO-B. Furthermore, these inhibitors are competitive MAO-B inhibitors.

Future recommendations

The following recommendations can be made for future studies:

- Compounds **1a** and **1d** are the most potent inhibitors of MAO-B and are thus most appropriate leads for the future design of MAO inhibitors.
- Since **1a** and **1d** are only moderately potent MAO-B inhibitors, their structures should be modified to enhance MAO-B inhibition. For a series of 1-tetralones, it was shown that substitution of 1-tetralone with relatively large substituents such as the benzyloxy moiety enhances MAO-B inhibition. For example, the IC_{50} value of 6-benzyloxy-1-tetralone is 0.063 µM for the inhibition of MAO-B, while that of 1-tetralone is 18.6 µM (Legoabe *et al*., 2014). Benzyloxy substitution therefore enhances MAO-B inhibition by 295-fold. The enhanced potency of 6-benzyloxy-1-tetralone compared to 1-tetralone may be due to the possibility that the benzyloxy moiety binds within the entrance cavity of MAO-B while the 1-tetralone moiety binds within the substrate cavity. Such cavity-spanning inhibitors are more potent MAO-B inhibitors than compounds such as 1-tetralone that are expected to only bind to the substrate cavity. This study therefore recommends that the benzyloxy substituted 1-benzosuberone derivatives shown in figure 5.1 be synthesised and evaluated as potential MAO inhibitors. The position of the benzyloxy substituent on the benzosuberone derivative may be varied to discover the optimum position for MAO-B

inhibition. Based on the above discussion, it is anticipated that the benzyloxy substituted 1-benzosuberone derivatives should by highly potent and specific MAO-B inhibitors.

- It should be noted that the 1-benzosuberone derivatives investigated here are chiral and represent the racemic mixtures of two enantiomers. In a chiral environment such as the active sites of the MAOs, two enantiomers will exhibit differing interactions with the protein residues and therefore differing inhibition potencies. It is recommended that the enantiomers of the 1-benzosuberone derivatives of this study should by separated. In this manner, most active enantiomer could be identified and used as lead for the design of more potent MAO inhibitors.

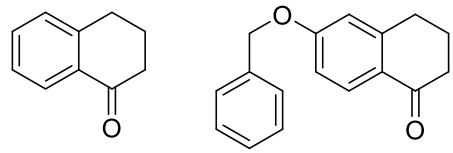

1-Tetralone 6-Benzyloxy-1-tetralone

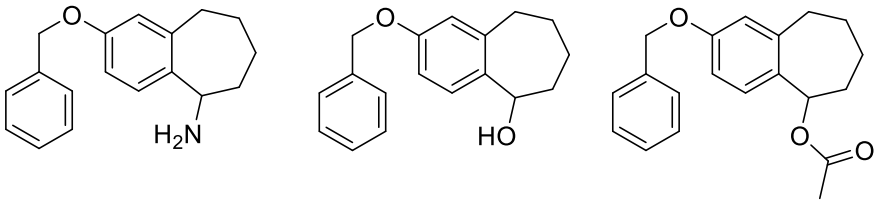

Benzyloxy substitution of the 1-benzosuberone derivatives for future studies

Figure 5-1 The structures of 1-tetralone, 6-benzyloxy-1-tetralone and the benzyloxy substituted 1-benzosuberone derivatives for future studies

BIBLIOGRAPHY

Adli, M., Pilhatsch, M., Bauer, M., Koberle, U., Ricken, R., Janssen, G., Ulrich, S. & Bschor, T. 2008. Safety of high-intensity treatment with the irreversible monoamine oxidase inhibitor trancylcypromine in patients with treatment-resistant depression. *Pharmacopsychiatry*. 41(6):252-257.

Agid, Y. 1998. Levodopa: is toxicity a myth? *Neurology*. 50:858-863.

Allain, H., Lieury, A., Brunet-Bourgin, F., Mirabaud, C., Trebon, P., Le Coz, F. & Gandon, J.M. 1993. Antidepressants and cognition: comparative effects of moclobemide, viloxazine and maprotiline. *Psychopharmacology*. 106(Suppl):56-61.

Aluf, Y. Vaya, J., Khatib, S., Loboda, Y. & Finberg, J.P. 2013. Selective inhibition of monoamine oxidase A or B reduces striatal oxidative stress in rats with partial depletion of the nigro-striatal dopaminergic pathway. *Neuropharmacolgy*. 65:48-57.

Amrein, R., Hetzel, W., Stabl, M. & Schmid-Burgk, W. 1993. RIMA – a new concept in the treatment of depression with Moclobemide. *International clinical psychopharmacology*. 7:123-132.

Assal, F., Spahr, L., Hadengue, A., Rubbici-Brandt, L. & Burkhard, P.R. 1998. Tolcapone and fulminant hepatitis. *The lancet*. 352(9132):958.

Babin, E.J. & Gliese, M. 1995. Extraneuronal uptake of noradrenaline in human tissue (uptake 2). *Heart vessels*. 10:151-153.

Bach, A.W., Lan, N.C., Johnson, D.L., Abell, C.W., Bembenek, M.E. & Shih, S.K. 1988. cDNA cloning of human liver monoamine oxidase A and B: molecular basis of differences in enzymatic properties. *Proceedings of the national academy of sciences of the United States of America*. 85:4934-4938.

Baker, G.B., Coutts, R.T., McKenna, K.F. & Sherry-McKenna, R.I. 1992. Insights into the mechanisms of action of the MAO inhibitors phenelzine and tranylcypromine: a review. *Journal of psychiatry & neuroscience*. 17(5):206-214.

Bar Am, O., Amit, T. & Youdim, M.B.H. 2004. Contrasting neuroprotective and neurotoxic actions of respective metabolites of anti-Parkinson drugs rasagiline and selegiline. *Neuroscience letters.* 355:169-172.

Barbry, P., Champe, M., Chassande, O., Munemitsu, S., Champigny, G., Lingueglia, E., Maes, P., Frelin, C., Tartar, A. & Ullrich, A. 1990. Human Kidney amiloride-binding protein: cDNA structure and functional expression. *Proceedings of the national academy of sciences of the United States of America*. 87:7347-7351.

Bentue-Ferrer, D., Menard, G. & Allain, H. 1996. Monoamine oxidase B inhibitors. Current status and future potential. *Central nervous system drugs*. 6:217-236.

Bieck, P.R., Antonin, K.H. & Schmidt, E.1993. Clinical pharmacology of reversible monoamine oxidase-A inhibitors. *Clinical neuropharmacology*. 16(Suppl 2):S34-S41.

Billett, E.E. 2004. Monoamine oxidase (MAO) in human peripheral tissues. *Neurotoxicology*. 25:139-148.

Binda, C., Coda, A., Angelini, R., Federico, R., Ascenzi, P. & Mattevi, A. 1999. A 30 Å long U-shaped catalytic tunnel in the crystal structure of polyamine oxidase. *Structure.* 7: 265-276.

Binda, C., Newton-Vinson, P., Hubalek, F., Edmondson, D.E. & Mattevi, A. 2002. Structure of human monoamine oxidase B, a drug target for the treatment of neurological disorders. *Nature structural & molecular biology*. 9(1):22-26.

Binda, C., Li, M., Hubalek, F., Herzig, Y., Sterling, J., Edmondson, D.E. & Mattevi, A. 2004. Crystal structures of monoamine oxidase B in complex with four inhibitors of N-Propargylaminiondan class*. Journal of medicinal chemistry*. 47:1767-1774.

Binda, C., Wang, J., Pisani, L., Caccia, C., Carotti, A., Salvati, P., Edmonson, D.E. & Mattevi, A. 2007. Structures of Human Monoamine Oxidase B complexes with selective noncovalent inhibitors: Safianmide and coumarin analogs. *Journal of medicinal chemistry*. 50:5848-5852.

Birkmayer, W., Knoll, J., Riederer, P., Youdim, M.B., Hars, V. & Marton, J. 1985. Increased life expectancy resulting from addition of L-deprenyl to Madopar treatment in Parkinson's disease: a longterm study. *Journal of neural transmission*. 64:113–127.

Braak, H., Del, Tredici, K., Rüb, U., de Vos, R.A., Steur, E.N.J. & Braak, E. 2003. Staging of brain pathology related to sporadic Parkinson's disease. *Neurobiology of aging*. 24:197-211.

Bryan-Lluka, L.J. & O'Donnell, S.R. 1992. Dopamine and adrenaline, but not isoprenaline, are substrates for uptake and metabolism in isolated perfused lungs of rats. *Naunyn-Schmiedeberg's archives of pharmacology*. 346:20-26.

Buffoni, F. 1966. Histaminase and related amine oxidases. *Pharmacological reviews*. 18:1163-1199.

Burke, R.E. 1998. (*In* Koliatos, V.E. & Rattan, R.R., *ed*. Parkinson's disease, Cell Death and Disease of the Nervous System. Totowa, NJ: Humana Press Inc. p. 459-475).

Caccia, C., Maj, R., Calabresi, M., Maestronoi, S., Faravelli, L., Curatolo, L., Salvati, P. & Fariello, R.G. 2006. Safinamide: From molecular targets to a new anti-parkinson drug. *Neurology*. 67: S18-S23.

Callaghan, R.C., Cunningham, J.K., Sykes, J. & Kish, S.J. 2012. Increased risk of Parkinson's disease in individuals hospitalized with conditions related to the use of methamphetamine or other amphetamine-type drugs. *Drug and alcohol dependence*. 120:35-40.

Christen, Y. 2000. Oxidative stress and Alzheimer's disease. *The American journal of clinical nutrition*. 71:621S-629S.

Ciccone, C.D. 1998. Free-radical toxicity and antioxidant medications in Parkinson's disease. *Physical therapy*. 78:313-319.

Cohen, G. 1990. Monoamine oxidase and oxidative stress at dopaminergic synapses. *Journal of neural transmission. Supplementum*. 18:431-435.

Colzi, A., d'Agostini, F., Cesura, A.M. & Da Prada, M. 1992. Brain microdialysis in rats: a technique to reveal competition in vivo between endogenous dopamine and moclobemide, a RIMA antidepressant. *Psychopharmacology (Berl).* 106(Suppl):S217-20.

Comella, C.L. & Tanner, C.M. 1995. (*In* Koller, W.C. & Paulson, G., *ed*. Therapy of Parkinson's Disease. 2nd Edition. New York, USA: Mercel Dekker Inc. p. 109-122).

Cooper, A. 1997. Glutathione in the brain: disorders of glutathione metabolism (*In* Rosenberg, R., Prusiner, S., DiMauro, S., Barchi, R. & Klunk, L., *ed*. The molecular and genetic basis of neurological disease. Boston: Butterworth-Heinemann. p. 1242–1245).

Coutts, R.T., Mozayani, A., Danielson, T.J. & Baker, G.B. 1991. Tissue levels and some pharmacological properties of an acetylated metabolite of phenelzine in the rat. *Journal of pharmaceutical sciences*. 80(8):765-767.

Da Prada, M., Zurcher, G., Wüthrich, I. & Haefely, W.E. 1987. On tyramine, food, beverages and reversible MAO inhibitor moclobemide. *Journal of neural transmission*. 26(Suppl):31-56.

Da Prada, M., Kettler, R., Keller, H.H., Cesura, A.M., Richards, J.G., Saura Marti, J., Muggli-Maniglio, D., Wyss, P.C., Kyburz, E. & Imhof, R. 1990. From Moclobemide to Ro 19-6327 and Ro 41-1049: the development of a new class of reversible, selective MAO-A and MAO-B inhibitors. *Journal of neural transmission*. 29:279-292.

Dauer, W. & Przedborski, S. 2003. Parkinson's disease: mechanisms and models. *Neuron*. 39:889–909.

Dixon, M. 1952. The determination of enzyme inhibitor constants. *Biochemical journal*. 55:170-171.

Edmondson, D.E., Mattevi, A., Binda, C., Li, M. & Hubálek, F. 2004. Structure and mechanism of monoamine oxidase. *Current medicinal chemistry*. 11:1983-1993.

Edmondson, D.E., Binda, C. & Mattevi, A. 2007. Structural insights into the mechanism of amine oxidation by monoamine oxidase A and B. *Archives of biochemistry and biophysics*. 464:269-276.

Edmondson, D.E., Binda, C., Wang, J., Upadhyay, A.K. & Mattevi, A. 2009. Molecular and mechanistic properties of the membrane-bound mitochondrial monoamine oxidases. *Biochemistry*. 48:4220-4230.

Fairweather, D.B. Kerr, J.S. & Hindmarch, I.1993. The effects of moclobemide on psychomotor performance and cognitive function. *International clinical psychopharmacology*. 8(1):43-47.

Finberg, J.P. 2014. Update on the pharmacology of selective inhibitors of MAO-A and MAO-B: focus on modulation of CNS monoamine neurotransmitter release. *Pharmacology & therapeutics*. 143:133-152.

Finberg, J.P., Tenne, M. & Youdim, M.B.H. 1981. Tyramine antagonistic properties of AGN 1135, an irreversible inhibitor of monoamine oxidase type B. *British journal of pharmacology*. 73:65–74.

Foley, P., Gerlach, M., Youdim, M.B.H. & Riederer, P. 2000. MAO-B inhibitors: multiple roles in the therapy of neurodegenerative disorders? *Parkinsonism and related disorders*. 6:25-47.

Fraaije, M.W. & Mattevi, A. 2000. Flavoenzymes: diverse catalysts with recurrent features. *Trends in biochemical sciences*. 25(3):126-132.

Fulton, B. & Benfield, P. 1996. Moclobemide. An update of its pharmacological properties and therapeutic use. *Drugs*. 52:450-474.

Garcia-Alberca, J.M., Paplo Lara, J., Gonzalez-Baron, S., Barbancho, M.A., Porta, D. & Berthier, M. 2008. Prevalence and comorbidity of neuropsychiatric symptoms in Alzheimer's disease. *Actas espanolas de psiquiatria*. 36:265-270.

Gillman, P.K. 2011. Advances pertaining to the pharmacology and interactions of irreversible nonselective monoamine oxidase inhibitors. *Journal of clinical psychopharmacology*. 31(1);66-74.

Goldberg, J.F. & Thase, M.E. 2013. Monoamine oxidase inhibitors revisited: what you should know. *Journal of clinical psychiatry*. 74(2):189-191.

Gotz, M.E., Kunig, G., Riederer, P. & Youdim, M.B. 1994. Oxidative stress: free radical production in neural degeneration. *Pharmacology & therapeutics*. 63:37-122.

Green, A.R., Mitchell, B.D., Tordoff, A.F. & Youdim, M.B. 1977. Evidence for dopamine deamination by both type A and type B monoamine oxidase in rat brain in vivo and for the degree of inhibition of enzyme necessary for increased functional activity of dopamine and 5-hydroxytryptamine. *British journal of pharmacology*. 60:343-349.

Grünblatt, E. 2004. The benefits of microarrays as tools for studying neuropsychiatric disorders. *Drugs of today (Barcelona, Spain).* 40(2):147-156.

Guentert, T.W., Holford, N.H., Pfefen, J.P. & Dingemanse, J. 1994. Mixed linear and non-linear disposition of lazabemide, a reversible and selective inhibitor of monoamine oxidase B. *British journal of clinical pharmacology*. 37:553-557.

Haefely, W., Burkard, W.P., Cesura, A.M., Kettler, R., Lorez, H.P., Martin, J.R., Richards, J.G., Scherschlicht, R. & Da Prada, M. 1992. Biochemistry and pharmacology of moclobemide, a prototype RIMA. *Psychopharmacology (berl).* 106(Suppl):S6-S14.

Hinze, C., Kaschube, M. & Hardenberg, J. 1994. Pharmacodynamics of MDL 72974A: absence of effect on the pressor response to oral tyramine. *Journal of neural transmission*. 41:371-375.

Hubert, H., Fernandez, M.D. & Chen, J.J. 2007. Monoamine oxidase-B inhibition in the treatment of Parkinson's disease. *Pharmacotherapy*. 27(12 Pt 12):174S-185S.

Hughes, A.J., Ben-Shlomo, Y., Daniel, S.E. & Lees, A.J. 1992. What features improve the accuracy of clinical diagnosis in Parkinson's disease: a clinicopathologic study? *Neurology*. 42:1142-1146.

Ioannidas, J.P. 2008. Effectiveness of antidepressants: an evidence myth constructed from a thousand randomized trials? *Philosophy, ethics, and humanities in medicine*. 3:14.

Jalkanen, S. & Salmi, M. 2001. Cell surface monoamine oxidases: enzymes in search of a function. *The EMBO journal*. 20(15):3893-3901.

Jankovic, J. 2008. Parkinson's disease: clinical features and diagnosis. *Journal of neurology, neurosurgery & psychiatry*. 79:368–376.

Katzung, B.G. 2001. Pharmacological management of parkinsonism and other movement disorders. (*In* Katzung, B.G., Masters, S.B. & Trevor, A.J. *ed.* Basic and Clinical Pharmacology, 8th edition. New York: Lange Medical Books/ McGraw Hill Companies Inc. p. 483-500).

Kerr, J.S., Fairweather, D.B. & Hindmarch, I. 1992. The effects of acute and repeated doses of moclobemide on psychomotor performance and cognitive function in healthy elderly volunteers. *Human psychopharmacology*. 7:273-279.

Klinman, J.P. 1996. New quinocofactors in eukaryotes. *The journal of biological chemistry*. 271:27189-27192.

Klinman, J.P. & Mu, D. 1994. Quinoenzymes in biology. *Annual review of biochemistry.* 63:299-344.

Knoll, J. 2000. (-)Deprenyl (selegiline): past, present and future. *Neurobiology (Bp).* 8:179-199.

Knoll, J. & Magyar, K. 1972. Some puzzling pharmacological effects of monoamine oxidase inhibitors. *Advances in biochemical psychopharmacology*. 5:393-408.

Kopin, I.J. 1994. Monoamine oxidase sand catecholamine metabolism. *Journal of neural transmission.* 41:57-67.

Korn, A., Da Prada, M. Raffesberg, W., Allen, S. & Gasic S. 1987. Tyramine pressor effect in man: studies with moclobemide, a novel, reversible monoamine oxidase inhibitor. *Journal of neural transmission.* 26(Suppl):57-71.

Kumar, M.J., Nicholls, D.G. & Anderson, J.K. 2003. Oxidative alpha-ketoglutarate dehydrogenase inhibition via subtle elevations in monoamine oxidase B levels results in loss of spare respiratory capacity: implications for Parkinson's disease. *The journal of biological chemistry*. 278(47):46432-9.

Langston, J.W. 2006. The Parkinson’s complex: Parkinsonism is just the tip of the iceberg. *Annals of neurology*. 59:591–596.

Lee, M.G., Wynder, C., Schmidt, D.M., McCafferty, D.G. & Shiekhattar, R. 2006. Histone H3 lysine 4 demethylation is a target of nonselective antidepressive medications. *Chemistry & biology*. 13(6):563-567.

Lee, M.R. 1982. Dopamine and the kidney. *Clinical science.* 62:439-448.

LeWitt, P.A. & Nyholm, D. 2004. New developments in levodopa therapy. *Neurology*. 62:S9-S16.

LeWitt, P.A., Segel, S.A., Mistura, K.L. & Schork, M.A. 1993. Symptomatic anti-parkinsonian effects of monoamine oxidase-B inhibition: comparison of selegiline and lazabemide. *Clinical neuropharmacology*. 16:332-337.

Lees, A. 2005. Alternatives to levodopa in the initial treatment of early Parkinson’s disease. *Drugs aging*. 22(9):731-740

Legoabe, L.J., Petzer, A. & Petzer, J.P. 2014. α-Tetralone derivatives as inhibitors of monoamine oxidase. *Bioorganic & medicinal chemistry letters*. 24:2758-2763.

Leonard, N., Lamber, C., Depiereux, E. & Wouters, J. 2004. Modeling of human oxidase A: From low resolution threading models to accurate comparative models based on crystal structures. *Neurotoxicology.* 25:47-61.

Lum, T.L. & Stahl, S.M. 2012. Opportunities for reversible inhibitors of monoamine oxidase-A (RIMAs) in the treatment of depression. *CNS spectrums*. 17:107-120.

Lyles, G.A. 1996. Mammalian plasma and tissue-bound semicarbazide-sensitive amine oxidase: biochemical, pharmacological and toxicological aspects. *The international journal of biochemistry & cell biology*. 28:259-274.

Mandel, S., Weinreb, O., Amit, T. & Youdim, M.B.H. 2005. Mechanism of neuroprotective action of the anti-Parkinson drug rasagiline and its derivatives. *Brain research reviews*. 48:379-387.

Manley-King, C.I., Bergh, J.J. & Petzer, J.P. 2013. Inhibition of monoamine oxidase by selected C5- and C6-substituted isatin analogues. *Bioorganic & medicinal chemistry*. 19(1):261-274.

Meissner, W.G., Frasier, M., Gasser, T., Goetz, C.G., Lozano, A, Piccini, P. Obeso, J.A., Rascol, O., Schapira, A., Voon, V., Weiner, D.M., Tison, F. & Bezard, E. 2011. Priorities in Parkinson's disease research. *Nature reviews drug discovery*. 10(5):377-393.

Mercuri, N.B. & Bernardi, G. 2005 The 'magic' of l-dopa: why is it the gold standard Parkinson's disease therapy? *Trends in pharmacological sciences*. 26(7):341-344.

Meyer, J.H., Ginovart, N. & Boovariwala, A. 2006. Elevated monoamine oxidase a levels in the brain: an explanation for the monoamine imbalance of major depression. *Archives of general psychiatry*. 63(110):1209-1216.

Milczek, E.M., Binda, C., Rovida, S., Mattevi, A. & Edmondson, D.E. 2011. The 'gating' residues Ile199 and Tyr326 in human oxidase B function in substrate and inhibitor recognition. *FEBS journal*. 278(24):4860-4869.

Nagatsu, T. 2004. Progress in monoamine oxidase (MAO) research in relation to genetic engineering. *Neurotoxicology*. 25:11–20.

Newton-Vinson, P., Hubalek, F. & Edmondson, D.E. 2000. High-level expression of human liver monoamine oxidase B in pichia pastoris. *Protein expression and purification*. 20:334-345.

O'Carroll, A.M., Fowler, C.J., Phillips, J.P., Tobbia, I. & Tipton, K.F. 1983. The deamination of dopamine by human brain monoamine oxidase. Specificity for the two enzyme forms in seven brain areas. *Naunyn-Schmiedeberg's Archives of pharmacology*. 322:198-202.

Olanow, C.W., Hauser, R.A., Gauger, L., Malapira, T., Koller, W., Hubble, J., Bushenbark, K., Lilienfeld, D. & Esterlitz, J. 1995. The effect of deprenyl and levodopa on the progression of the signs and symptoms in Parkinson's disease. *Annals of neurology*. 38:771 – 777.

Olanow, C.W., Watts, R.L. & Koller, W.C. 2001. An algotithm (decision tree) for the management of Parkinson's disease (2001): treatment guidelines. *Neurology*. 56(suppl 5):S1-S88.

Oreland, L., Arai, Y., Strenstrom, A. & Fowler CJ. 1983. Monoamine oxidase activity and localization in the brain and the activity in relation to psychiatric disorders. (*In* Beckmann, H., Riederer, P., *ed*. Modern problems in pharmacopsychiatry. Monoamine oxidase and its selective inhibitors. Basel: Karger, p. 246–254).

Palfreyman, M.G., McDonald, I.A., Bey, P., Danzin, C., Zreika, M. & Cremer, G. 1994. Haloallylamine inhibitors of MAO and SSAO and their therapeutic potential. *Journal of neural transmission.* 41:407-414.

Pedrosa, D.J. & Timmermann, L. 2013. Review: management of Parkinson's disease. *Neuropsychiatric disease and treatment*. 9:321-340.

Petzer, A., Pienaar, A. & Petzer, J.P. 2013a. The Inhibition of Monoamine Oxidase by Esomeprazole. *Drug research*. 63: 462–467

Petzer, A., Pienaar, A. & Petzer, J.P. 2013b. The interactions of caffeine with monoamine oxidase. *Life sciences*. 93(7):283-287.

Postuma, R.B., Lang, A.E., Munhoz, R.P., Charland, K., Pelletier, A., Moscovich, M., Filla, L., Zanatta, D., Romenets, S.R., Altman, R., Chuang, R. & Shah, B. 2012. Caffeine for treatment of Parkinson's disease: a randomized controlled trial. *Neurology*. 79(7):651-658.

Prediger, R.D. 2010. Effects of caffeine in Parkinson's disease: from neuroprotection to the management of motor and non-motor symptoms. *Journal of Alzheimer's disease*. 20:205-220.

Quik, M. 2004. Smoking, nicotine and Parkinson's disease. *Trends in neurosciences*. 27:561-568.

Quik, M. Bordia, T. & O'Leary, K. 2007. Nicotinic receptors as CNS targets in Parkinson's diseas. *Biochemical pharmacology*. 74(8):1224-1234.

Rajput, A.H., Martin, W., Saint-Hilaire, M.H. Dorflinger, E. & Pedder, S. 1997. Tolcapone improves motor function in parkinsonian patients with the wearing off phenomenon: a double blind, placebo-controlled, multicentre trial. *Neurology.* 49:1066-1071.

Riederer, P. & Youdim, M. 1993. The therapeutic place and value of present and future MAO-B inhibitors L-deprenyl as the gold standard. (*In* Szelenyi, J., *ed*. Inhibition of monoamine oxidase b, pharmacology and clinical use in neurodegenerative disorders. Basel: Birkhäuser. p. 327–338).

Riederer, P., Sofic, E., Rausch, W.D., Schmidt, B., Reynolds, G.P., Jellinger, K. & Youdim, M.B. 1989. Transition metals, ferritin, glutathione, and ascorbic acid in parkinsonian brains. *Journal of neurochemistry*. 52:515-520.

Riederer, P., Danielczyk, W. & Grunblatt, E. 2004. Monoamine oxidase-B inhibition in Alzheimer's disease. *Neurotoxicology.* 25:271–277.

Robakis, D. and Fahn, S. 2015. Defining the role of the monoamine oxidase-B inhibitors for Parkinson's disease. *CNS drugs*. 29:433-441.

Robinson-White, A., Baylin, S.B., Olivecrons, T. & Beaven, M.A. 1985. Binding of diamine oxidase activity to rat and guinea pig microvascular endothelial cells. Comparisons with lipoprotein lipase binding. *The journal of clinical investigation*. 76:93-100.

Sajja, Y., Vanguru, S., Jilla, L., Vulupala, H.R., Bantu, R., Yogeswari, P., Sriram, D. & Nagarapu, L. 2016. A convenient synthesis and screening of benzosuberone bearing 1,2,3-triazoles against Mycobacterium tuberculosis. *Bioorganic & medicinal chemistry letters*. 26:4292-4295.

Salach, J.I. 1979. Monoamine oxidase from beef liver mitochondria: Simplified isolation procedure, properties, and determination of its cysteinyl flavin content. *Archives of biochemistry and biophysics*. 192:128-137.

Saura, J., Kettler, R., Da, P.M. & Richards, J.G. 1992. Quantitative enzyme radioautography with 3H-Ro 41-1049 and 3H-Ro 19-6327 in vitro: localization and abundance of MAO-A and MAO-B in rat CNS, peripheral organs, and human brain. *Journal of neuroscience.* 12:1977-1999.

Schmidt, D.M. & McCafferty, D.G. 2007. Trans-2-Phenylcyclopropylamine is a mechanism-based inactivator of the histone demethylase LSD1. *Biochemistry*. 46(14):4408-4416.

Seiler, N. 1990. Polyamine metabolism. *Digestion*. 46:319-330.

Shapiro, M.A., Chang, Y.L., Munson, S.K., Jacobson, C.E., Rodriguez, R.L., Skidmore, F.M., Okun, M.S. & Fernandez, H.H. 2007. The four A's associated with pathological Parkinson gamblers: anxiety, anger, age and agonists*. Neuropsychiatric disease and treatment.* 3(1):161-167.

Shih, J.C., Chen, K. & Ridd, M.J. 1999. Monoamine oxidase: from genes to behaviour. *Annual review of neuroscience*. 22:197-217.

Silver, D.E. & Ruggieri, S. 1998. Initiating therapy for Parkinson's disease. *Neurology* 50(6):S18-S22.

Singh, N., Pillay, P. & Choonara, Y.E. 2007. Advances in the treatment of Parkinson's disease. *Progress in neurobiology*. 81:29-44.

Sivasubramaniam, S.D., Finch, C.C., Rodriguez, M.JL Mahy, N. & Billett E.E. 2003. A comparative study of the expression of monoamine oxidase-A and –B mRNA and protein in non-CNS human tissues. *Cell and tissue research*. 313:291-300

Son, S., Ma, J., Kondou, Y., Yoshimura, M., Yamashita, E. and Tsukihara, T. 2008. Structure of human monoamine oxidase A at 2.2-Å resolution: The control of opening the entry for substrates/inhibitors. *The national academy of sciences of the USA*. 105:5739-5744.

Stahl, S.M. 2008. Stahl's Essential Psychopharmacology: Neuroscientific Basis and Practical Applications. 3rd ed. Fully rev. expanded ed. Cambridge, UK: Cambridge University Press. 1057p.

Stewart, J.T. 2007. Not all monoamine oxidase inhibitors are created equal. *Journal of the American geriatrics society*. 11:1890.

Stoof, J.C., Booij, J. & Drukarch, B. 1992. Amantadine as a N-methyl-D-aspartic acid receptor antagonist: new possibilities for therapeutic application? *Clinical neurology and neurosurgery*. 93:S4-S6.

Strydom, B., Malan, S.F., Castagnoli Jr, N., Bergh, J.J. and Petzer, J.P. 2010. Inhibition of monoamine oxidase by 8-benzyloxycaffeine analogues. *Bioorganic & medicinal chemistry*. 18:1018-1028.

Tabor, C.W., Tabor, H. & Rosenthal, S.M. 1954. Purification of amine oxidase from beef plasma. *The journal of biological chemistry*. 208: 645-661.

Tiller, J.W. 1993. Clinical overview on Moclobemide. *Progress in neuro-psychopharmacology & biological psychiatry*. 17:703-712.

Tipton, K.F. 1980. Kinetic mechanism and enzyme function. *Biochemical society transactions.* 8:242.

Tipton, K.F. 1986. Enzymology of monoamine oxidase. *Cell biochemistry and function*. 4:79-87.

Thomas, T. 2000. Monoamine oxidase-B inhibitors in the treatment of Alzheimer's disease. *Neurobiology of aging.* 21:343-348.

Von Strauss, E., Viitanen, M., De Ronchi, D., Winblad, B. & Fratiglioni, L. 1999. Aging and the occurrence of dementia: findings from a population-based cohort with a large sample of nonagenarians. *Archives of neurology*. 56:587-592.

Walmeier, P.C., Felner, A.E. & Maitre, L. 1981. Long term effects on selective MAO inhibitors on MAO activity and amine metabolism. (*In* Youdim, M.B. & Paykel, E.S., *ed*. Monoamine oxidase inhibitors: the state of the art. Chichester: Wiley. p. 87-102).

Walker, W.H., Kearney, E.B., Seng, R.L. & Singer, T.P. 1971. The covantly bound flavin of hepatic monoamine oxidase. 2. Identification and properties of cysteinyl riboflavin. *European journal of biochemistry*. 24:328-331.

Weinreb, O., Amit, T., Bar-Am, O., & Youdim, M.B.H. 2010. Rasagiline: A novel anti-Parkinsonion monoamine oxidase-B inhibitor with neuroprotective activity. *Progress in neurobiology*, 92:330-344.

Westlund, K.N., Denney, R.M., Kochersperger, L.M., Rose, R.M. & Abell, C.W. 1985. Distinct monoamine oxidase A and B populations in primate brain. *Science*. 230:181-183.

Westlund, K.N., Denney, R.M., Rose, R.M. & Abell, C.W. 1988. Localization of distinct monoamine oxidase A and monoamine oxidase B cell populations in human brain stem. *Neuroscience*. 25:439–56.

Weyler, W. & Salach, J.I. 1985. Purification and Properties of Mitochondrial Monoamine Oxidase Type A from Human Placenta. *The journal of biological chemistry*. 260:13199-13207.

Weyler, W., Hsu, Y.P. & Breakefield, X.O. 1990. Biochemistry and genetics of monoamine oxidase. *Pharmacology & therapeutics*. 47:391-417.

Weyler, W., Titlow, C.C. & Salach, J.I. 1990. Catalytically active monoamine oxidase type A from human liver expressed in Saccharomyces cerevisiae contains covalent FAD. *Biochemical and biophysical research communications.* 173:1205-1211.

Xu, K., Bastia, E. & Schwarzschild, M. 2005. Therapeutic potential of adenosine A(2A) receptor antagonists in Parkinson's Disease. *Pharmacology & therapeutics*. 105(3):267-310.

Yamada, Y. & Yasuhara, H. 2004. Clinical Pharmacology of MAO inhibitors: Safety and Future. *Neurotoxicology*. 25:215-221.

Yang, M., Culhane, J.C., Szewczuk, L.M., Jalili, P., Ball, H.L., Machius, M. Cole, P.A. & Yu, H. 2007. Structural basis for the inhibition of the LSD1 histone demethylase by the antidepressant trans-2-phenylcyclopropylamine. *Biochemistry*. 46(27):8058-8065.

Yokel, R.A. 2000. The toxicology of aluminium in the brain: a review. *Neurotoxicology.* 21:813-828.

Youdim, M.B.H. 1978. The active centers of monoamine oxidase types A and B; binding with ^{14}C-clogyline and ^{14}C-deprenyl. *Journal of neural transmission*. 43:199-208.

Youdim, M.B. & Finberg, J. 1985. Monoamine oxidase inhibitor antidepressants. (*In* Grahame-Smith, D.G., *ed*. Psychopharmacology 2:Part1: preclinical psychopharmacology. Amsterdam: Excerpta Medica. p. 35-70).

Youdim, M.B.H. & Weinstock, M. 2004. Therapeutic Applications of selective and non-selective inhibitors of monoamine oxidase A and B that do not cause significant tyramine potentiation. *Neurotoxicology*. 25:243-250.

Youdim, M.B.H. & Bakhle, Y.S. 2006. Monoamine oxidase: Isoforms and inhibitors in Parkinson's disease and depressive illness. *British journal of pharmacology*, 147(Suppl 1):S287-S296.

Youdim, M.B.H., Finberg, J.P.M. & Tipton, K.F. 1988. Monoamine oxidase. (*In* Trendelenburg, U., & Weiner, N., *ed*. Handbook of Experimental Pharmacology Vol.90. Berlin: Springer-Verlag. p. 119-192).

Youdim, M.B.H., Gross, A. & Fiberg, J.P.M. 2001. Rasagiline [N-propargyl-1R(+)-aminoindan], a selective and potent inhibitor of mitochondrial monoamine oxidase B. *British journal of pharmacology*. 132:500-506.

Youdim, M.B.H., Maruyama, W. & Naoi, M. 2005. Neuropharmacological, neuroprotective and amyloid precursor processing properties of selective MAO-B inhibitor anti-parkinsonian drug, rasagiline. *Drugs today*, 41, 369–391.

Youdim, M.B., Edmondson, D. & Tipton, K.F. 2006. The therapeutic potential of monoamine oxidase inhibitors. *Nature reviews*. *Neuroscience*. 7(4):295–309.

Zreika, M., Fozard, J.R., Dudley, M.W., Bey, P., McDonald, I.A. & Palfreyman, M.G. 1989. MDL 72.974A: a potent and selective enzyme activated irreversible inhibitor of monoamine type B with potential use in Parkinson's disease. *Journal of neural transmission*. 1:243-254.

ANNEXURE A: NMR SPECTRA

6,7,8,9-tetrahydro-5*H*-benzo[7]annulen-5-amine (1a)

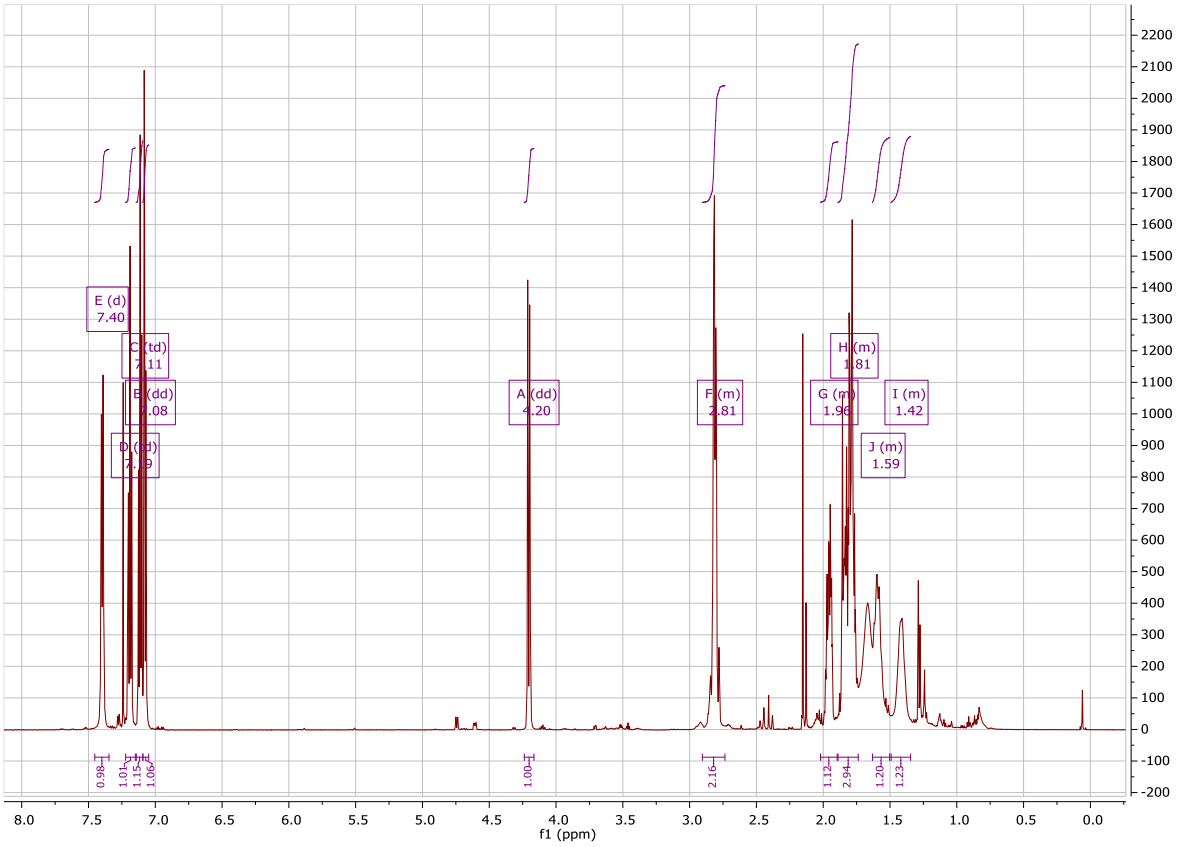

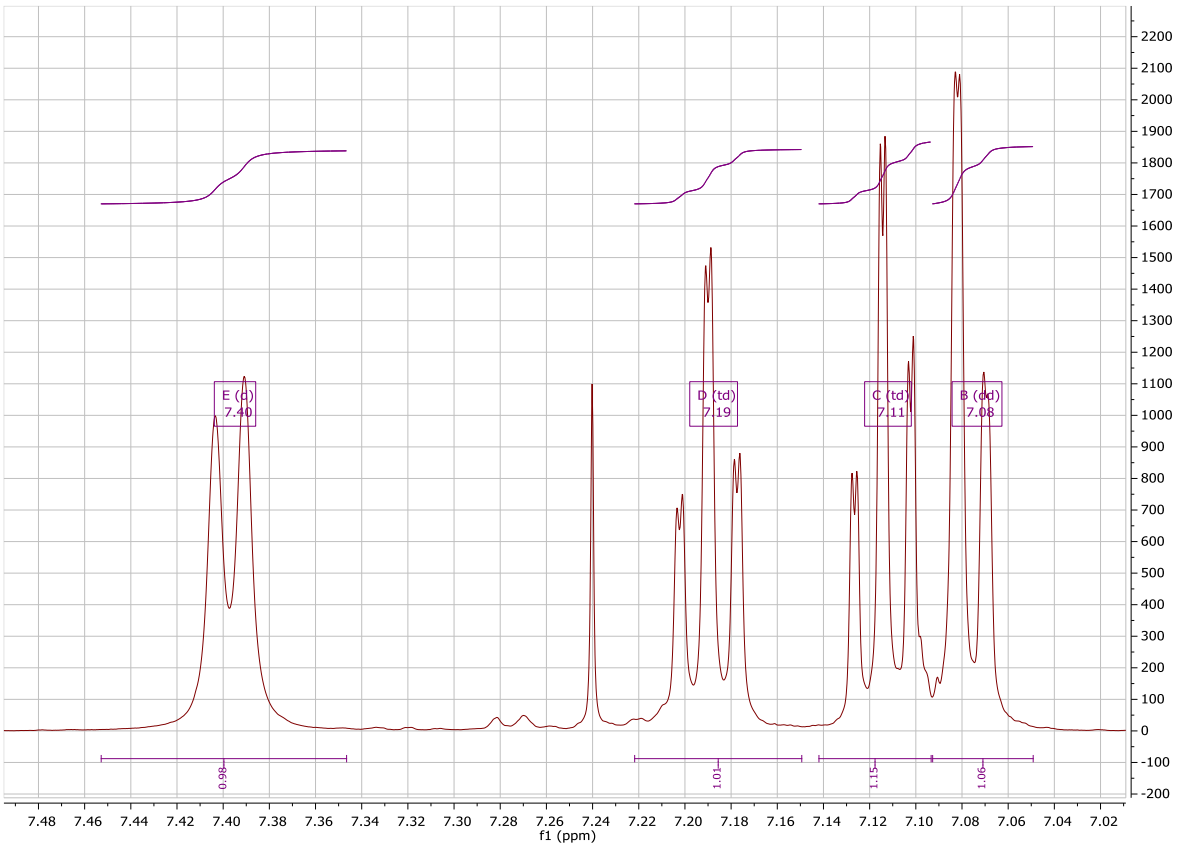
E (d)
7.40
D (td)
7.19
C (td)
7.11
B (dd)
7.08
0.98
1.01
1.15
1.06
f1 (ppm)

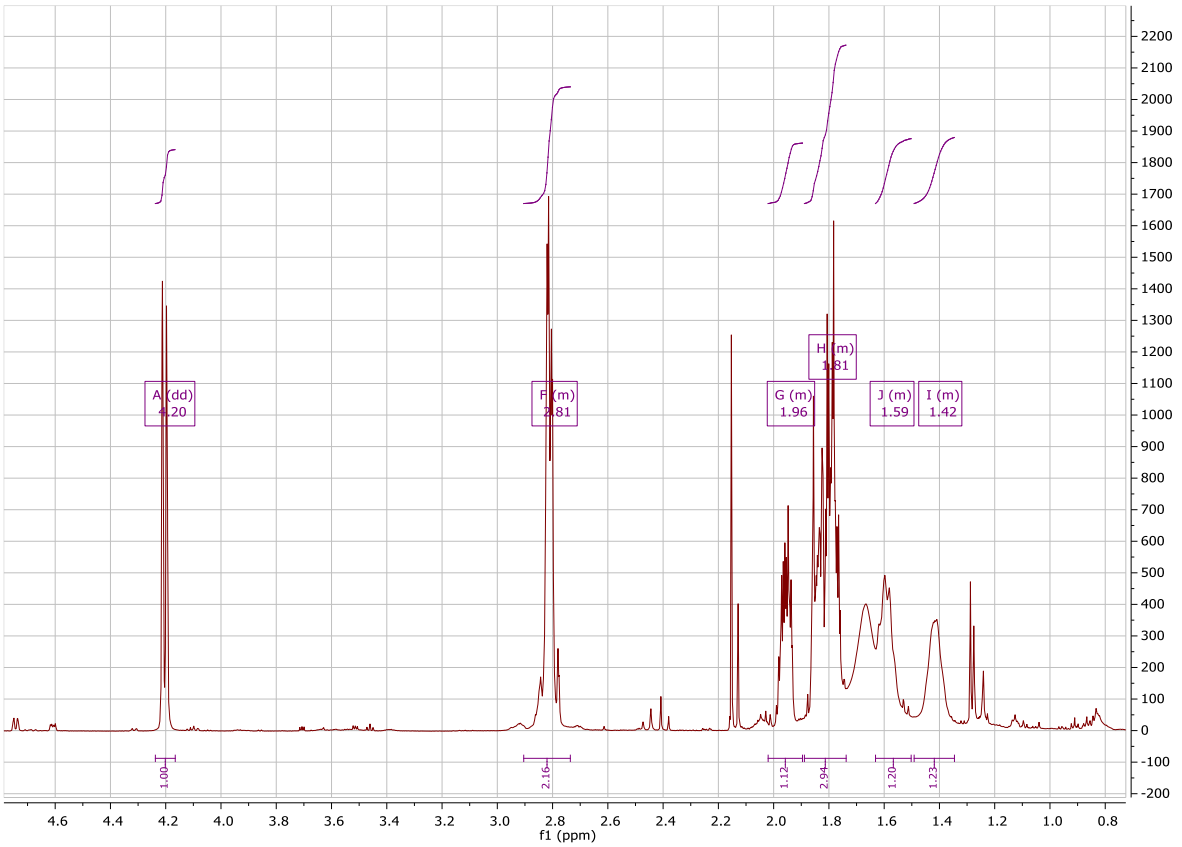
A (dd)
4.20
F (m)
2.81
H (m)
1.81
G (m)
1.96
J (m)
1.59
I (m)
1.42
1.00
2.16
1.12
2.94
1.20
1.23
f1 (ppm)

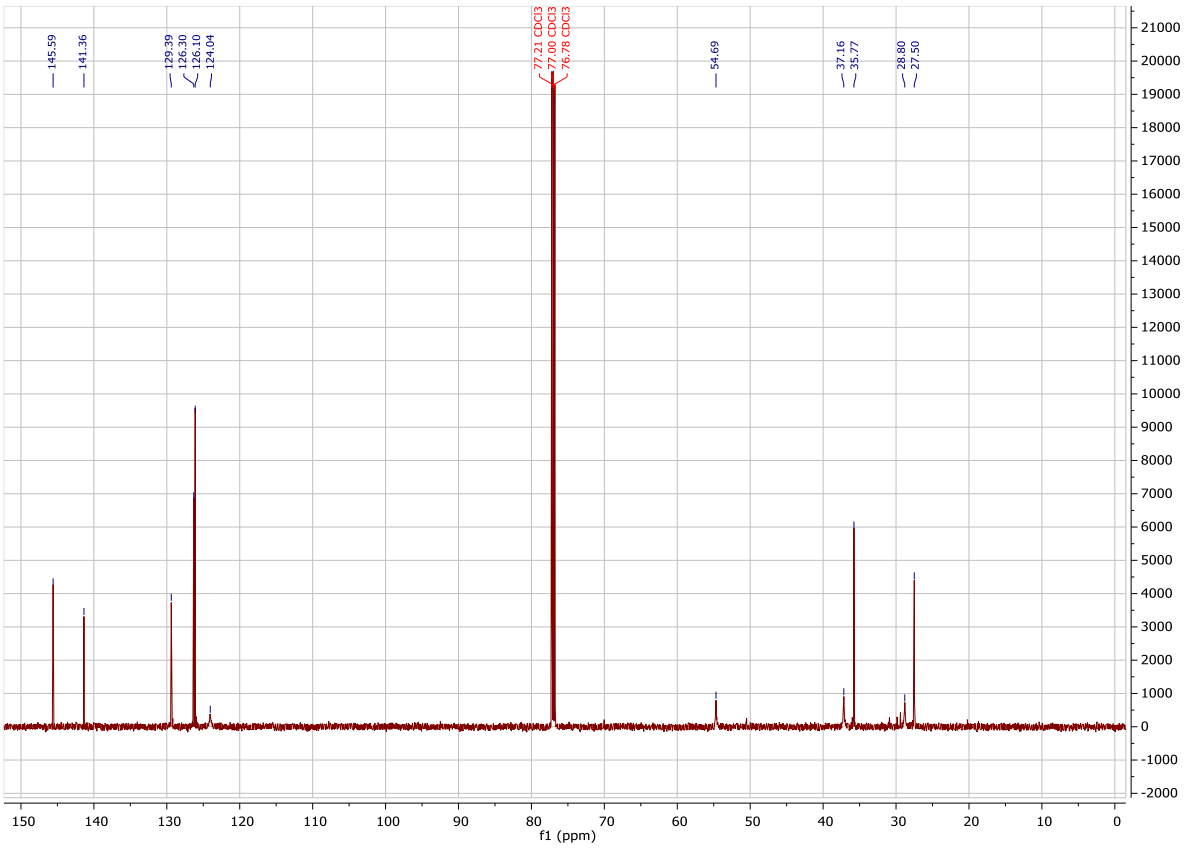

6,7,8,9-tertahydro-5*H*-benzo[7]annulen-5-ol (1b)

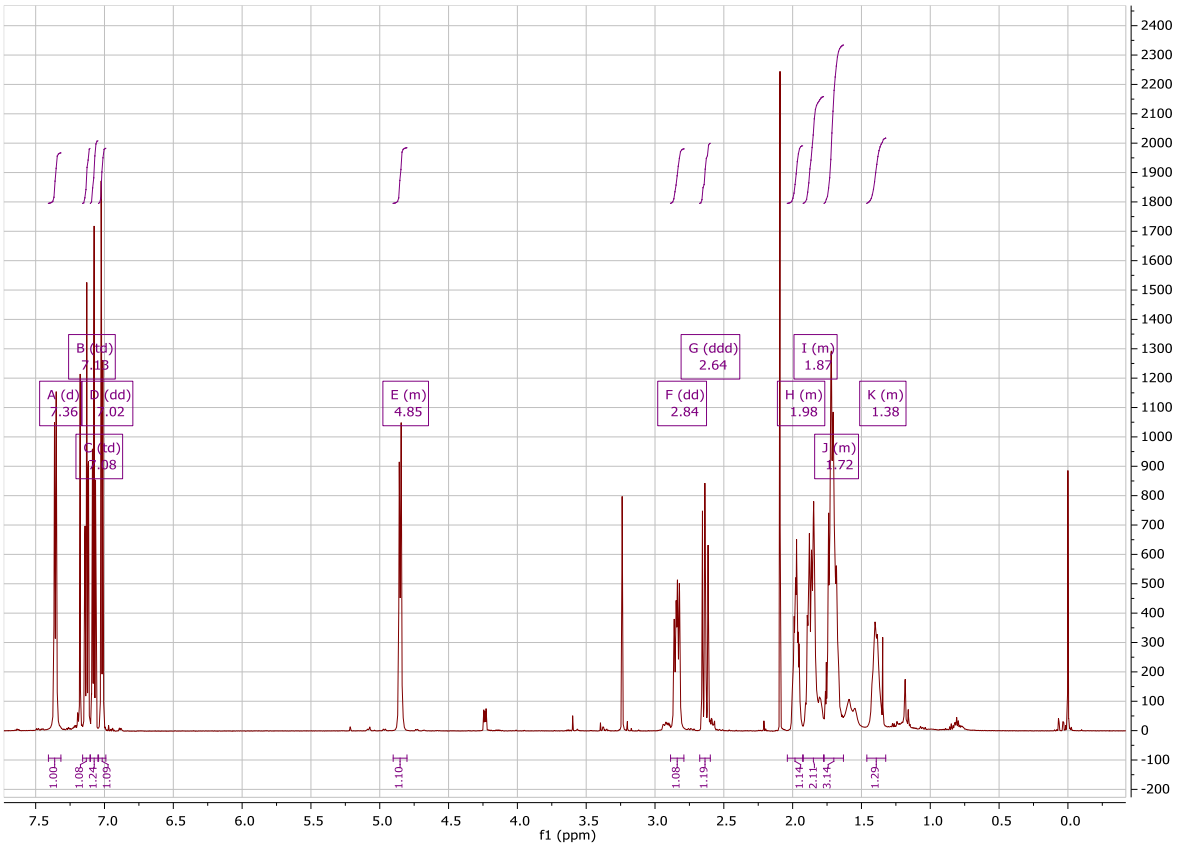

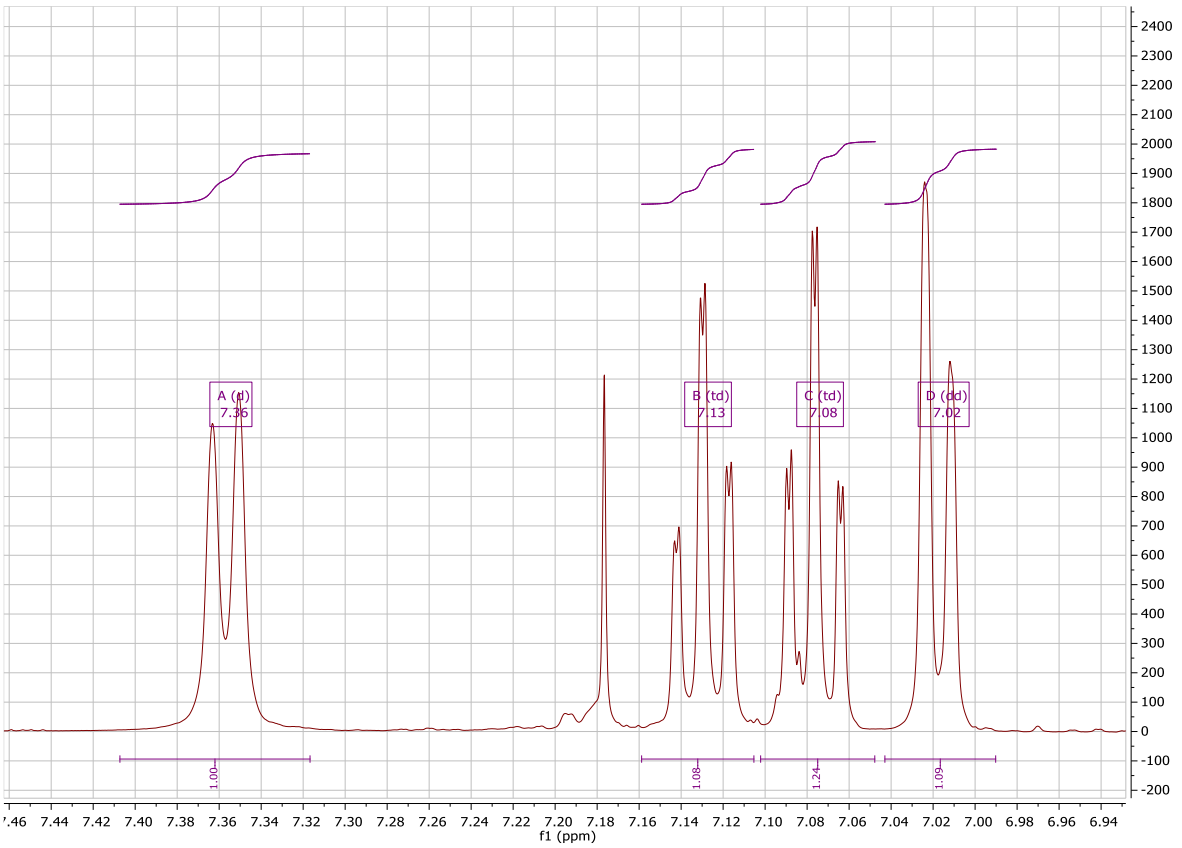
A (d)
7.36
B (td)
7.13
C (td)
7.08
D (dd)
7.02
1.00
1.08
1.24
1.09
f1 (ppm)

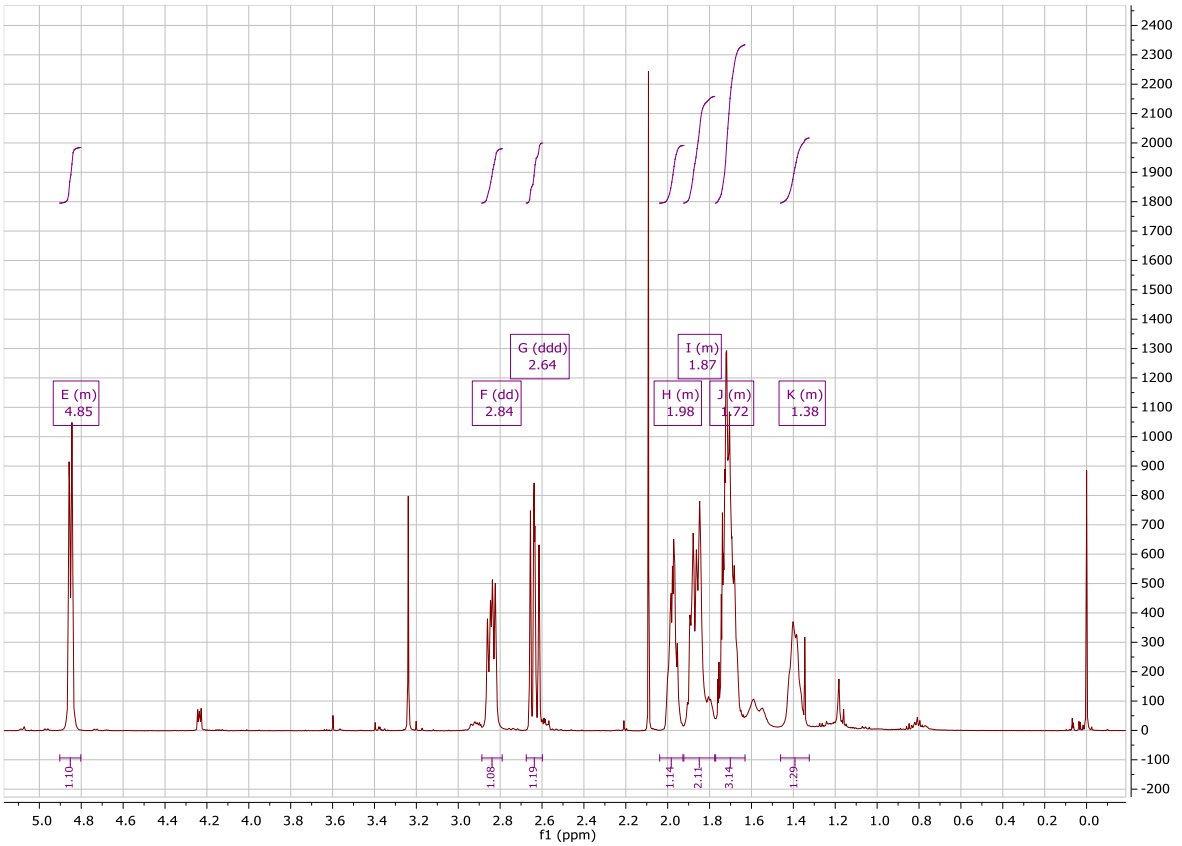
E (m)
4.85
F (dd)
2.84
G (ddd)
2.64
H (m)
1.98
I (m)
1.87
J (m)
1.72
K (m)
1.38
1.10
1.08
1.19
1.14
2.11
3.14
1.29
f1 (ppm)

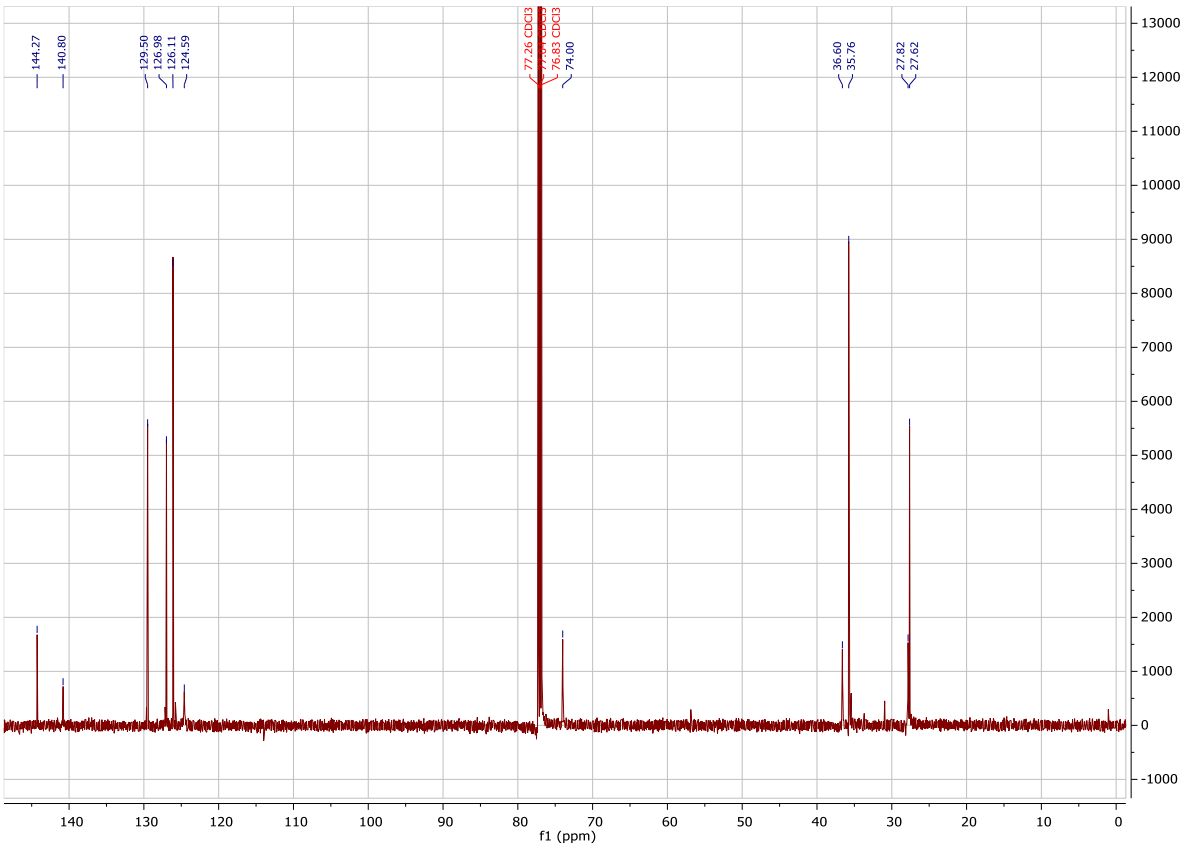

6,7-dihydro-5*H*-benzo[7]annulene (1c)

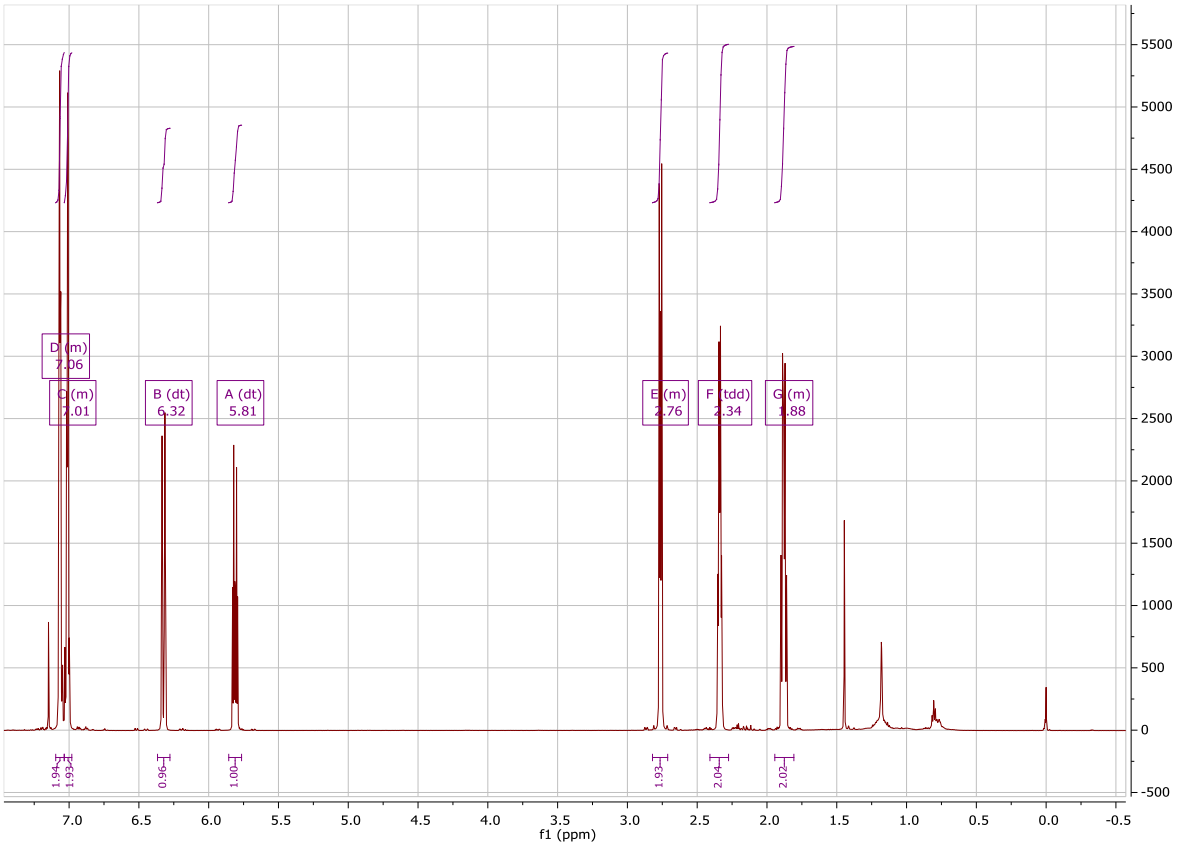

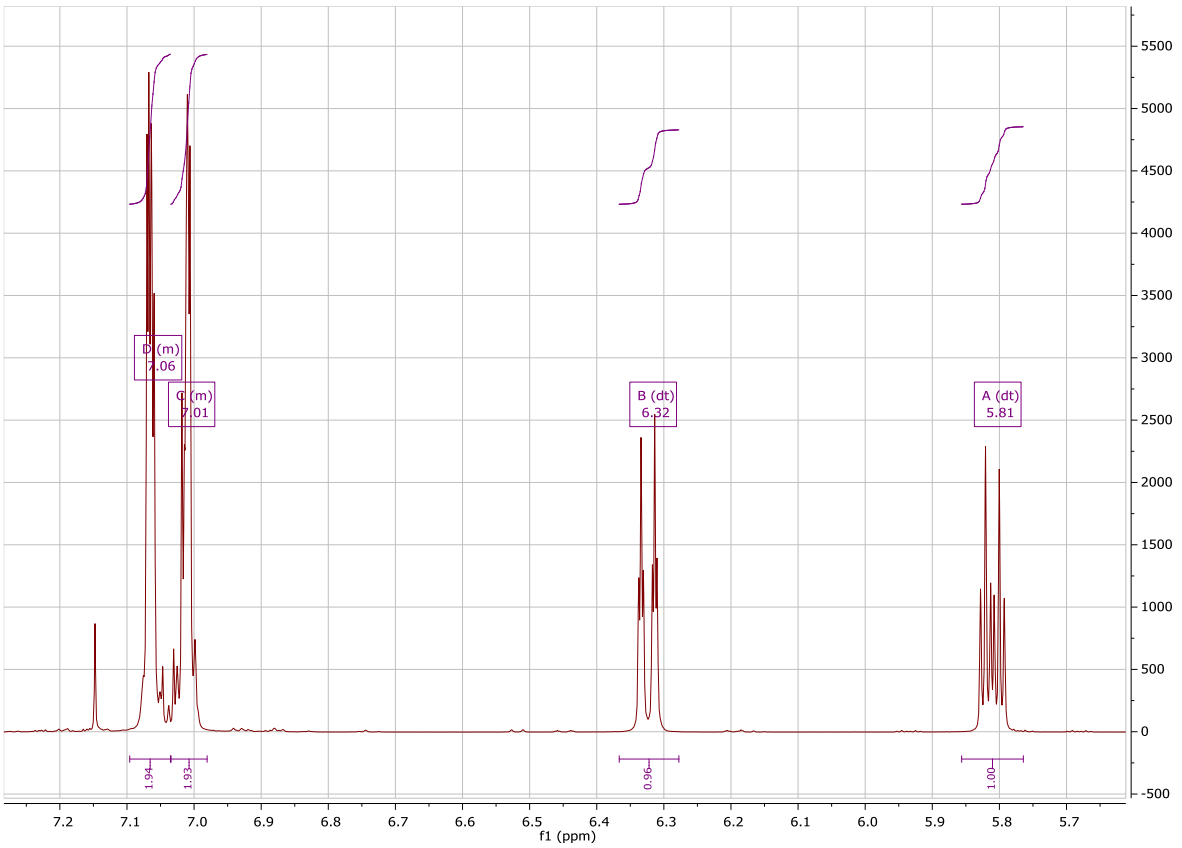
D (m)
7.06
C (m)
7.01
B (dt)
6.32
A (dt)
5.81
1.94
1.93
0.96
1.00
f1 (ppm)

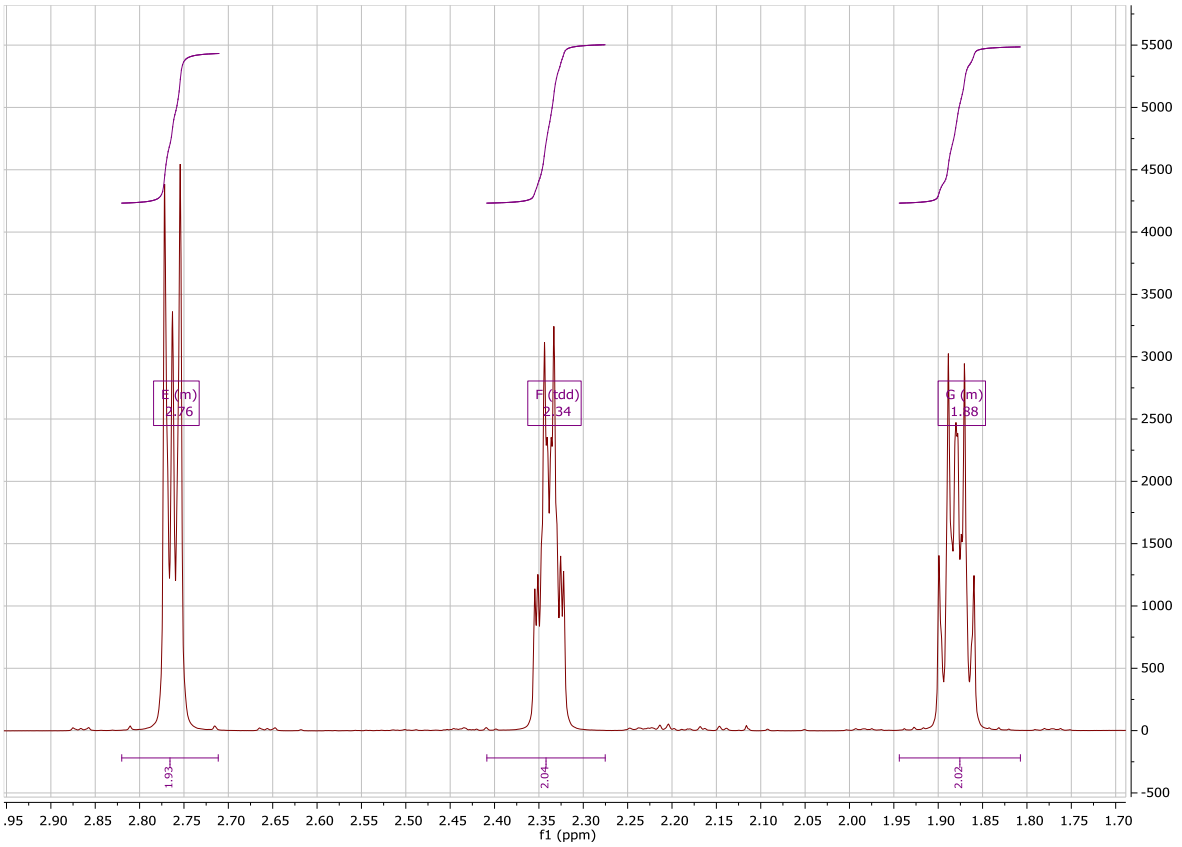
E (m)
2.76
F (tdd)
2.34
G (m)
1.38
1.93
2.04
2.02
f1 (ppm)

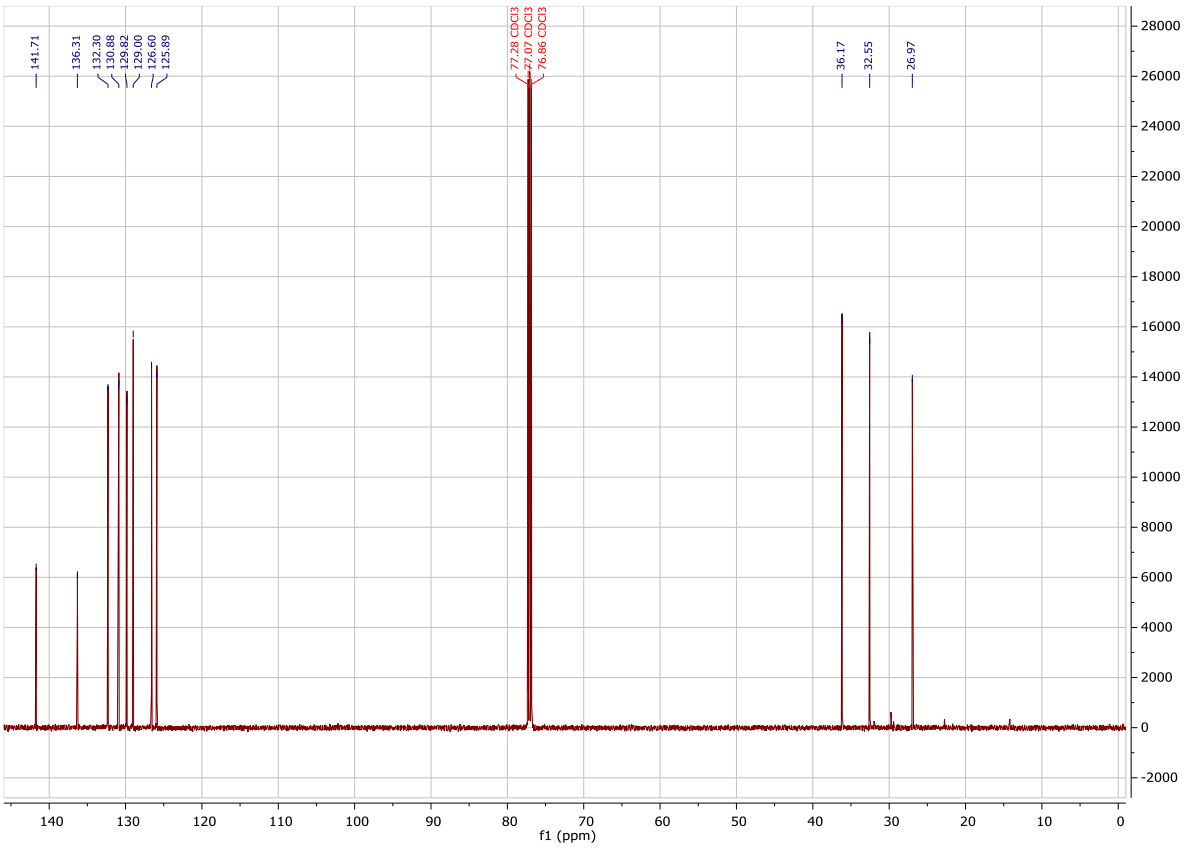

6,7,8,9-tetrahydro-5*H*-benzo[7]annulen-5-yl acetate (1d)

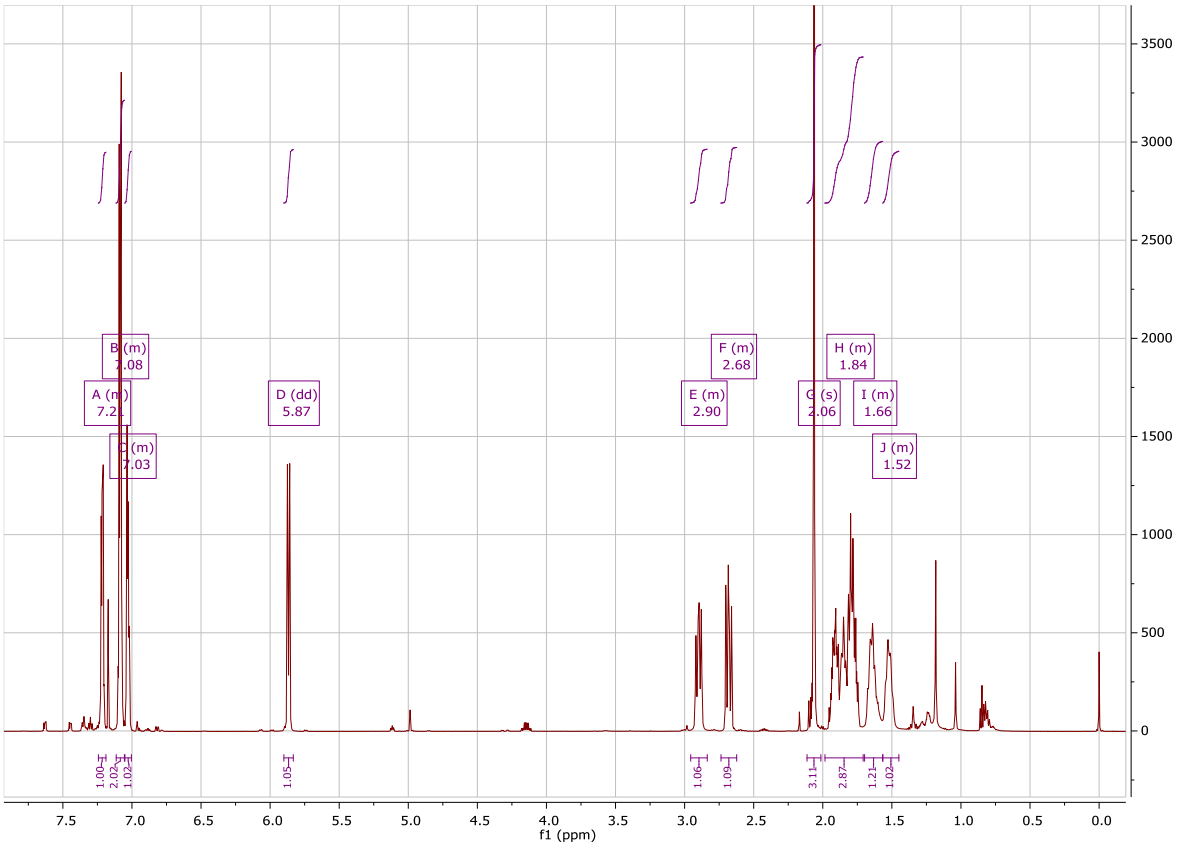

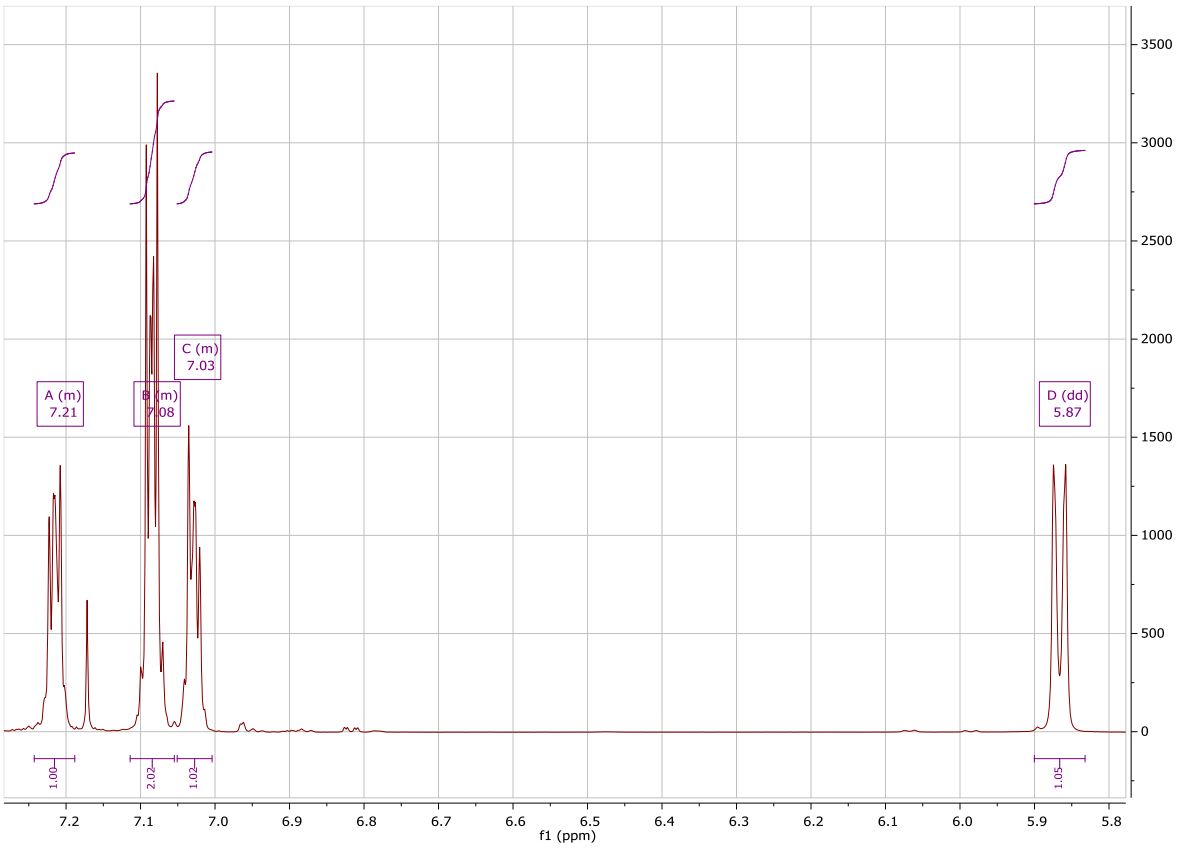
A (m)
7.21
B (m)
7.08
C (m)
7.03
D (dd)
5.87
1.00
2.02
1.02
1.05
f1 (ppm)

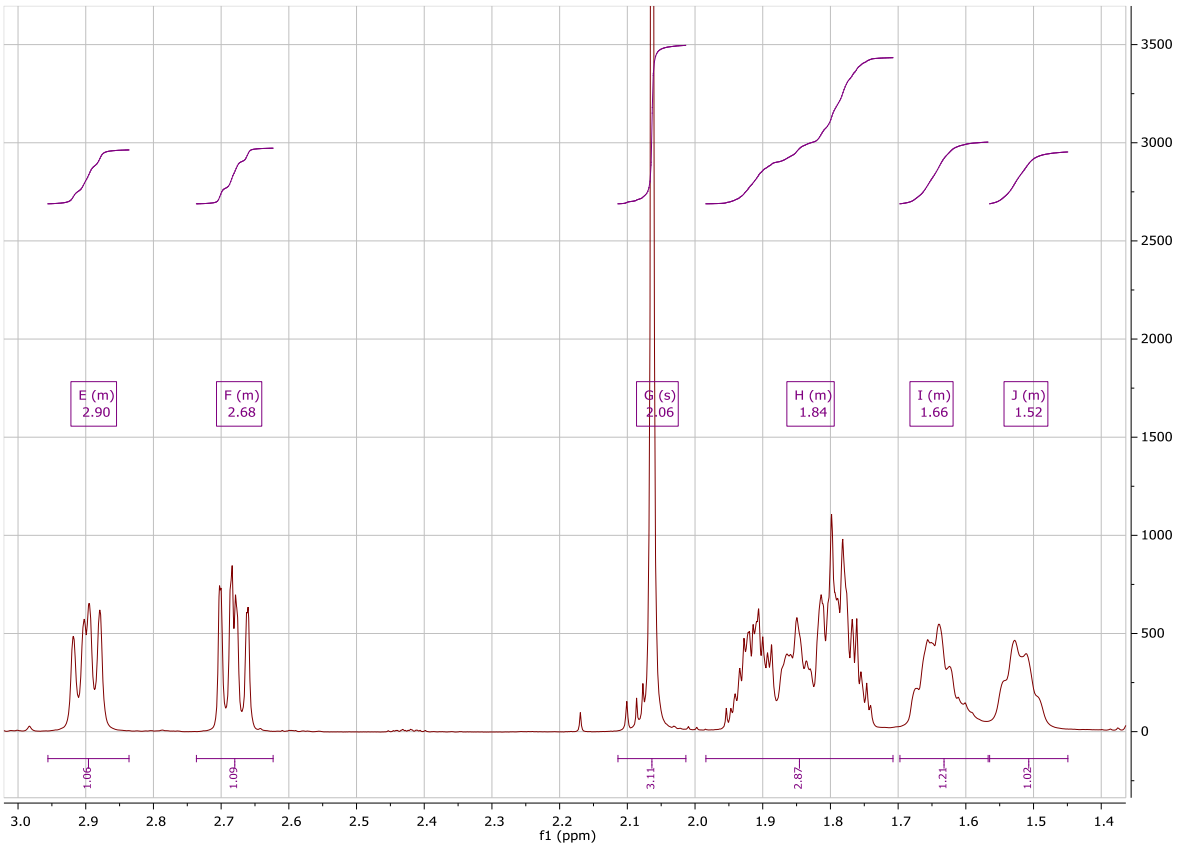
E (m)
2.90
F (m)
2.68
G (s)
2.06
H (m)
1.84
I (m)
1.66
J (m)
1.52
1.06
1.09
3.11
2.87
1.21
1.02
f1 (ppm)

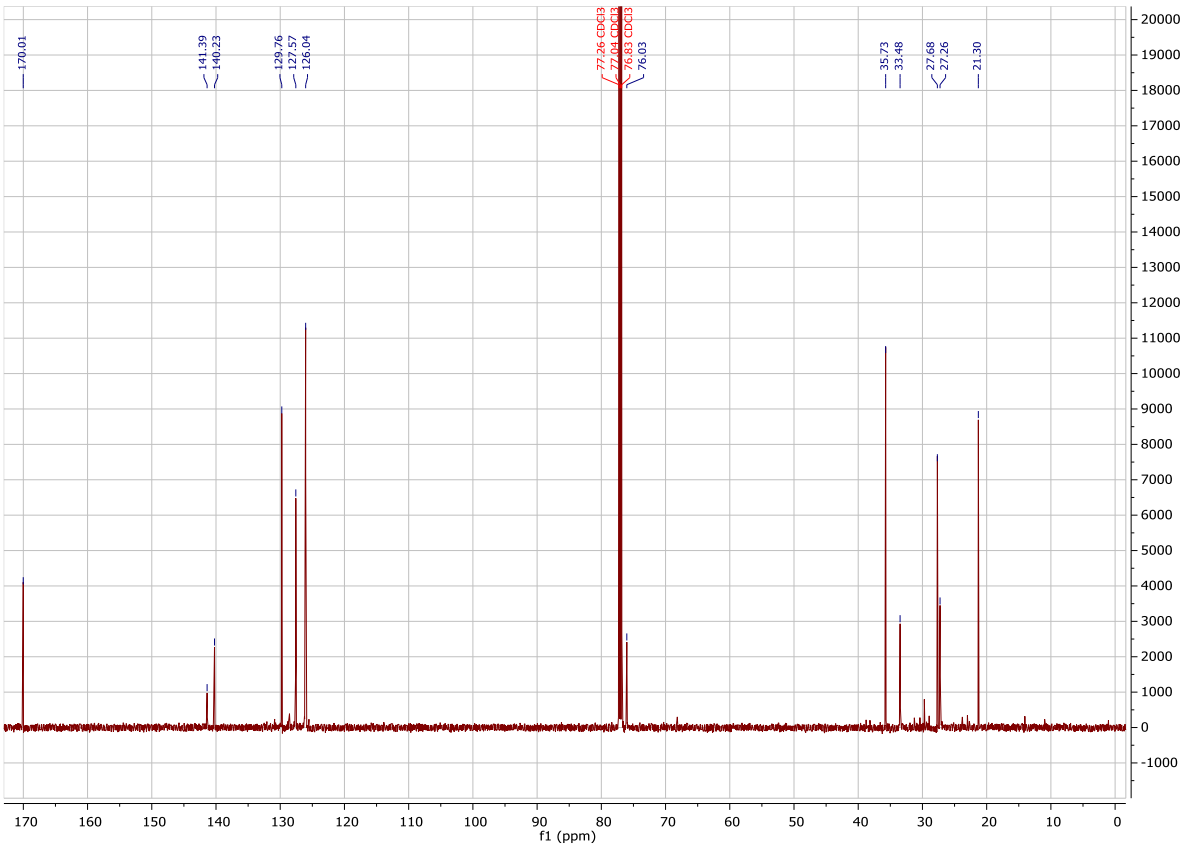
170.01
141.39
140.23
129.76
127.57
126.04
77.26 CDCl3
77.04 CDCl3
76.83 CDCl3
76.03
35.73
33.48
27.68
27.26
21.30
f1 (ppm)

ANNEXURE B: MASS SPECTRA

6,7,8,9-tetrahydro-5*H*-benzo[7]annulen-5-amine (1a)

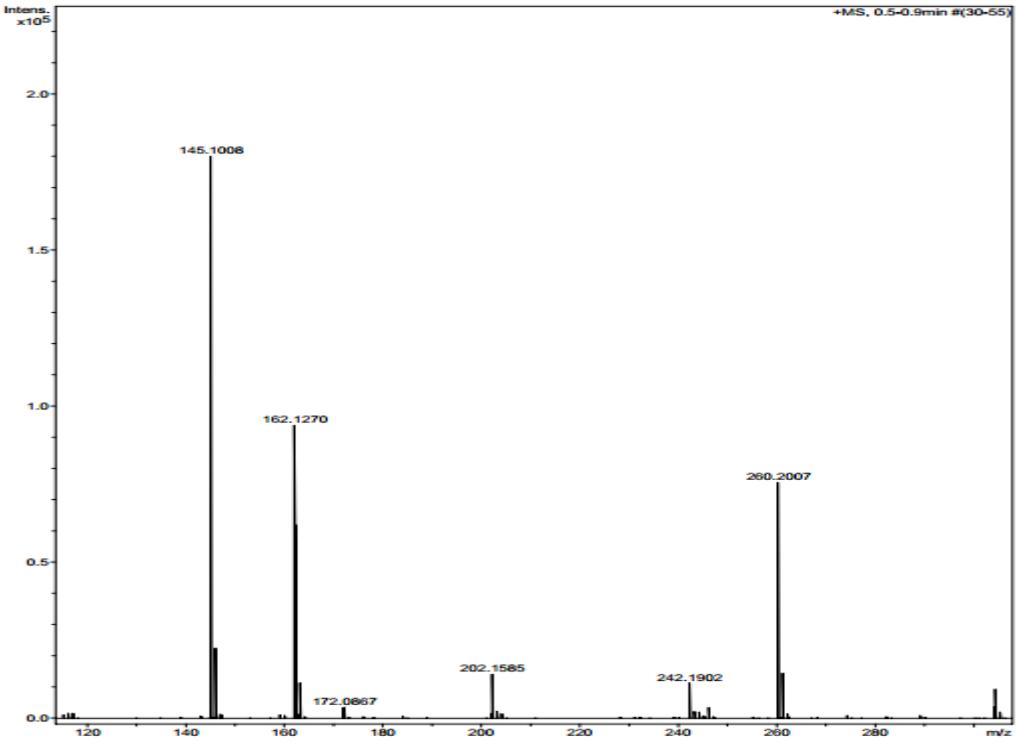

6,7,8,9-tertahydro-5*H*-benzo[7]annulen-5-ol (1b)

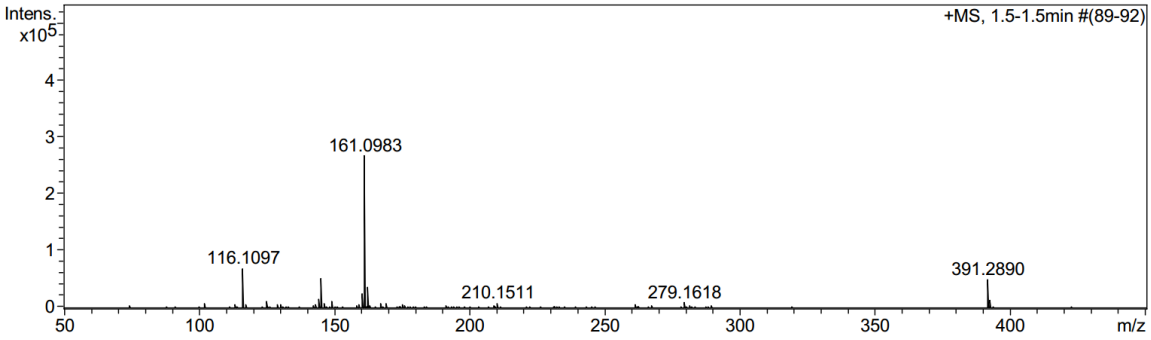

Meas. m/z	#	Formula	Score	m/z	err [mDa]	err [ppm]	mSigma	rdb	N-Rule	e⁻ Conf
145.1025	1	C 11 H 13	100.00	145.1012	-1.3	-9.1	8.0	5.5	ok	even
161.0983	1	C 11 H 13 O	100.00	161.0961	-2.2	-13.5	8.2	5.5	ok	even
391.2890	1	C 24 H 39 O 4	100.00	391.2843	-4.7	-12.0	2.4	5.5	ok	even

6,7-dihydro-5*H*-benzo[7]annulene (1c)

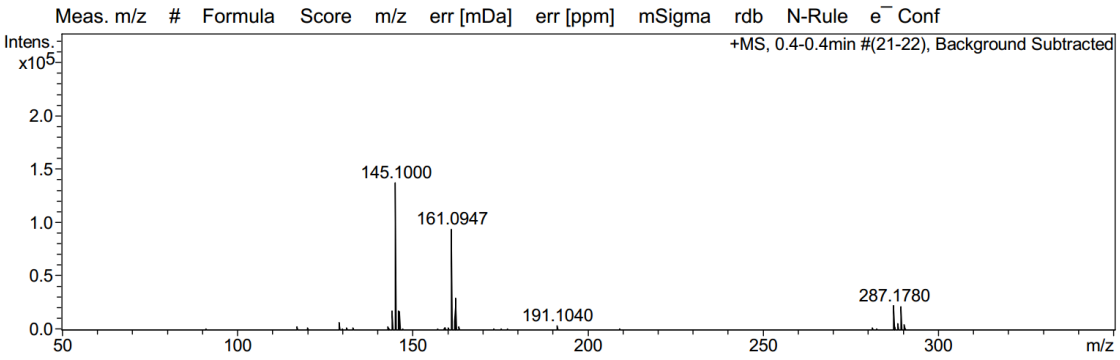

Meas. m/z	#	Formula	Score	m/z	err [mDa]	err [ppm]	mSigma	rdb	N-Rule	e¯ Conf
145.1000	1	C 11 H 13	100.00	145.1012	1.2	8.4	8.4	5.5	ok	even
161.0947	1	C 11 H 13 O	100.00	161.0961	1.4	8.4	113.1	5.5	ok	even

ANNEXURE C: HPLC TRACES

6,7,8,9-tetrahydro-5*H*-benzo[7]annulen-5-amine (1a)

1 mM

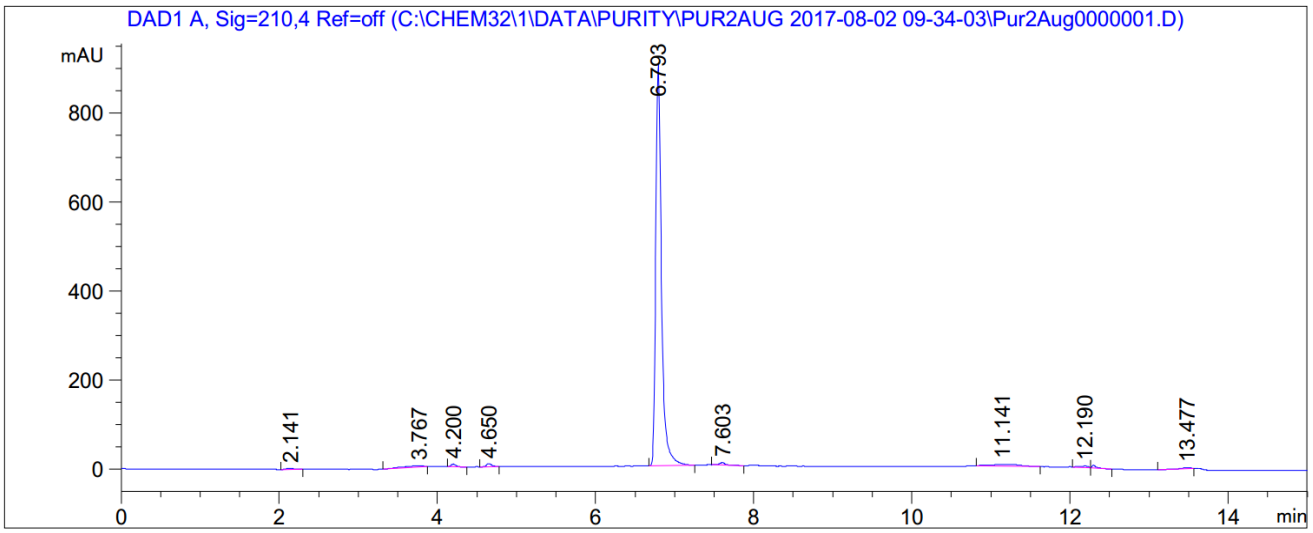

6,7,8,9-tertahydro-5*H*-benzo[7]annulen-5-ol (1b)

1 mM

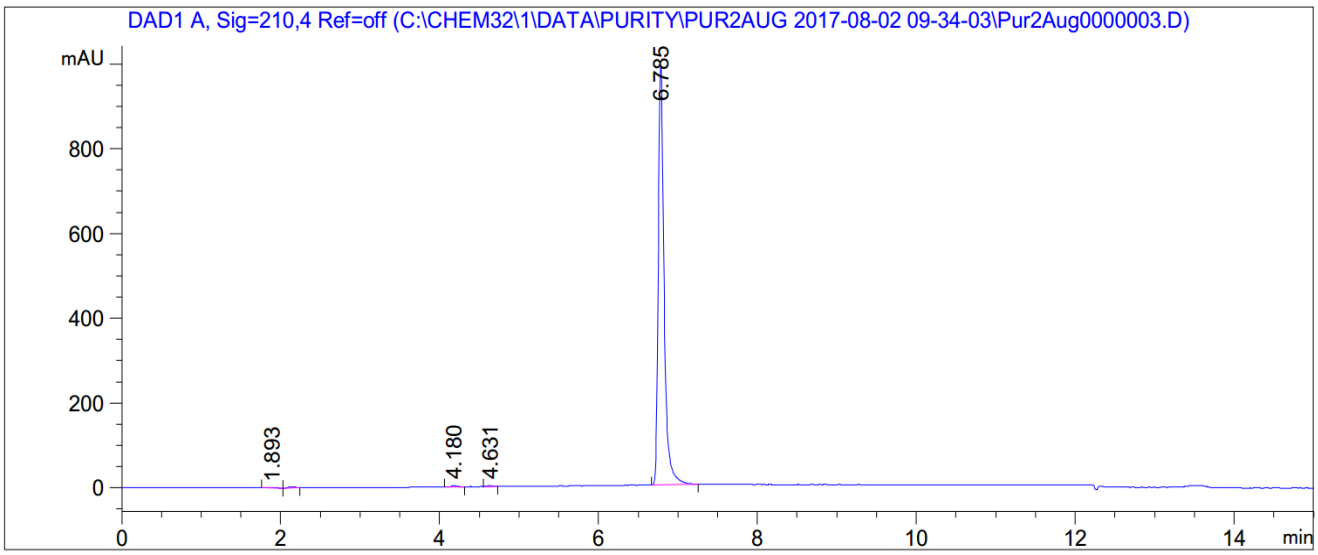

6,7-dihydro-*5H*-benzo[7]annulene (1c)

1 mM